University of Kerbala
College of Science
Department of Chemistry

Synthesis and theoretical study of new imidazole derivatives dyes and their application in dye sensitized solar cells

A Thesis

Submitted to the council of the College of Science/

University of Kerbala

In partial Fulfillment of the requirements for the Degree of Master of Science in Chemistry

By

Saifaldeen Fahim Abdulhussein

Supervised by

Prof. Dr. Haitham Dalol Hanoon

Assist.Prof. Dr. Saifaldeen Muwafag Abdulhadi

2022 A.D ***1443 A.H***

Supervisors Certification

I certify this thesis conducted under my supervision at the department of chemistry, College of science, University of Kerbala, as a partial fulfillment of the requirements for the degree of M.Sc. in organic chemistry.

Signature:
Name: Prof. Dr. Haitham Dalol Hanoon
Address: University of Kerbala – College of Science
Date: 3 / 7 /2022

Signature:
Name: Assist.Prof. Dr. Saifaldeen Muwafag Abdulhadi
Address: University of Al-Karkh for Science – College of Reomte Sensing and Geophysics
Date: 3 / 7 /2022

Report of the Head of the Chemistry Department

According to the recommendation presented by the Chairman of the Postgraduate Studies Committee, I forward this thesis **"Synthesis and theoretical study of new imidazole derivatives dyes and their application in dye sensitized solar cells"** for examination.

Signature:

Prof.Dr. Luma M. Ahmed

Head of Chemistry Department

Address: University of Kerbala, College of Science, Department of Chemistry

Date: 4 / 7 /2022

Examination Committee Certification

We certify that we have read this thesis entitled "**Synthesis and theoretical study of new imidazole derivatives dyes and their application in dye sensitized solar cells** " as the examining committee, examined the student " **Saifaldeen Fahim Abdulhussein** " on its contents, and that in our opinion, it is adequate for the partial fulfillment of the requirements for the Degree of Master in Science of chemistry.

:Signature
Name: **Dr. Mohanad Mousa Kareem**
Title: Professor
Address: University of Babylon, College of Science, Department of Chemistry
Date: 3 / 7 /2022
(Chairman)

Signature
Name: **Dr. Ghazwan Ali Salman**
Title: Assistant Professor
Address: University of Mustansiriyah, College of Science, Department of Chemistry.
Date: 3 / 7 /2022
(Member)

Signature
Name: **Dr. Jalal Hasan Mohammed**
Title: Assistant Professor
Address: University of Kerbala, College of Pharmacy.
Date: 3 /7 /2022
(Member)

Signature:
Name: **Dr. Haitham Dalol Hanoon**
Title: Professor
Address: University of Kerbala, College of Science, Department of Chemistry
Date: 3 / 7 /2022
(Member & Supervisor)

Signature:
Name: **Dr. Saifaldeen Muwafag Abdulhadi**
Title: Assistant Professor
Address: University of Al-Karkh for Science, College of Reomte Sensing and Geophysics.
Date: 3 / 7 /2022
(Member & Supervisor)

Approved by the council of the College of Science

Signature:
Name: **Dr. Jasem Hanoon Hashim Al-Awadi**
Title: Assistant Professor
Address: **Dean of College of Science, University of Kerbala.**
Date: 5/7 9/2022

بسم الله الرحمن الرحيم

نَرْفَعُ دَرَجَاتٍ مَّن نَّشَاءُ ۗ وَفَوْقَ كُلِّ ذِي عِلْمٍ عَلِيمٌ

صدق الله العلي العظيم

سورة يوسف: الآية (76)

Dedication

To

Fatima al-Zahra, her father,

her husband and her sons,

peace be upon them

Acknowledgments

In the beginning, I would like to thank Allah for its blessings…

I would like to thank those who sponsored me as a master's student, and for preparing this research, my esteemed professor and supervisors, **Prof. Dr. Haitham Dalol Hanoon** and **Assist.Prof. Dr. Saifaldeen**

Muwafag Abdulhadi. Those who have the credit - after God Almighty - for research and researcher since the topic was a title and an idea until it became a thesis and research. They have all my thanks, appreciation and gratitude.

I also extend my heartfelt thanks whoever help me from the teaching staff at the University of Kerbala, College of science, Department of chemistry.

I would like to express my deep appreciation to all of members my family and friends for their material and spiritual support.

Saifaldeen

Abstract

In this work, six free metal-organic dyes were designed and synthesized as the donor-π bridge-acceptor system in a one-pot condensation reaction and used as a sensitizer in DSSCs. The dyes that were recorded are imidazole derivatives, which are of two types. Type I are basically 2,4,5-trisubstituted imidazole derivatives (Scheme I) and the type II of dyes are 1,2,4,5-tetrasubstituted imidazole derivatives (Scheme II).

The first type is PP1 and the second type are containing five different substituents on (N-imidazole) ring such as (nitrobenzene (PP2), *N*,*N*-diethylpropan-1-amine (PP3), phenyl (PP4), chlorobenzene (PP5) and dichlorobenzene (PP6)) with investigation the effect of these substituents in the efficiency of the synthesized compounds as a DSSCs. Benzene and imidazole units were chosen as donor groups, for their electron-donating character and to avoid dye aggregation on the TiO_2 surface. Basically, 2,4,5-trisubstituted imidazole units were used to comparative study of the performance of the sensitizers in the final devices. Benzene ring was chosen as the termination of the π-bridge. Carboxylic acid was chosen as both acceptor and anchor group on the TiO_2 surface. All these dyes are characterized by FTIR, ^{1}H-NMR, ^{13}C-NMR, Mass spectra and supported by computational calculation. The dye PP3 with the alkyl chain substitution displayed the highest power conversion efficiency (PCE) of 2.01% (J_{sc} = 3.75 mA cm^{-2}, V_{oc} = 0.73 mV, FF = 73.9%) while the PP2 dye with the nitrobenzene substitution showed the lowest energy gap (E_g = 2.55 eV) and lowest PCE 0.96% (J_{sc} = 1.59 mA cm^{-2}, V_{oc} = 0.080 mV, FF = 61.6%).

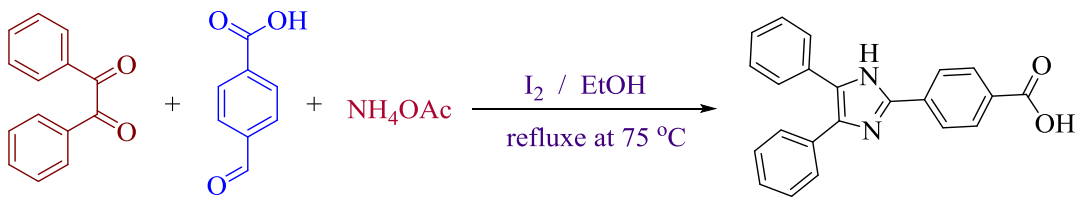

PP1

Scheme I: Synthetic route for 2,4,5-trisubstituted imidazole derivatives

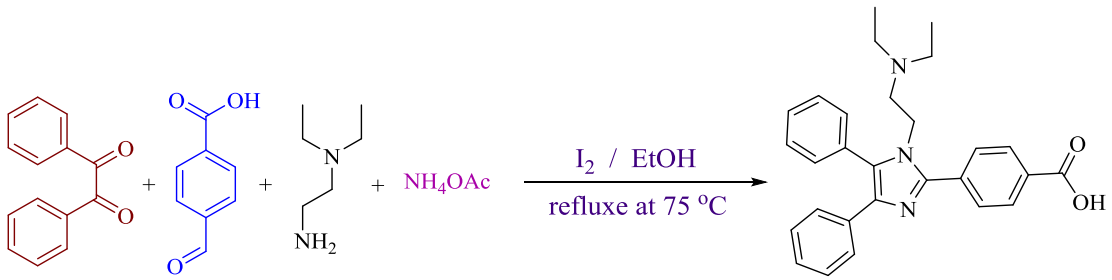

PP3

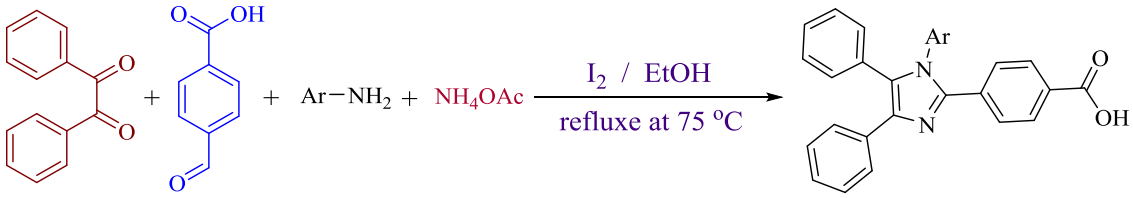

PP2, PP4, PP5 and PP6

Where Ar = 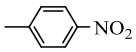 **(PP2),**  **(PP4),**  **(PP5),** 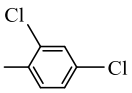 **(PP6)**

Scheme II: Synthetic route for 1,2,4,5- tetrasubstituted imidazole derivatives

Contents

List of Tables

List of Figures

List of Schemes

List of Equation

Abbreviations

Symbol	Definition
A	Absorption
a-Si	Amorphous Silicon Thin Film Solar Cell
b.p.	Boiling point
CdTe	Cadmium Telluride Thin Film Solar Cell
^{13}C-NMR	Carbon Nuclear Magnetic Resonance
c	Concentration
CB	Conduction band
CIGS	Copper Indium Gallium Di-Selenide Solar Cells
DFT	Density functional theory
DMSO	Dimethyl sulfoxide
D-π-A	Donor- π-bridge-Acceptor
d	doublet
D	Dye
D*	Photoexcited dye
DSSCs	Dye sensitized solar cells
η	Efficiency
E_g	Energy gap
$Eg\ opt$	Optical energy gap
EtOH	Ethanol
ε	Extinction coefficient
FF	Fill factor
FTO	Fluorine-doped Tin Oxide
FTIR	Fourier Transform Infrared
^{1}H-NMR	Proton Nuclear Magnetic Resonance
HOMO	Highest occupied molecular orbital
I_o	Total incident irradiance
ITO	Indium tin oxide
J_{max}	Maximum power point current
J_{sc}	Short circuit current
J	Coupling constant
LUMO	Lowest unoccupied molecular orbital
l	Pathlength
MS	Mass spectrometry
m.p.	Melting point

NREL	National Renewable Energy Laboratory
PCE	Power conversion efficiency
PV	Photovoltaic
PVC	Photovoltaic cell
Ref.	References
SMO	Semiconducting metal oxide
s	singlet
SLS	Sodium lauryl sulfate
THF	Tetrahydrofuran
TLC	Thin Layer Chromatography
TCO	Transparent conducting oxide
t	triplet
v	Wavenumber
V_{max}	Maximum power point voltage
V_{oc}	Open circuit voltage
USA	United states of America
UV	Ultraviolet

Chapter one

Introduction

1.1 Imidazole

1.1.1 Structure

Imidazole is a five-membered heterocyclic molecule that contains three carbon atoms and two nitrogen atoms at positions 1 and 3 and usually referred as 1,3-diazole. The nitrogen atom at position 1 is pyrrole-type nitrogen because it contains a hydrogen atom. The second nitrogen atom at position 3 is analogous to the nitrogen atom in pyridine and is hence referred to as pyridine-type nitrogen. (Fig.1-1)

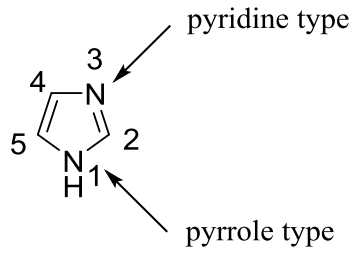

Figure 1-1: Structure of imidazole

Imidazole has a structure that combines the structural characteristics of pyrrole and pyridine. Three carbon atoms and the pyridine-type nitrogen each donate one electron to the aromatic sextet, whereas the pyrrole-type nitrogen contributes two electrons. Imidazole is a heterocyclic aromatic compound with resonance energy of 59 kJ/mol and is thought to be a resonance hybrid of the following resonating structures (Fig. 1-2) [1].

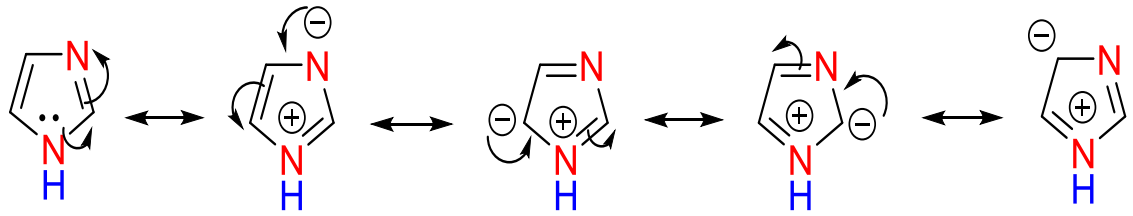

Figure 1-2: Resonance structures of imidazole

1.1.2 Physical properties

Imidazole is a colorless crystal with a melting point of 90°C and a boiling point of 256°C. It is soluble in water and most of the polar solvents. Imidazole has a comparatively high boiling point (b.p. 256°C) when compared to other five-membered heterocyclic systems. The increased boiling point of imidazole is due to the presence of intermolecular hydrogen bonds of the type NH-N (Fig. 1-3). Imidazole, such as water, is an excellent giver of hydrogen bonds and an excellent acceptor; the imine nitrogen provides an electron pair and the N- hydrogen accepts them. Imidazoles have an extraordinarily high thermal stability. Above 500°C, imidazole decomposes [2].

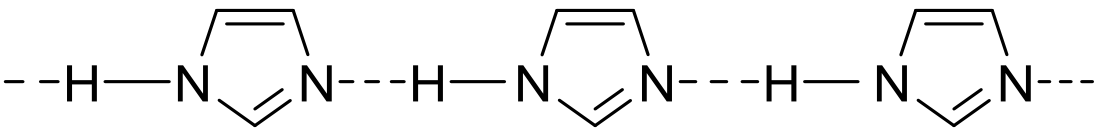

Figure 1-3: Hydrogen bonding in imidazole[47]

1.1.3 Chemical properties

Imidazole is considered a strong base, if compared to other heterocyclic amines such as pyrrole, pyridine, or pyrazole. Pyrazine and imidazole are more stable in acidic media than other cyclic amines. Pyrazine and imidazole both contain two nitrogen atoms and when they are protonated, the positive charge associated with them is delocalized. However, imidazole is a stronger base than pyrazole due to the fact that the pyrazolium ion has a positive charge that is less delocalized than the imidazolium ion (Fig.1-4). Imidazole can undergo acid-base reaction due to the fact that imidazole is a mono acidic base; it has weak acid characteristics and produces acids with crystalline salts [3].

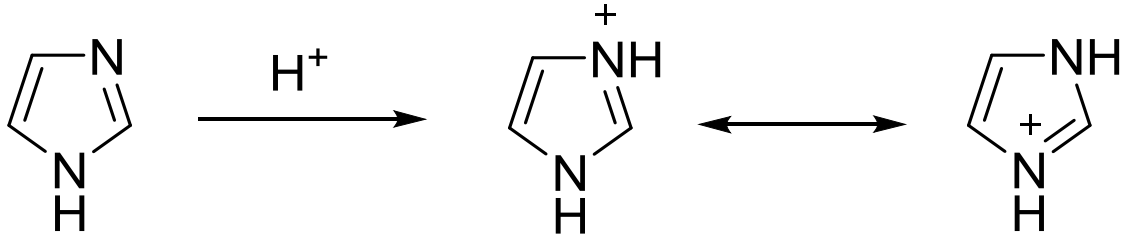

Figure 1-4: Imidazole has Weak Acid Properties[47]

Because the hydrogen atom may be positioned on any of the two nitrogen atoms, imidazole exists in two equivalent tautomeric forms (Fig.1-5). As indicated by its predicted dipole moment of 3.61 D, imidazole is a strongly polar molecule amphoteric and has a pKa of 14.5 [4].

Figure 1-5: Tautomerism in imidazoles.

The imidazole contains two distinct forms of electrons lone-pair. One of them is on pyrrolic nitrogen, which has been delocalized and so becomes acidic. Another is on the basic pyridinic type of N, which has a non-Huckle-lone pair. As a result of their distinct pKa values (7.0 and 14.9), in nature imidazole is amphoteric. Any modification at the pyrrolic position may improve its basicity, hence lessening the difference in the pKa values of the two nitrogen positions in the imidazole moiety, which aids in better electron delocalization in the aromatic ring [5,6].

1.1.4 Synthesis of Imidazole Derivatives

There are many synthetic ways to produce the imidazole and the synthetic approaches are described below [7]:

M. Waheed and co-worker described a unique technique for the synthesis of 2,4,5-trisubstituted and 1,2,4,5-tetrasubstituted imidazole derivatives using a novel organocatalyst based on dihydroquinoline as cost-effective and ecologically friendly organocatalyst. The synthesis of 2,4,5-trisubstituted (Equation 1-1) and 1,2,4,5-tetrasubstituted (Equation 1-2) imidazole derivatives using this process were not need column chromatography. The reaction proces was very simple and pure, allowing for straightforward work-up and purification of products with no detected side products [8].

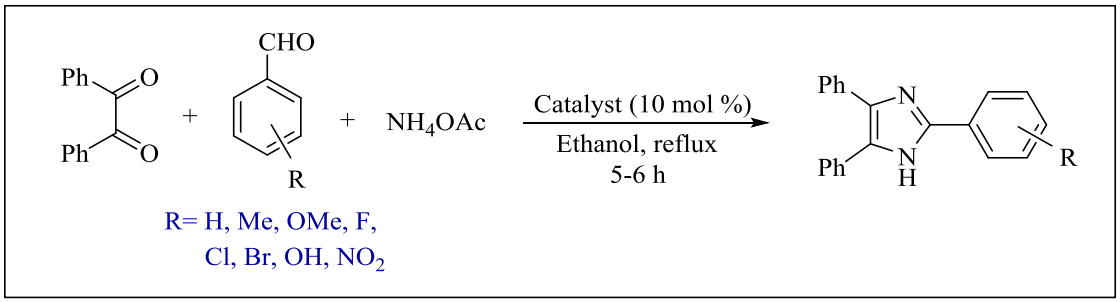

Equation 1-1: Synthesis of 2,4,5-trisubstituted imidazole derivatives

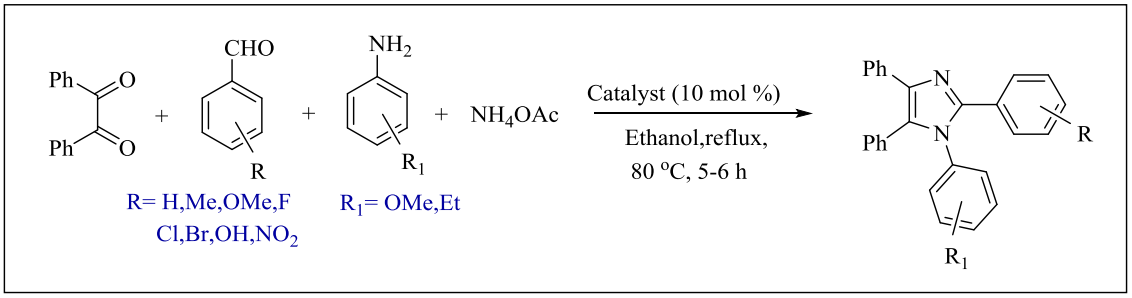

Equation 1-2: Synthetic route of 1,2,4,5-tetrasubstituted imidazole derivatives

Radiszewski reaction was usually used to prepare a imidazole drevitaves by using dicarbonyl chemical such as glyoxal, keto aldehyde, or diketones with an aldehyde in the presence of ammonia, for example, benzyl,

with benzaldehyde and ammonia results in the formation of 2,4,5-triphenylimidazole. Frequently, formamide is used instead of ammonia (Equation 1-3) [4,7].

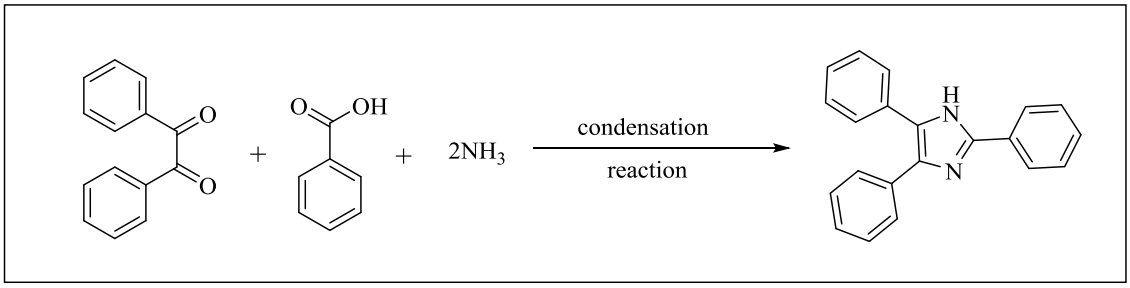

Equation 1-3: Formation of 2,4,5-triphenylimidazole.

R. Bansal and co-workers synthesized 1,2,4,5-tetrasubstituted (Equation 1-4) and 2,4,5-trisubstituted imidazole derivatives (Equation 1-5) through one-pot multicomponent processes at 80°C using water as solvent. This technique has many benefits, including a metal-free reaction, non-chromatographic purification of products, and outstanding yields [9].

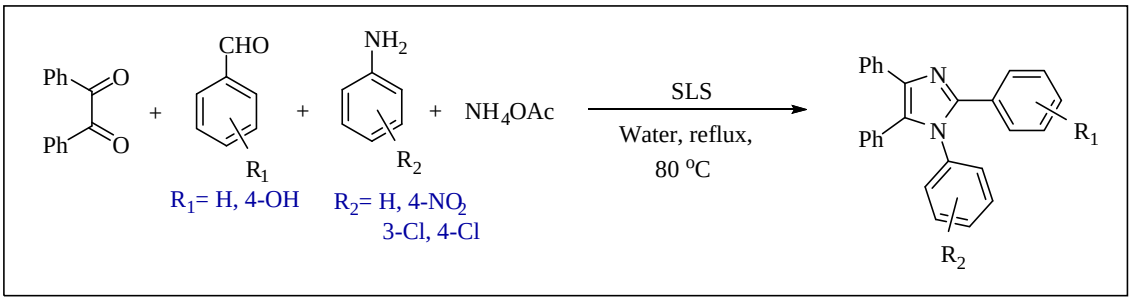

Equation 1-4: Synthetic route of 1,2,4,5-tetrasubstituted imidazole derivatives.

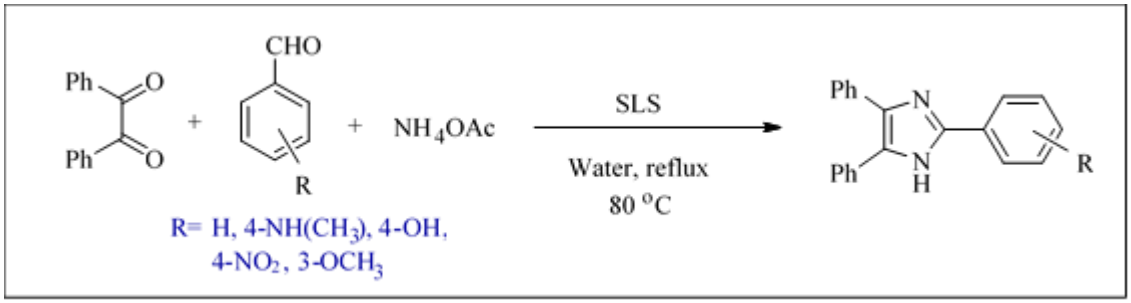

Equation 1-5: Synthesis of 2,4,5-trisubstituted imidazole derivatives.

S. Walki and co-workers synthesized 4-(1-(3-chloro-4-nitrophenyl)-4,5-diphenyl-1*H*-imidazol-2-yl)benzoic acid *via* a one-pot by condensation reaction for 4-5 hrs. with good yields (70-80%) (Equation 1-6) [10].

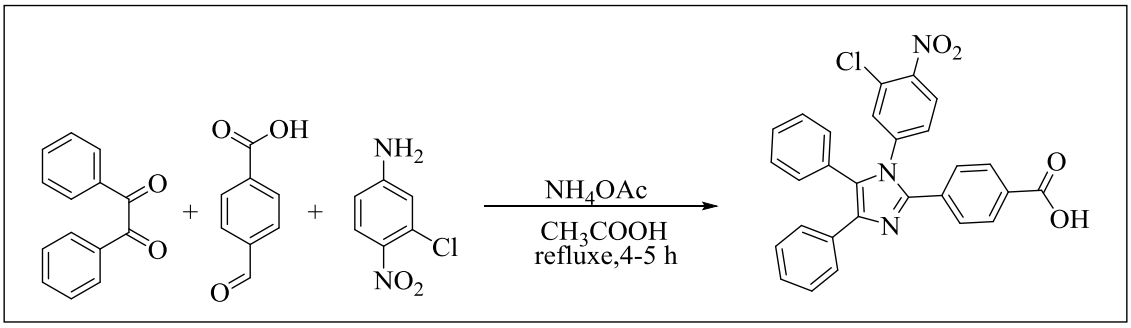

Equation 1-6: Synthetic route of 1,2,4,5-tetrasubstituted imidazole derivatives.

1.1.5 Imidazole Derivatives in DSSCs

Due to the favorable properties of imidazole, researchers have recently brought it into organic light-emitting diode and DSSC applications. According to previous studies, putting electron donors into the 4,5-position of imidazole and an electron acceptor into the 2-position, allows for the formation of conjugated dipolar sensitizers while also enhancing their light-harvesting capability [11]. Additionally, by reducing the positive charge density at the donor group through electronic delocalization of the two substituents in the imidazolyl ring's 4,5-position, charge recombination after electron injection may be decreased [12].

Charge recombination may be slowed after electron injection due to the reduced positive charge density at the donor caused by the electronic delocalization of the two substituents at positions 4 and 5 of the imidazolyl ring [13-15].

In 2007, M. S. Tsai and co-workers reported that the effectiveness of DSSC was 4.68 percent when they used 3-(4-(6,9-Bis(4-(diphenylamino)phenyl)-1*H*-phenanthro-[9,10-d]imidazol-2-yl)phenyl)-2-cyano-acryli acid (**DPPPIPC**) is a molecule in which the electron-donating

1H-phenanthro[9,10-d]imidazole and the electron-accepting 2-cyano-acrylic acid are connected by conjugated spacers. Incorporation of arylamine moieties at 1*H*phenanthro[9,10-d]imidazole was found to retard the charge recombination of the electrons in the conduction band of TiO_2 with the oxidized dyes, possibly through a series of charge separations [16].

In 2014, X. Chen and coworkers reported a 4.11 percent efficiency for DSSC when synthesizing imidazole derivatives using triphenylamine and 2-cyanoacetic acid as acceptor groups and the imidazole unit as the imidazole unit as π- bridge to prepare new 2D-π-A dye 3-(4-((4-(4,5-bis(4-methoxyphenyl)-1H-imidazol-2-yl)phenyl)(phenyl)amino)phenyl)-2-cyanoacrylic acid coded as (**CD-4)** by heated to reflux under a nitrogen atmosphere for 10 h, this dye which exhibited a J_{sc} of 8.60 mA cm^{-2} , V_{oc} of 0.63 V and ff of 0.75 [17].

In 2015, Y. S. Yen and co-worker achieved the highest cell efficiency of 4.97 percent by synthesizing and using a new imidazole-based organic dye 3,3-([2-(9-Hexyl-9H-carbazol-3-yl)-1H-cyanoacrylic Acid) **(TL-5)** with two 2-cyanoacetic acid acceptors/anchors connected at the C-4 and C-5 positions, and a carbazole donor connected at. **(TL-5)** exhibited a J_{sc} of 11.11 mA cm^{-2} , V_{oc} of 0.62 V and ff of 0.72 [18].

In 2020, J. Sivanadanam and co-workers synthesized the dye 2-cyano-3-yl)phenyl)acrylic acid (**4**). They incorporated the imidazole moiety as a -bridge and achieved the maximum power conversion efficiency (PCE) of 7.16 percent, dye 4 having phenanthrene donor and anisole ancillary donor showed maximum power conversion efficiency (PCE) of 7.16% (J_{SC} = 13.07 mA/cm^2 , V_{OC} = 0.831 V, FF = 0.659) [5]. The efficacy of various dyes in DSSCs is shown in Table (1-1).

Table 1-1: The efficiency of DSSCs using the dyes

Code of dye	Structure	Efficiency η%	Ref
DPPPIPC	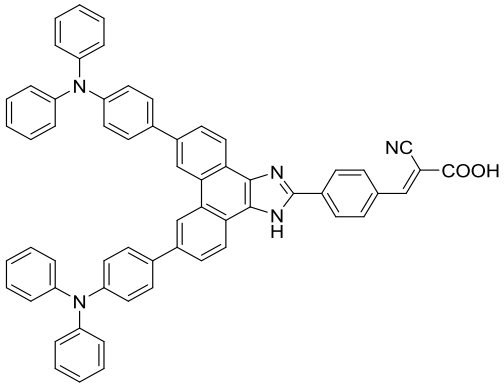	4.68	[17]
CD-4	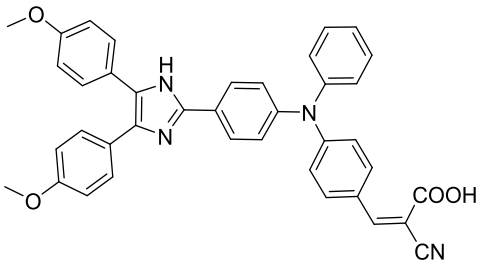	4.11	[18]
TL-5	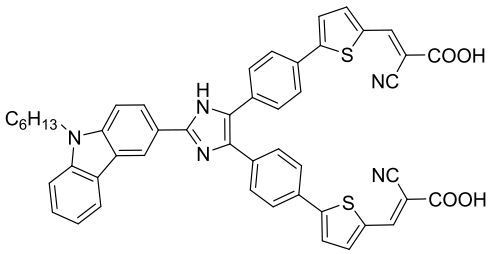	4.97	[19]
2-cyano-3-yl)phenyl)acrylic acid	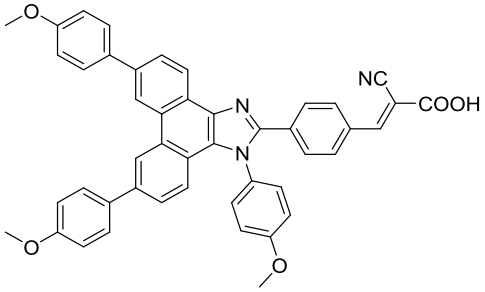	7.16	[6]

1.2. Solar Energy

The Pollution and impressive energy consumption are one of the most critical and greatest challenges of the global today. The major problems of these challenges are related with the health effect, environmental impact, and limitation of resources. For these reasons, the growing global interest in finding alternative energy sources is increased through the last two decade. The supply of clean sustainable energy is considered as one of the most important scientific and technical challenges facing humanity in the 21st century. Renewable energy sources include wind, tidal, thermal, and, most notably, solar cells. These sources have the potential to significantly decrease pollution and its associated consequences on the climate [20].

Generally, the amount of solar energy received by the Earth in a single hour is more than the total energy used by the whole globe in a single year [21] and the solar energy alone has the potential to fulfil the planet's energy needs in the near future. Solar photovoltaic (PV) technology is the most frequently deployed solar energy today which are powered by light, operate at near-ambient temperatures and have no moving components [22] as well as solar energy is an infinite source of energy that is completely free. [23]

1.3. Historical background of the solar cells

The first description of photovoltaic was started in 1839, when the photovoltaic effect was discovered by French physicist Edmond Becquerel through the electrolytic cell. In 1876, the first tests using selenium-based solid-state photocells were conducted in London by Adam and Day. The earliest solar photocells with an efficiency of somewhat more than 1% took more than half a century to build [24]. Solar cells and photovoltaic (PV) modules have been the subject of intense research since the 1950s, when the

first Si-based p/n junction capable of converting sunlight to electrical energy was created. After that, solar photovoltaics entered the modern age in 1954, when Daryl Chapin, Calvin Fuller, and Gerald Pearson of Bell Telephone Laboratories in the United States of America produced the first silicon-based photovoltaic device; initially named a solar battery, the device is now called a solar cell [25]. This device made use of the fundamental p-n junction concepts discovered in the early 1950s with initial energy conversion efficiency of 6% [26]. However, it had increased to 11% by 1957 [27] and 14% by 1960 [28]. Since 1980, the National Renewable Energy Laboratory (NREL, USA) has published an efficiency table for several kinds of solar cells (Fig. 1-6)

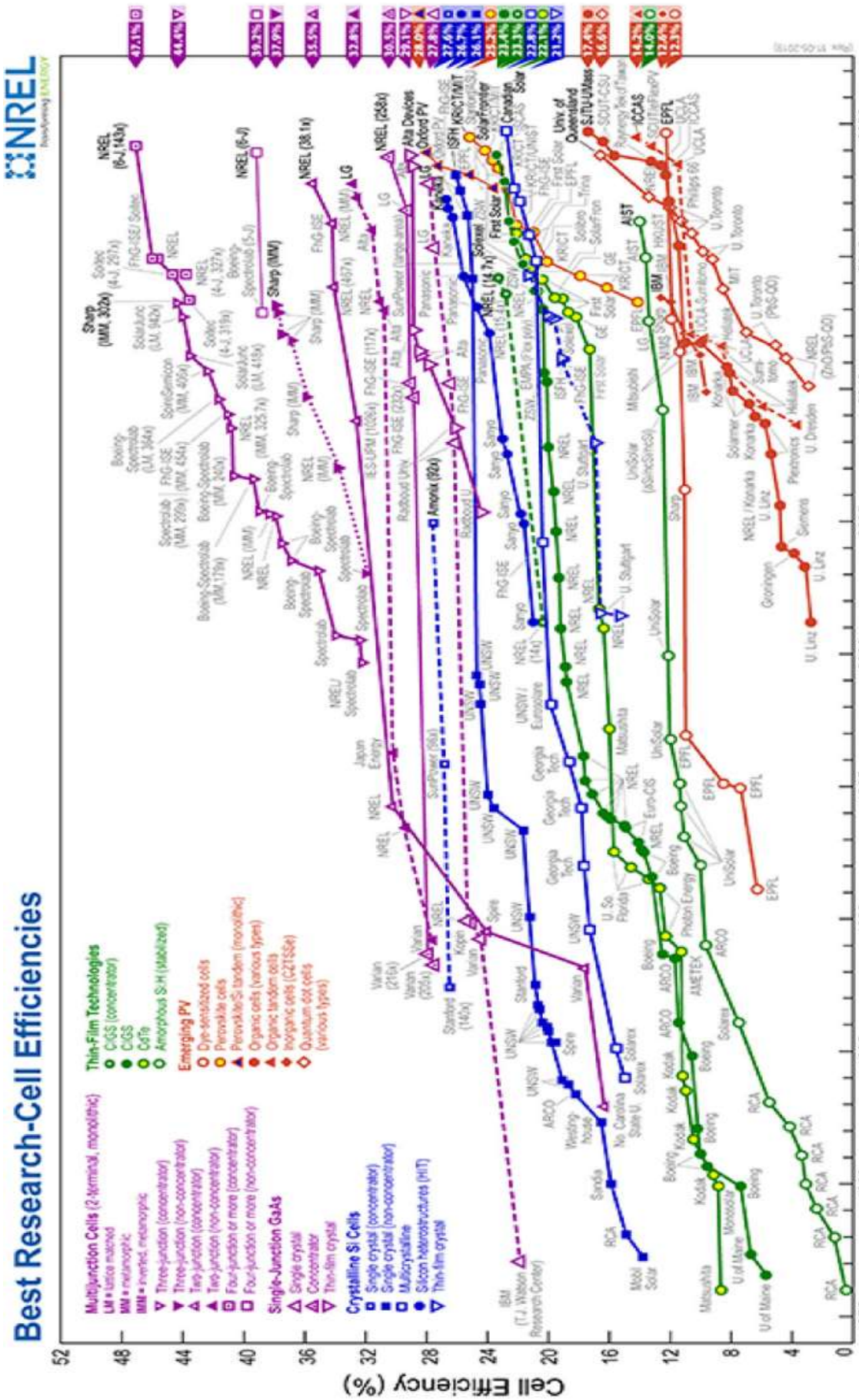

Figure 1-6: Annual efficiency of various photovoltaic solar cells [29].

PV has developed into a variety of uses, including public utility buildings, solar farms, concentrated solar power systems, street lighting, and floating systems. Whereas other kinds of renewable energy have struggled to gain market adoption, rooftop photovoltaic systems have thrived in the residential sector [30].

1.4. Classification of solar cells

Solar PVC technologies have evolved through three generations; based on the manufacturing process and light-absorbing substance employed, they may be further classified into the following categories:

- Crystalline Silicon (Wafer based)
- Thin Film
- Emerging thin films

1.4.1 First-Generation-Wafer based Solar Cells

As previously stated, the first generation of solar cells are fabricated on silicon wafers. It is the most widely and used oldest technology because to its high energy efficiency ~27%. The silicon wafer-based technology is further subdivided into two subcategories, indicated by the abbreviations (Fig. 1-7) [31-33].

- Single/ Mono-crystalline silicon solar cell.
- Poly/Multi-crystalline silicon solar cell.

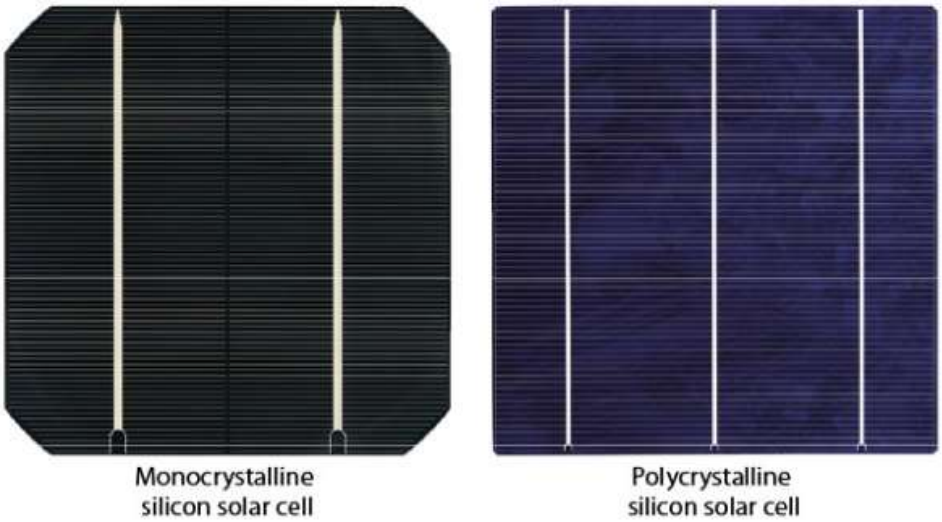

Figure 1-7: Monocrystalline and polycrystalline silicon solar cell

1.4.2 Second Generation - Thin Film Solar Cells

The majority of thin film and a-Si solar cells are second generation solar cells that are more cost effective than first generation silicon wafer solar cells. The light-absorbing layers of silicon wafer solar cells up to 350 μm thick, while thin-film solar cells have light-absorbing layers that are typically less than silicon wafer solar cells thick [32,34]. Thin film solar cells are classified into the following categories (Fig. 1-8):

- A-Si (Amorphous Silicon Thin Film Solar Cell).
- CdTe (Cadmium Telluride Thin Film Solar Cell).
- CIGS (Copper Indium Gallium Di-Selenide Solar Cells).

Figure 1-8: Copper Indium Gallium Selenide Solar Cells Module Market

1.4.3 Third Generation- Emerging Thin Films

Third generation cells are emerging as potential technology, these solar cells are designed to combine between both first and second solar cells. The majority of developed third generation solar cell types are as follows [32,35]:

- Nano crystal based solar cells.
- Polymer based solar cells.
- Dye sensitized solar cells.
- Concentrated solar cells.

Among solar cell technologies, dye-sensitized solar cells (DSSCs) have gained considerable attention owing to their simplicity of manufacturing and ability to achieve modest power conversion efficiency (PCE) [36].

1.5. Dye Sensitized Solar Cells (DSSCs)

Gratzel and his colleagues investigated a new type of solar cell which called DSSCs and was dubbed the Gratzel Cell in honor of its discoverer. In 1991, O'Regan and Gratzel were the first to combine dye based on Ru with TiO_2 and reported as a power conversion efficency 7.1%. Gratzel's group also investigated the cobalt-based electrolyte with a donor-acceptor design, using zinc porphyrin as a sensitizer, and saw an increase in efficiency to 13% in 2014 (Fig. 1-9) [37,38].

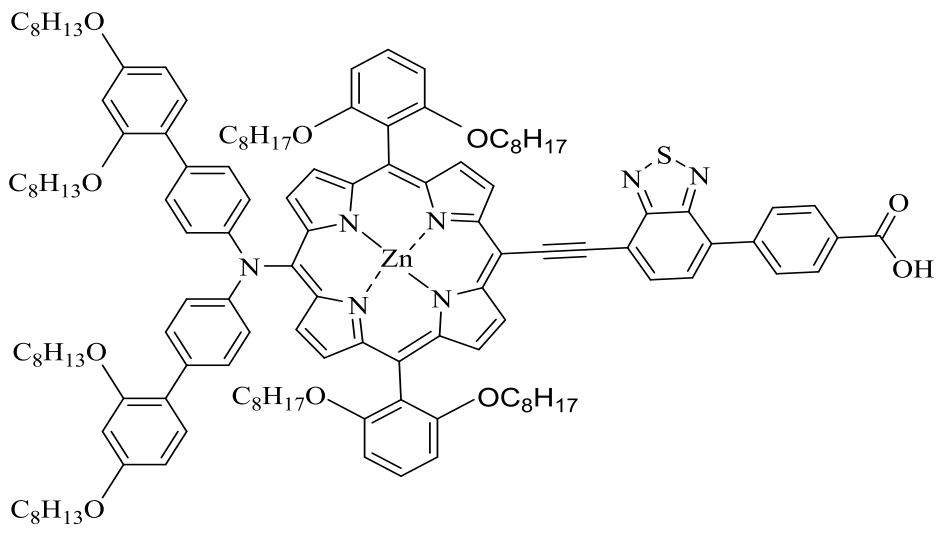

Figure 1-9: Structure of Zinc Porphyrin

Natural and synthetic dyes are employed in the DSSCs, while synthetic dyes are further classified as metal–organic complex and metal-free organic dyes [39]. Metal–organic dyes, such as cis-[Ru (2,2′-bipyridil-4,4′-dicarboxylic acid)$_2$(NCS)$_2$] coded (N3) and (Bu4N)$_2$[Ru(2,2′-bypiridil-4,4′-dicarboxylic acid)$_2$(NCS)$_2$] coded (N719) (Fig. 1-10) are widely used as standard dyes with highest PCEs of 11% and 12%, respectively, that have strong absorption of visible light, chemical nature of light conversion, and stability of excitation states across the full visible light spectrum [40]. On the other hand, metal–organic dyes are hazardous due to the presence of heavy precious metals and are damaging to the environment. Additionally, Ru complex dyes are difficult to produce and costly, which makes them unsuitable for commercialization of DSSCs. As a result, metal-free organic dyes are used instead of metal–organic complex as a sensitizer in the manufacture of DSSCs. Metal-free organic dyes is more affordable and simple to synthesize, however the achieved efficiency is still less than 10% [41].

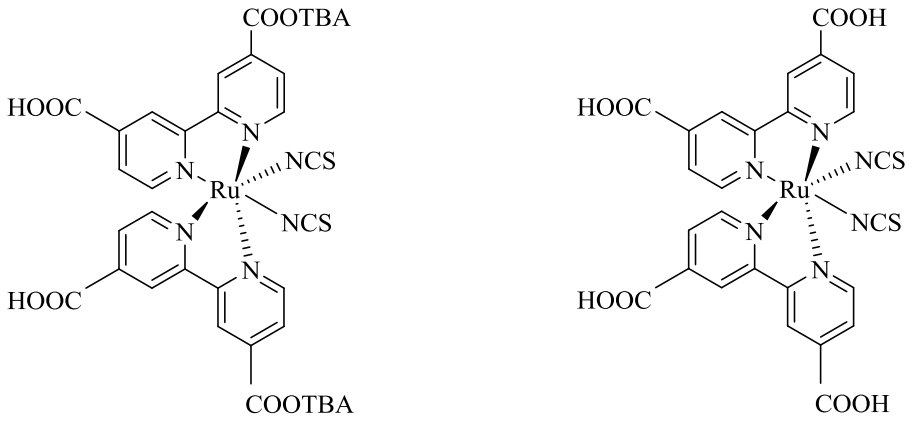

N719 **N3**

Figure 1-10 Structure of N3 and N719

1.5.1 Advantages of DSSCs

1-The materials used to make DSSCs are non-toxic and plentiful.

2- Economical and readily accessible.

3- Environmentally beneficial, since there are no pollutants or noise.

4- Flexibility and portability [42-44].

1.5.2 Materials in DSSCs

A schematic representation the main parts of configuration of a typical dye sensitized solar cell is shown in (Fig.1-11). Typically, a DSSC consists of four components: a photoanode, a photosensitizer (dye), an electrolyte, and a counter electrode. The next sections cover the general characteristics of these components.

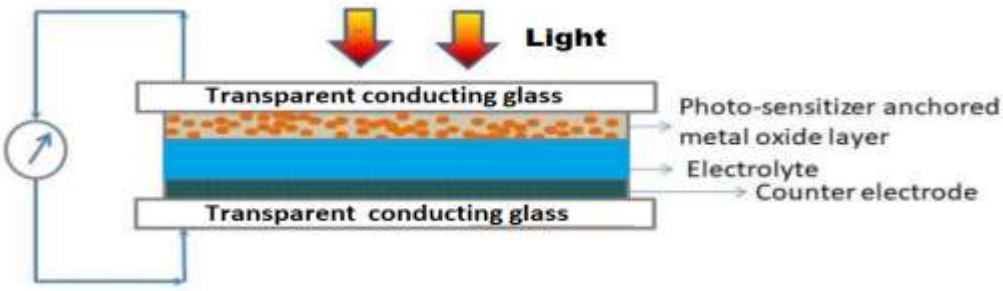

Figure 1-11: Schematic Configuration of a DSSC[45].

1.5.2.1 Photoanode

Photoanode are made from transparent conducting glass substrates which are coated by TiO_2 or ZnO as semiconducting metal oxides (SMOs). Photosensitizer is subsequently adsorbed onto the metal-oxide layer [44]. The transparent conducting glass is used as conductive substrates such as Indium tin oxide (ITO) and Fluorine-doped Tin Oxide (FTO). The properties of transparent conducting glass are represented by the following points.

a) The substrate should be transparent to more than 80% of the light impinging on the cell's effective area.
b) A high electrical conductivity substrate is required for effective charge transfer and low power losses in DSSCs [46].

1.5.2.2 Photosensitizer

Numerous photosensitizers have been tested for DSSCs, including synthetic and natural dyes [47]. Synthetic dyes might be classed as organometallic or organic materials. Organometallic dyes are composed of transition metals, while organic dyes are composed of a variety of organic chromophores.

The dye is often designed around a push-pull structural moiety of the general form D-π-A (Fig. 1-13), where D is an electron donor group connected to an electron acceptor group A through a conjugated moiety (π-bridge) [48]. The electron density moves from the donor region of the dye molecule (where the HOMO is localized) to the electron acceptor section of the dye molecule (where the LUMO is localized) during photoexcitation, resulting in electron injection into the conduction band of the nanocrystal line semiconductor (TiO_2). The sensitization process is highly dependent on the capacity of both the donor and acceptor parts to donate and take electrons, as well as the electrical characteristics of the π-bridge utilized. The π-bridge conjugated component is composed of many chemical groups, including

coumarin, phenoxazine, and oligothiophene, while the donor groups include dialkylamine, diphenylamine, and triphenylamine [49]. Carboxylic acid, Rhodanine-3-acetic acid, and Cyanoacrylic acid moieties are often utilized as anchoring groups on the TiO_2 surface (Fig 1-12) [50-52].

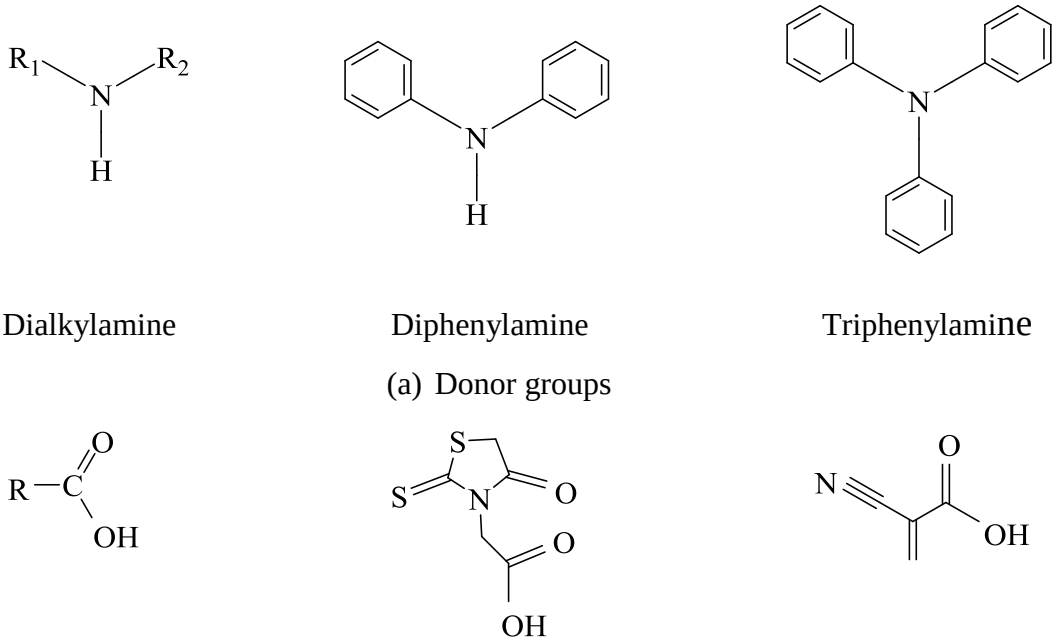

Figure 1-12: Some of donor and accepter groups

The following properties of an effective dye for dye sensitized solar cell applications are proposed.

a) The dye should absorb light throughout the visible and near-infrared spectrums [53].
b) Dye must have a significant affinity for the metal oxides that will be adsorbed on the semiconductor layer. To establish ester bonds with the metal oxide, response groups such as phosphates and carboxylates are added. This excitation of the absorbed photons and electrons to the lowest unoccupied molecular orbital (LUMO) results

in their direct interposition into conduction band (CB) of the metal oxide's.

c) Energy levels of the dye's must be compatible with those of the metal oxide and electrolyte ((LUMO) dye > (CB) metal oxide ;(HOMO) dye > (HOMO) electrolyte) (HOMO stands for highest occupied molecular orbital).

d) Avoid dye aggregation to keep the excited state's nonradioactive decline to the ground state to a minimum [54].

e) The dye must be chemically, thermally, and light stable for an extended length of time, which is now the primary barrier to commercialization [55].

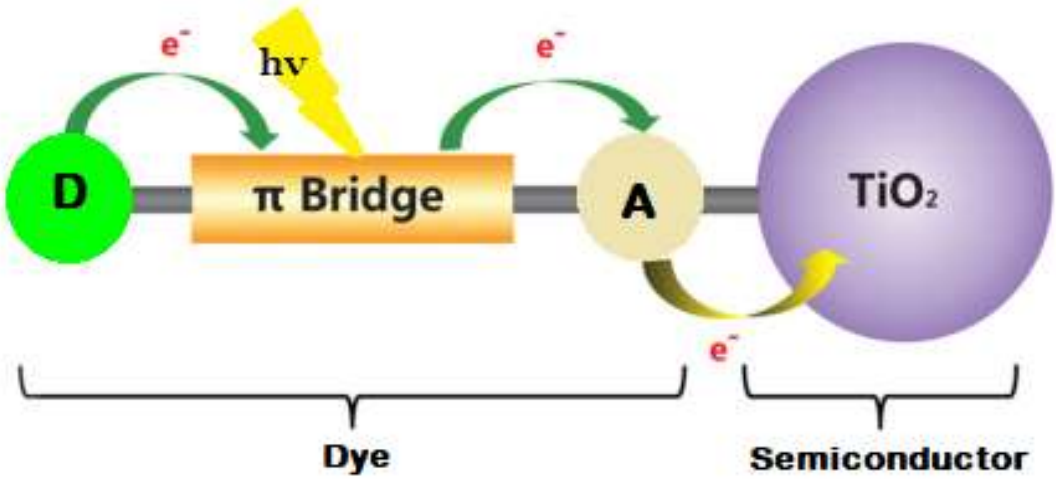

Figure 1-13: Structure of Organic dye[37]

Dye molecules should be attached to the surface of a metal oxide substrate by a variety of methods, including monodentate ester, bidentate chelating, bidentate bridging, and monodentate H-bonding. Due of the close interaction between carboxylate anchor-based dyes and the metal oxide surface, structures with bidentate modes (chelating or bridging) typically

demonstrate more stability than structures with other anchoring modes (Scheme 1-1) [57].

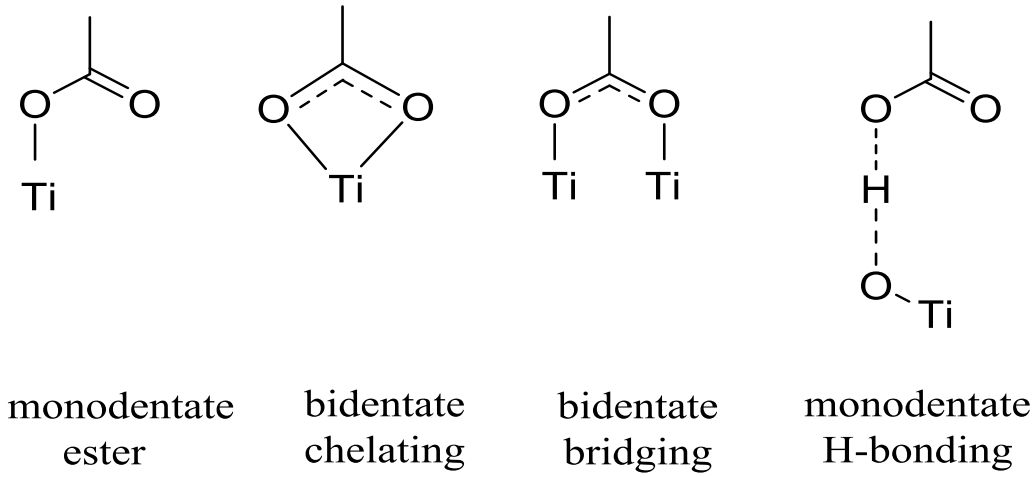

Scheme (1-1): Possible Carboxylic Acid Anchor Binding to TiO_2 [38]

1.5.2.3 Electrolyte

The electrolyte is critical in regenerating the oxidized photosensitizer to its starting condition inside a DSSC. Typically, an electrolyte contains a redox couple, additives, a solvent, cations, and ionic liquids. To be considered as an electrolyte, a prospective substance must possess the following features [58,59].

a) The couple of redox should having the ability of renewing the oxidized dye effectively.
b) The electrolyte used must be stable throughout time.
c) The electrolyte used in the DSSC should be non-corrosive to the other parts in DSSC.
d) It must be allow for rapid charge carrier diffusion between electrodes.
e) The absorption spectra was used of the electrolyte should not interfere with those of the dye [29].

However, the most efficient and least expensive electrolytes continue to be those based on iodide/tri-iodide (I^-/I_3^-) redox couple (liquid-phase) of systems. For DSSCs, the electrolyte system (I^-/I_3^-) demonstrates modest

penetration through SMO films, minimal recombination losses and fast dye regeneration [54].

1.5.2.4 Counter electrode

The counter electrode in DSSCs was flowed electrons from the external circuit and catalyzes the redox electrolyte's operation. To produce the counter electrodes for DSSCs, thin layers of Pt, Ag, or Au are typically deposited to clear conductive glass substrates. However, researchers have developed counter electrodes for DSSCs using low-cost conductive carbonaceous materials [60].

1.4.3 Operation principle of DSSCs

In a DSSC, photocurrent is generated when the dye sensitizer (D) absorbs a photon (from sunlight) and then the photoexcited dye (D*) injects an electron into the CB of TiO_2 [61]. Once the dye sensitizer absorbs sunlight (energy, hv), electrons in the dye molecules are stimulated from the HOMO to the LUMO levels, increasing the probability of LUMO electrons being injected into the CB of TiO_2 (Fig. 1-14). Following that, the injected electrons flow through the network of connected TiO2 nanoparticles to the TCO layer, where they go through the external circuit (load) to the counter electrode (Pt coated glass) [62]. The oxidized dye is then reduced to its neutral state by absorbing one electron from the I^- ions in the redox mediator, resulting in the formation of I_3^-. This process is called dye regeneration or re-reduction. To complete the circuit, electron donation from the external circuit happens at the counter electrode into I_3^- to renew I^- [63,64].

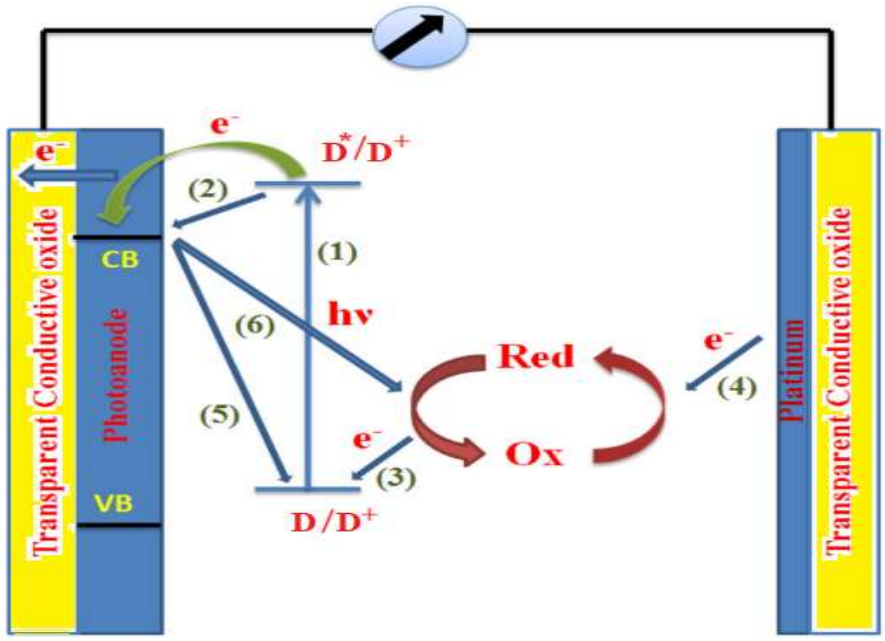

Figure 1-14: A Schematic diagram and operational principle of DSSC where D:dye[64]

This process is summarized as follows [38]:

1) Electron photoexcitation in a dye

D (adsorbed at TiO_2) + $h\upsilon$ → D^*(adsorbed at TiO_2)

2) The injection of electron from the dye into the semiconducting oxide layer's conduction band.

D^*(adsorbed at TiO_2) → D^+ (adsorbed at TiO_2) + e^- (injected at TiO_2)

3) Electron transfer from the semiconducting oxide layer to the TCO substrate

I_3^- + $2e^-$ (cathode) → $3I^-$ (cathode)

4) Electron conduction from the anode to the cathode

$2D^+$ (at TiO_2) + $3I^-$ → $2D$ (at TiO_2) + I_3^-

5) Recombination, electron diffusion from cathode to electrolyte

D^+ (adsorbed at TiO_2) + e^- (TiO_2) → D (adsorbed at TiO_2)

6) Recombination, dye regeneration

I_3^- + $2e^-$ (TiO_2) → $3I^-$ (anode)

1.6 Aim of study

The aim of this study is:

1. Synthesis of six new imidazole derivatives designed according to the D-π-A geometry to be used as dyes in DSSCs.
2. Characterization of the synthesized imidazole derivatives by spectroscopic techniques; FTIR, ^{1}HNMR, ^{13}CNMR and Mass spectroscopy.
3. Investigating the efficiency of these dyes by their application in dye sensitized solar cells.

Chapter two

Experimental

2.1. Chemicals and Techniques

2.1.1 Chemicals

All reagents and solvents were purchased from Merck, BDH, Sigma-Aldrich, and Fluka chemical companies and used without further purification.

2.1.2 Techniques

1. Thin layer chromatography (TLC) (silica gel plates 60 F254, 0.2 mm) was used to monitor the reactions by using UV light (ware length = 254 nm).
2. Melting points were determined using a capillary melting apparatus, Electro thermal Stuart SMP 30.
3. Infrared spectra were acquired at the University of Kerbala, College of Science, Department of Chemistry using a SHIMADZU FTIR-8400S Infrared Spectrophotometer.
4. λ_{max} was determined using a UV spectrophotometer SHIMADZU (UV 1800) at the University of Kerbala's College of Science.
5. ^{1}H NMR and ^{13}C NMR were carried out on Bruker Avance III 400 and recorded at 400 MHz and 100 MHz spectra, respectively, University of Tehran, Central Laboratory.
6. Mass spectrometry was obtained on a Bruker (Micro ToF QII), University of Tehran, Central Laboratory.
7. Elemental analysis was recorded on a Horeaus (CHN Rapid analyzer), College of Education for Pure Science (Ibn Al-Haitham).
8. The performances of the solar cells are investigated by SMU unit, Ketly 2450 (simulator), and all dyes were measured under standard condition AM 1.5 at 100 mW cm^{-2}, University of Nahrain, Nanorenewable Energy Research Center.

2.2 Synthesis of imidazoles derivatives

2.2.1 Synthesis of 2,4,5-trisubstituted imidazole [4-(4,5-diphenyl-1*H*-imidazole-2-yl) benzoic acid] (PP1)

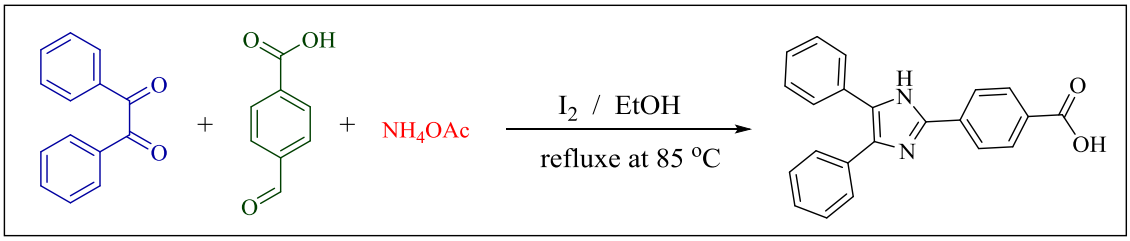

Equation 2-1: Synthetic pathway of PP1 compound

1.05g (5 mmol) benzil, 0.75 g (5 mmol) terephthalaldehydic acid, 0.77 g (10 mmol) ammonium acetate, and 0.127 g (0.5 mmol) iodine were dissolved in 7 mL of ethanol and stirred at 85°C for 11 hrs. The completion of reaction was monitored by TLC and the eluent was (n-hexane/EtOAc, 9:1). After the reaction was completed, the reaction mixture was treated with a solution of $Na_2S_2O_3$ (5%). After filtering, the crud mixture was washed with diethyl ether and dichloromethane to remove unreacted aldehyde and benzil. Finally, using hot ethanol, the product was recrystallized to produce a pale yellow powder product with 76% as a yield, m.p 264–266℃ [64-66]. FTIR (v, cm^{-1}): N-H (3356), O-H (2400-3200), C=O (1689), C=N (1606). ^1H NMR δ, 400 MHz, DMSO-d_6: 12.99 (s, 1H, O-H), 10.09 (s, 1H, N-H), 8.22 (d, J= 8.0 Hz, 2H, Ar-H), 8.14 (d, J = 8.0 Hz, 2H, Ar-H), 8.06 (d, J = 8.0 Hz, 4H, Ar-H), 8.02-7.38 (m, 6H, Ar-H),). ^{13}C NMR δ, 101 MHz, DMSO-d_6: 193.0, 167.57, 166.73, 144.57, 138.81, 136.11, 134.12, 130.09, 129.96, 129.89, 129.56, 128.51, 125.07. MS (EI, m/z): calcd. for $C_{22}H_{16}N_2O_2$: 340.1, found 340.3. Elemental analysis, calcud (CHN): C, 77.63; H, 4.74; N, 8.23, found: C, 77.21; H, 4.62; N, 8.22.

2.2.2 Synthesis of 1,2,4,5-tetrasubstituted imidazole

2.2.2.1 Synthesis of 4-[1-(4-nitrophenyl)-4,5-diphenyl-1*H*-imidazol-2-benzoic acid] (PP2)

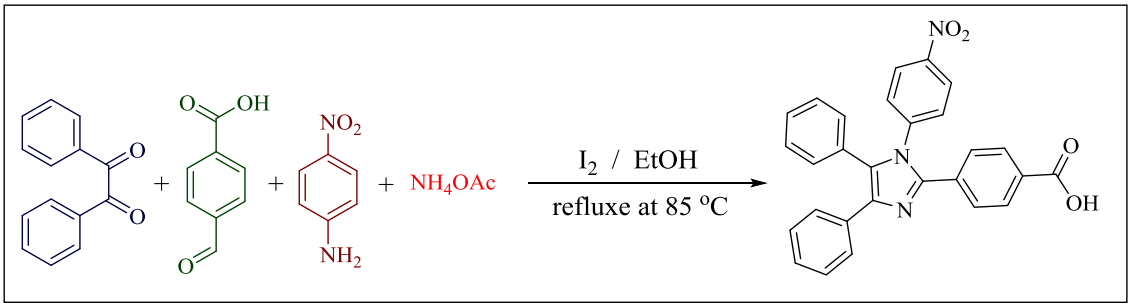

Equation 2-2: Synthetic pathway of PP2 compound

1.05 g (5 mmol) benzil, 0.75 g (5 mmol) terephthalaldehydic acid, 0.385 g (5 mmol) ammonium acetate, 0.69 g (5 mmol) 4-nitroaniline and 0.127 g (0.5 mmol) iodine were dissolved in 7 mL of ethanol and stirred at 85°C for 11 hrs. The completion of reaction was monitored by TLC and the eluent was (n-hexane/EtOAc, 9:1). After the reaction was completed, the reaction mixture was treated with a solution of $Na_2S_2O_3$ (5%). After filtering, the crud mixture was washed with diethyl ether and dichloromethane to remove unreacted aldehyde and benzil. Finally, using hot ethanol, the product was recrystallized. The yield is 70%, the color is yellow, and the melting point is 269-271℃ [64-66]. FTIR (ν, cm^{-1}): O-H (2400-3500), C=O (1687), C=N (1600), NO_2 (1535 and 1392). ^{1}H NMR δ, 400 MHz, DMSO-d_6: 12.97 (s, 1H, O-H), 8.23 (d, J = 8.0 Hz, 2H, ArH), 8.06 (d, J = 8.0 Hz, 2H, Ar-H), 7.56-7.37 (m, 14H, Ar-H). ^{13}C NMR δ, 101 MHz, DMSO-d_6: 192.96, 167.15, 163.12, 157.09, 145.21, 144.59, 138.88, 134.15, 130.06, 129.91, 129.84, 129.58, 129.28, 128.51, 126.47, 125.09, 125.01, 121.99, 112.44, 56.13, 18.63. MS (EI, m/z): calcud. for $C_{28}H_{19}N_3O_4$: 461.1, found 461.3. Elemental analysis, calcud (CHN): C, 72.88; H, 4.15; N, 9.11; found: C, 72.60; H, 4.12; N, 8.98.

2.2.2.2 Synthesis of 4-[1-(2-(diethylamino) ethyl)-4,5-diphenyl-1*H*-imidazol-2-yl] benzoic acid (PP3)

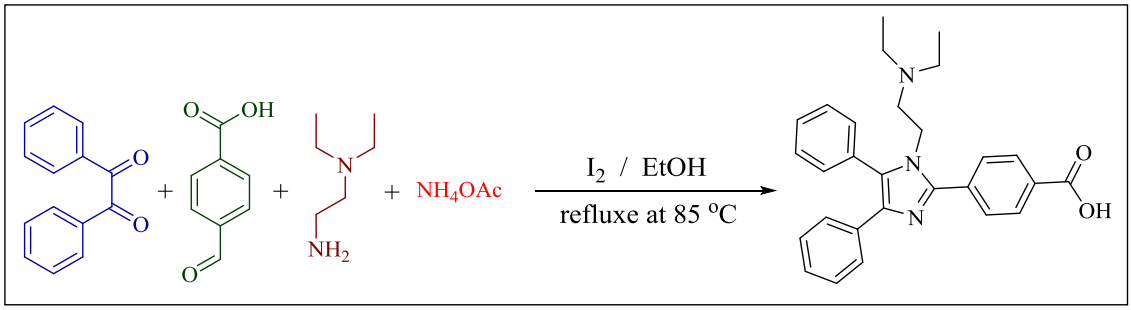

Equation 2-3: Synthetic pathway of PP3 compound

1.05 g (5 mmol) benzil, 0.75 g (5 mmol) terephthalaldehydic acid, 0.385 g (5 mmol) ammonium acetate, 1.4 mL (5 mmol) N^1,N^1-diethylethane-1,2-diamine and 0.127 g (0.5 mmol) iodine were dissolved in 7 mL of ethanol and stirred at 85°C for 11 hrs. The completion of reaction was monitored by TLC and the eluent was (n-hexane/EtOAc, 9:1). After the reaction was completed, the reaction mixture was treated with a solution of $Na_2S_2O_3$ (5%). After filtering, the crud mixture was washed with diethyl ether and dichloromethane to remove unreacted aldehyde and benzil. Finally, using hot ethanol, the product was recrystallized. The yield is 68%, the color is orange, and the melting point is 216-217℃. FTIR (ν, cm^{-1}): O-H (2400-3400), C-H aliphatic (2978), C=O (1682), C=N (1599). ^{1}H NMR δ, 400 MHz, DMSO-d_6: 10.10 (s, 1H, O-H), 8.07 (d, J = 8.0 Hz, 2H, Ar-H), 7.87 (d, J = 8.0 Hz, 2H, Ar-H), 7.57-7.11 (m, 10H, Ar-H), 3.97 (t, J = 8.0 Hz, 2H, -CH_2-), 2.24 (t, J = 8.0 Hz, 2H, -CH_2-), 2.10 (q, J_1 = 16 Hz, J_2 = 8 Hz, 4H, 2 × -CH_2-), 0.55 (t, J = 6.0 Hz, 6H, 2 × -CH_3). ^{13}C NMR δ, 101 MHz, DMSO-d_6: 167.33, 146.23, 136.92, 134.66, 134.50, 130.96, 130.83, 130.37, 129.64, 129.48, 129.22, 129.04, 128.67, 128.12, 126.26, 126.10,51.38, 46.72, 42.99, 11.50. MS (EI, m/z): calcd. for $C_{28}H_{29}N_3O_2$: 439.2, found 439.4. Elemental analysis, calcud (CHN): C, 76.51; H, 6.65; N, 9.56; found: C, 76.45; H, 6.67; N, 9.49

2.2.2.3 Synthesis of 4-(1,4,5-triphenyl-1*H*-imidazol-2-yl)benzoic acid (PP4)

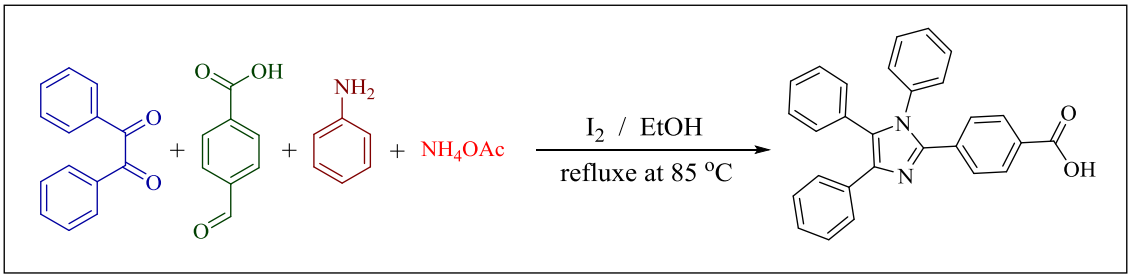

Equation 2-4: Synthetic pathway of PP4 compound

1.05 g (5 mmol) benzil, 0.75 g (5 mmol) terephthalaldehydic acid, 0.385 g (5 mmol) ammonium acetate, aniline 0.456 mL (5 mmol) and 0.127 g (0.5 mmol) iodine were dissolved in 7 mL of ethanol and stirred at 85°C for 11 hrs. The completion of reaction was monitored by TLC and the eluent was (n-hexane/EtOAc, 9:1). After the reaction was completed, the reaction mixture was treated with a solution of $Na_2S_2O_3$ (5%). After filtering, the crud mixture was washed with diethyl ether and dichloromethane to remove unreacted aldehyde and benzil. Finally, using hot ethanol, the product was recrystallized. The yield is 71.5%, the color is dark yellow, and the melting point is 250-252°C. FTIR (ν, cm^{-1}): O-H (2500-3400), C=O (1709), C=N (1606). ^{1}H NMR δ, 400 MHz, DMSO-d_6: 12.96 (s, 1H, O-H), 8.21 (d, J = 8.0 Hz, 2H, Ar-H), 8.04 (d, J = 12.0 Hz, 2H, Ar-H), 7.83 (d, J = 8.0 Hz, 2H, Ar-H), 7.49 (t, J = 10.0 Hz, 3H, Ar-H), 7.36-7.17 (m, 10H, Ar-H). ^{13}C NMR δ, 101 MHz, DMSO-d_6: 166.87, 145.01, 137.35, 136.44, 134.24, 134.18, 132.03, 131.14, 130.24, 130.15, 129.31, 129.14, 128.99, 128.69, 128.58, 128.52, 128.24, 128.14, 126.66, 126.41, 125.04. MS (EI, m/z): calcd. for $C_{28}H_{20}N_2O_2$: 416.1, found 416.3. Elemental analysis, calcud (CHN): C, 80.75; H, 4.84; N, 6.73; found: C, 80.62.45; H, 4.92; N, 6.71.

2.2.2.4 Synthesis of 4-[1-(2-chlorophenyl)-4,5-diphenyl-1*H*-imidazol-2-yl]benzoic acid (PP5)

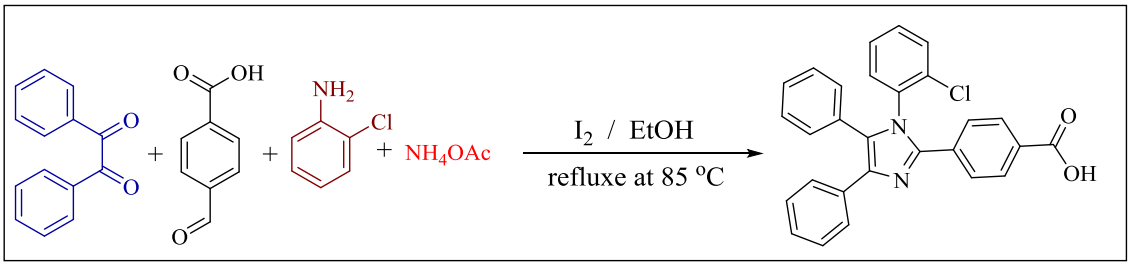

Equation 2-5: Synthetic pathway of PP5 compound

1.05 g (5 mmol) benzil, 0.75 g (5 mmol) terephthalaldehydic acid, 0.385 g (5 mmol) ammonium acetate, 2-chloroaniline 0.525 mL (5 mmol) and 0.127 g (0.5 mmol) iodine were dissolved in 7 mL of ethanol and stirred at 85°C for 11 hrs. The completion of reaction was monitored by TLC and the eluent was (n-hexane/EtOAc, 9:1). After the reaction was completed, the reaction mixture was treated with a solution of $Na_2S_2O_3$ (5%). After filtering, the crud mixture was washed with diethyl ether and dichloromethane to remove unreacted aldehyde and benzil. Finally, using hot ethanol, the product was recrystallized. The yield is 77%, the color is light brown, and the melting point is 220-222 ℃. FTIR (ν, cm^{-1}): O-H (2400-3500), C=O (1701), C=N (1608), C-Cl (771). ^{1}H NMR δ, 400 MHz, DMSO-d_6: 12.96 (s, 1H, O-H), 8.22 (d, J = 8.0 Hz, 2H, Ar-H), 8.14 (d, J = 8.0 Hz, 2H, Ar-H), 8.09-8.00 (m, 2H, Ar-H), 7.93 (d, J = 8.0 Hz, 1H, Ar-H), 7.87 (d, J = 8.0 Hz, 1H, Ar-H), 7.81-7.19 (m, 10H, Ar-H). ^{13}C NMR δ, 101 MHz, DMSO-d_6: 206.55, 194.87, 193.01, 167.11, 166.64, 161.96, 145.10, 144.55, 138.90, 137.57, 135.75, 135.60, 134.14, 133.93, 132.27, 131.90, 131.70, 131.43, 130.72, 130.56, 130.10, 130.01, 129.89, 129.84, 129.66, 129.59, 129.55, 129.38, 129.03, 128.89, 128,63, 128.31, 128.25, 127.51, 126.82, 126.36, 125.07, 120.30, 40.15, 30.74. MS (EI, m/z): calcd. for $C_{28}H_{19}ClN_2O_2$: 450.1, found 450.3. Elemental analysis, calcud (CHN): C, 74.58; H, 4.25; N, 6.21; found: C, 76.01.45; H, 4.12; N, 5.95.

2.2.2.5 Synthesis of 4-[1-(2,4-dichlorophenyl)-4,5-diphenyl-1*H*-imidazol-2-yl]benzoic acid (PP6)

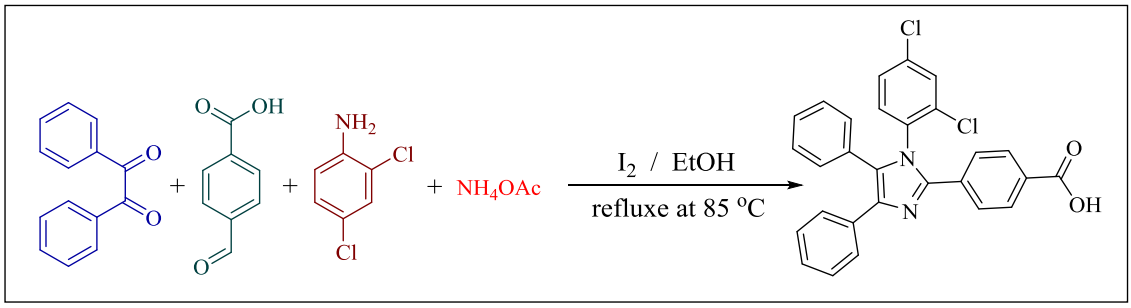

Equation 2-6: Synthetic pathway of PP6 compound

1.05 g (5 mmol) benzil, 0.75 g (5 mmol) terephthalaldehydic acid, 0.385 g (5 mmol) ammonium acetate, 2,4-dichloro aniline 0.81g (5 mmol) and 0.127 g (0.5 mmol) iodine were dissolved in 7 mL of ethanol and stirred at 85°C for 11 hrs. The completion of reaction was monitored by TLC and the eluent was (n-hexane/EtOAc, 9:1). After the reaction was completed, the reaction mixture was treated with a solution of $Na_2S_2O_3$ (5%). After filtering, the crud mixture was washed with diethyl ether and dichloromethane to remove unreacted aldehyde and benzil. Finally, using hot ethanol, the product was recrystallized. The yield is 73%, the color is brown, and the melting point is 234-235℃. FTIR (v, cm^{-1}): O-H (2400-3400), C=O (1680), C=N (1587), C-Cl (707). ^{1}H NMR δ, 400 MHz, DMSO-d_6: 13.25 (s, 1H, O-H), 8.67 (s, 1H, Ar-H), 8.22 (d, J = 8.0 Hz, 2H, Ar-H), 8.11-8.05 (m, 2H, Ar-H), 7.92 (d, J = 4.0 Hz, 1H, Ar-H), 7.78 (t, J = 8.0 Hz, 2H, Ar-H), 7.67-7.18 (m, 8H, Ar-H). ^{13}C NMR δ, 101 MHz, DMSO-d_6: 194.81, 166.87, 162.56, 147.33, 144.54, 142.00, 139.03, 135.54, 134.12, 133.63, 132.25, 130.72, 129.86, 129.81, 129.62, 129.51, 129.17, 129.09, 128.64, 128.28, 125.04, 121.55, 119.69, 118.36, 116.25, 113.37. MS (EI, m/z): calcd. for $C_{28}H_{18}Cl_2N_2O_2$: 484.0, found 484.1. Elemental analysis, calcud (CHN): C, 69.29; H, 3.74; N, 5.77; found: C, 67.82; H, 3.71; N, 6.13.

2.3 Fabrication DSSCs using Doctor Blade's method.

To make the TiO_2 paste, 3.00 mL of ethanol and 0.5 mL of concentrated acetic acid were added to 1.00 g of TiO_2 nanoparticles (10-20 nm). The mixture was sonicated until attained to a white pasty. A conductive glass (ITO) was cleaned twice with absolute ethanol, and then a tape was put on the conducting face of the glass to draw a border of TiO_2 paste and set the paste thickness between 50 and 60 nm. On the conductive surface of ITO, a few drops of TiO_2 paste were placed and flattened using the doctor's blade procedure. The homogeneous TiO_2 layer was annealed at 400 degrees Celsius for 45 minutes on a hot plate and then cooled to room temperature for 15 min. The counter electrode (ITO with TiO_2) was immersed for 2 hours in a solution of manufactured dye (EtOH : THF, 5:1) and then washed with ethanol to remove the aggregate dye. The counter electrode was created by scratching graphite pen on the conducting surface of another ITO glass.

The electrolyte solution was made using a volume ratio of 4:1 of 0.50 M KI, 0.05 M I_2 in ethylene glycol, and acetonitrile. A few drops of the electrolyte solution were applied to the surface of the TiO_2 and then the counter electrode was connected to the working electrode using a binder clip. The produced solar cell was then evaluated using a photon incident beam to determine its efficiency (Fig. 2-1) and (Fig.2-2). [67,68]

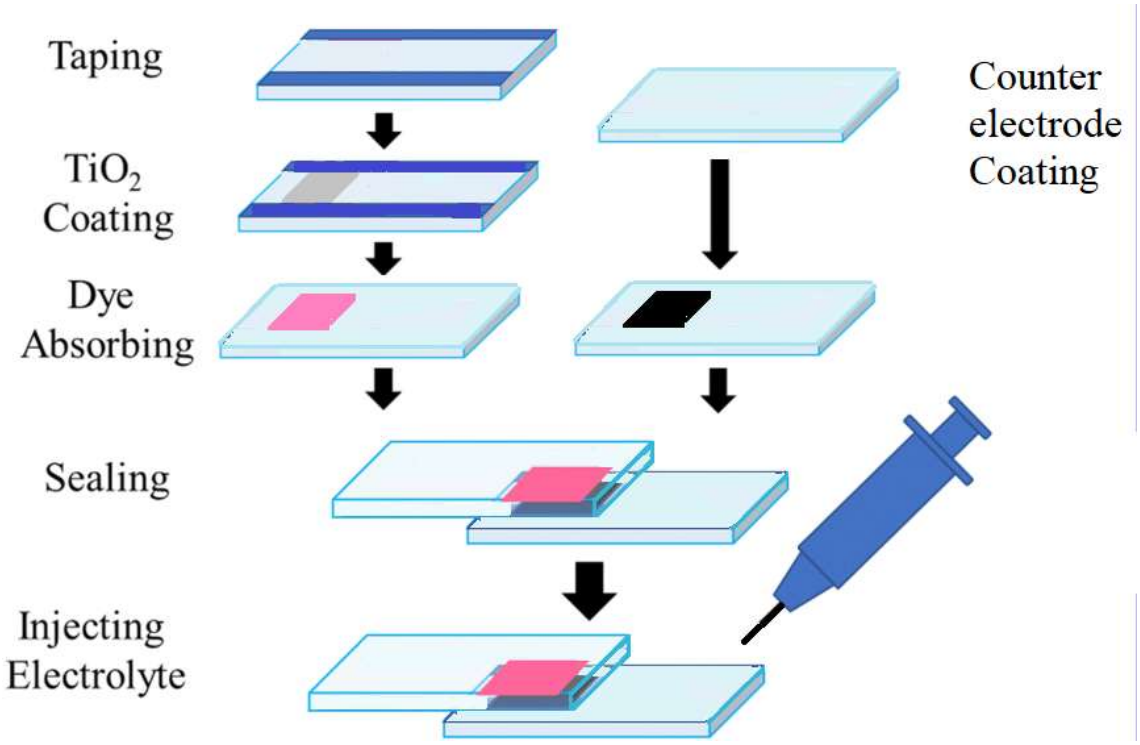

Figure 2-1: Schematic illustration of the dye-sensitized solar cells (DSSCs) assembly[69]

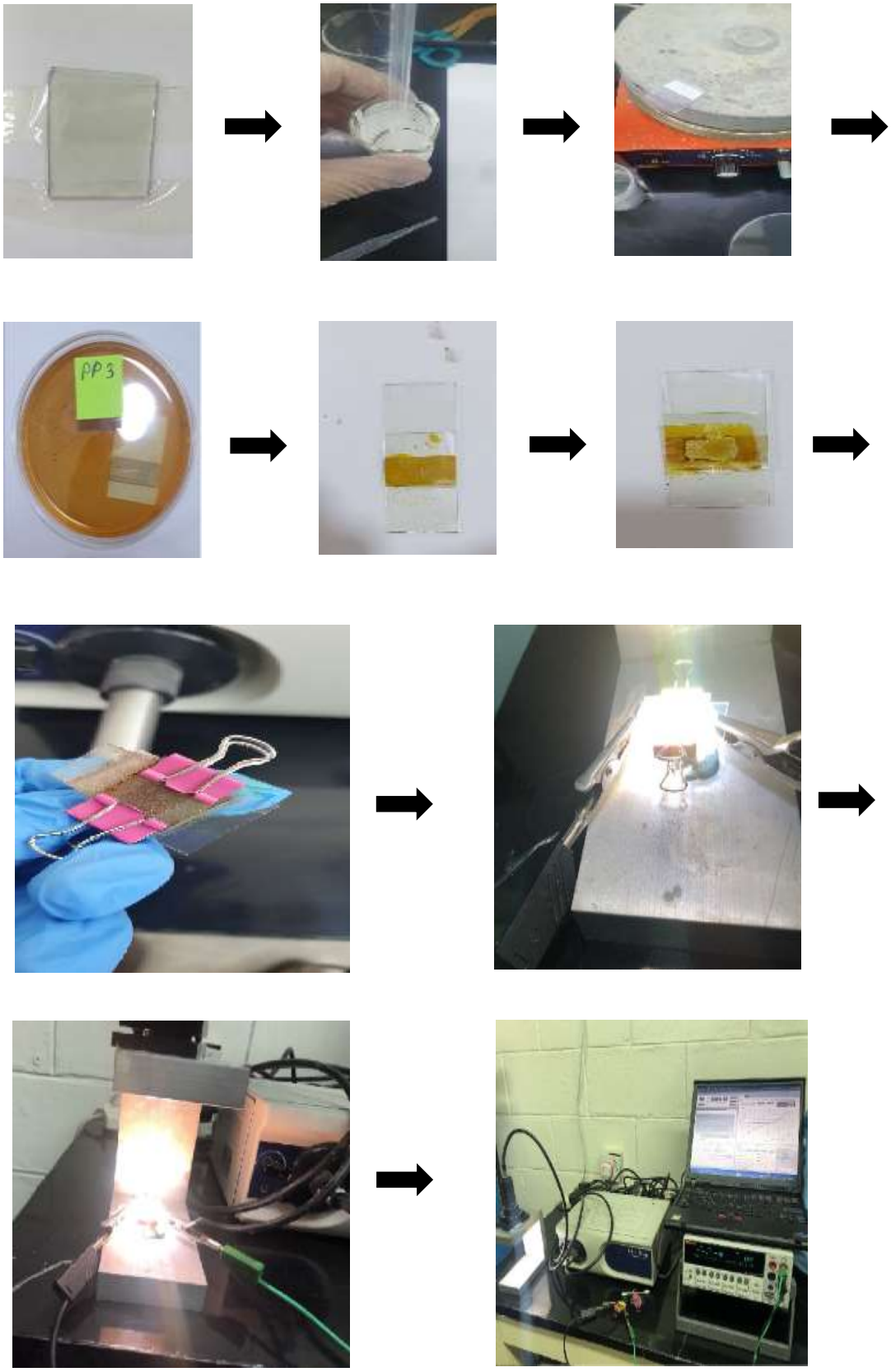

Figure 2-2: Steps of Fabrication DSSCs

Chapter three

Results and Discussion

3.1 General synthesis

Six substituted imidazole derivative dyes were synthesized using a method previously described in the literature [64-66]. The electron-donating and electron-withdrawing groups were employed as substituents on the imidazole by catalyzing the cyclo condensation process between aldehyde and benzil with ammonium acetate and iodine as the catalyst. The reaction was carried out by linkage the iodine molecule to the oxygen in the aldehyde and then increasing the reactivity of the carbonyl group due to The Lewis acidic nature of molecular iodine. Iodine facilitates the creation of a diamine intermediate (A), which condenses further with the carbonyl carbon of 1,2 diketone followed by dehydration afford the intermediate (B), which undergoes sigmatropic rearrangement to give the necessary imidazoles (scheme 3-1) [65,70,71,72]. Purification and characterization of all products were carried out using FTIR, ^{1}H NMR, ^{13}CNMR and Mass spectroscopy. The yields of the synthesized compounds are approximately 70%.

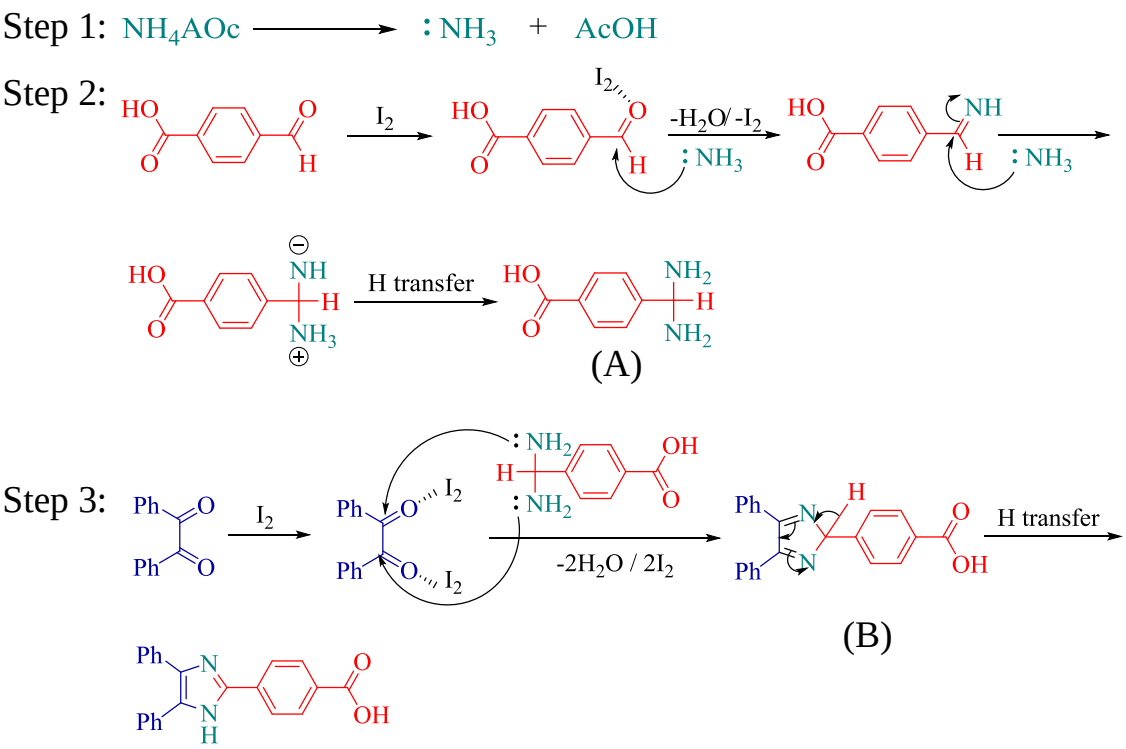

Scheme 3-1: Probable mechanism of synthesis trisubstituted imidazole [65,70-72].

In mechanism of synthesis tetrasubstituted imidazole, the difference is the presence of another nitrogen source (amine group) in addition to the ammonium acetate (scheme 3-2).

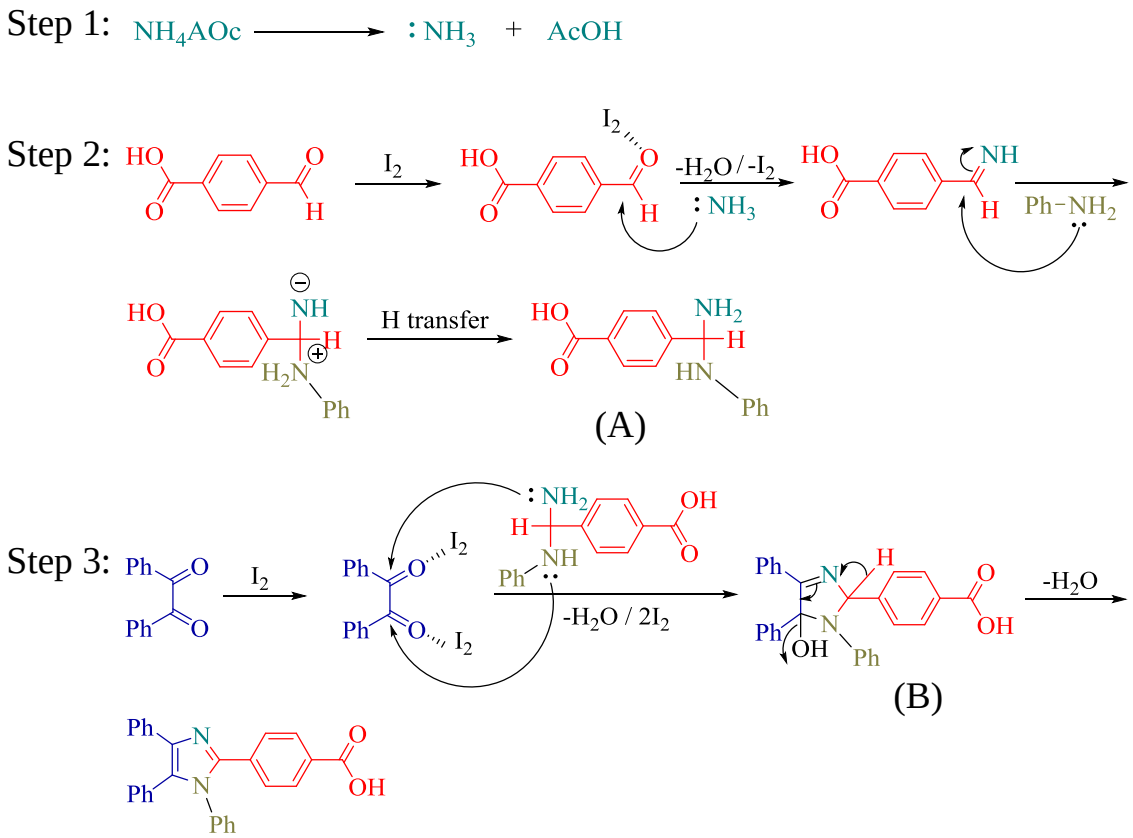

Scheme 3-2: Probable mechanism of synthesis tetrasubstituted imidazole [65,70-72].

3.2 Characterization of the dyes

FTIR spectra of (PP1, PP2, PP3, PP4, PP5 and PP6) (Fig. 3-1 to 3-6) showed a broad absorption band in the range (2400-3500 cm^{-1}) due to the stretching vibrations of the O–H bonds in carboxylic acids. At PP1 appeared one peak at 3356 cm^{-1} (Fig. 3-1) assigned to N–H in imidazole ring but in the other dyes, the peak of N–H was disappeared due to presence of a substituent group on N–H of imidazole ring. The spectra also showed six absorption bands between 1680-1708 cm^{-1} are attributed to the stretching vibration of the C=O bonds for all dyes, which correspond to the C=O in carboxylic acids. Beside that the dyes exhibit absorption bands (1575-1608) cm^{-1}, (1213-1292) cm^{-1} and (3076) cm^{-1} attributed to C=N, C-N bonds stretching in imidazole ring and C-H aromatic respectively. PP2 showed absorption bands at (1535 and 1392 cm^{-1}) (Fig. 3-2) assigned to NO_2 bond stretching and PP3 was appeared absorption bands at 1180 and 2978 cm^{-1} (Fig. 3-3) due to aliphatic amine was substituent on N-H of imidazole ring and C-H aliphatic on the same amine respectively. PP5 and PP6 showed two absorption bands at 771 and 707 cm^{-1} (Fig. 3-5 and 3-6) respectively due to C-Cl bond.

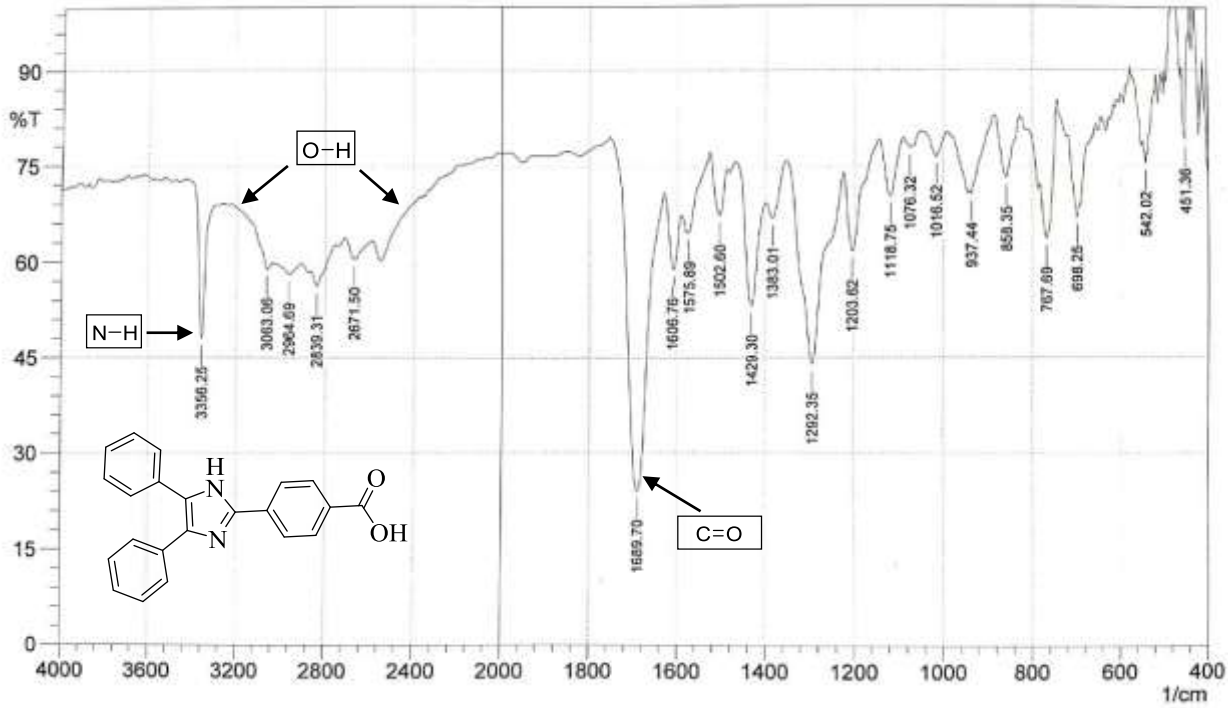

Figure 3-1: FTIR spectrum of (PP1)

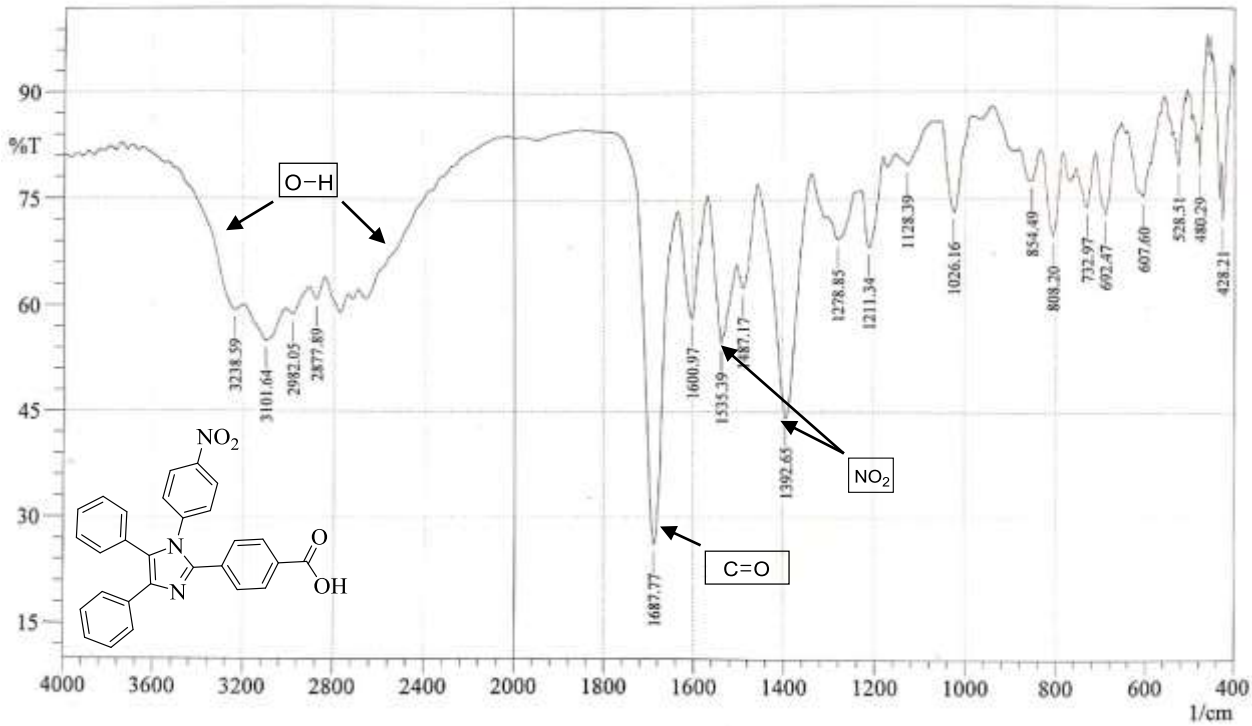

Figure 3-2: FTIR spectrum of (PP2)

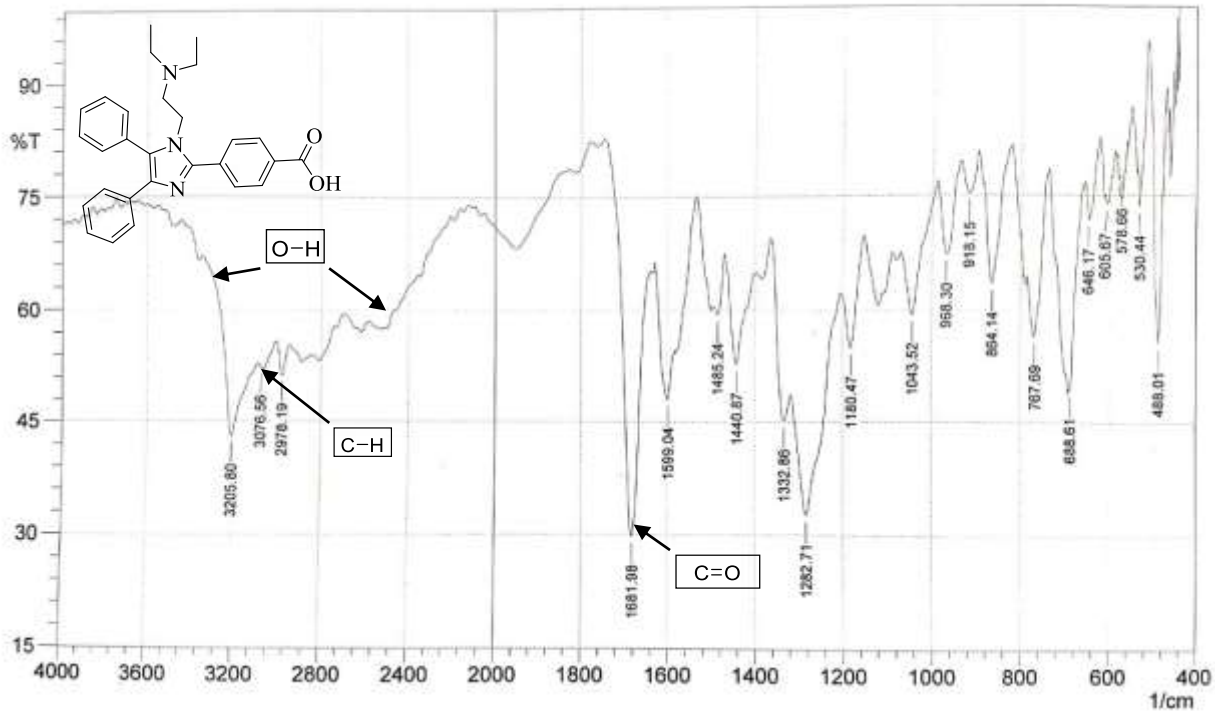

Figure 3-3: FTIR spectrum of (PP3)

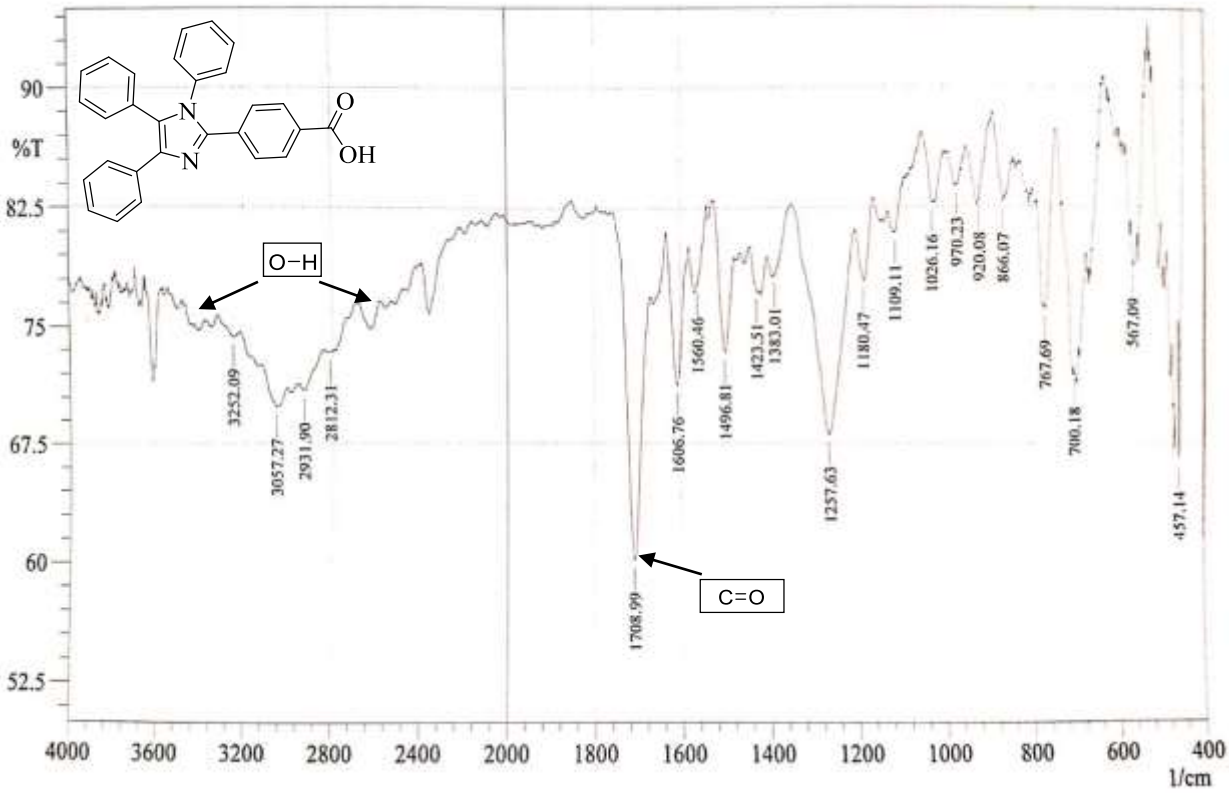

Figure 3-4: FTIR spectrum of (PP4)

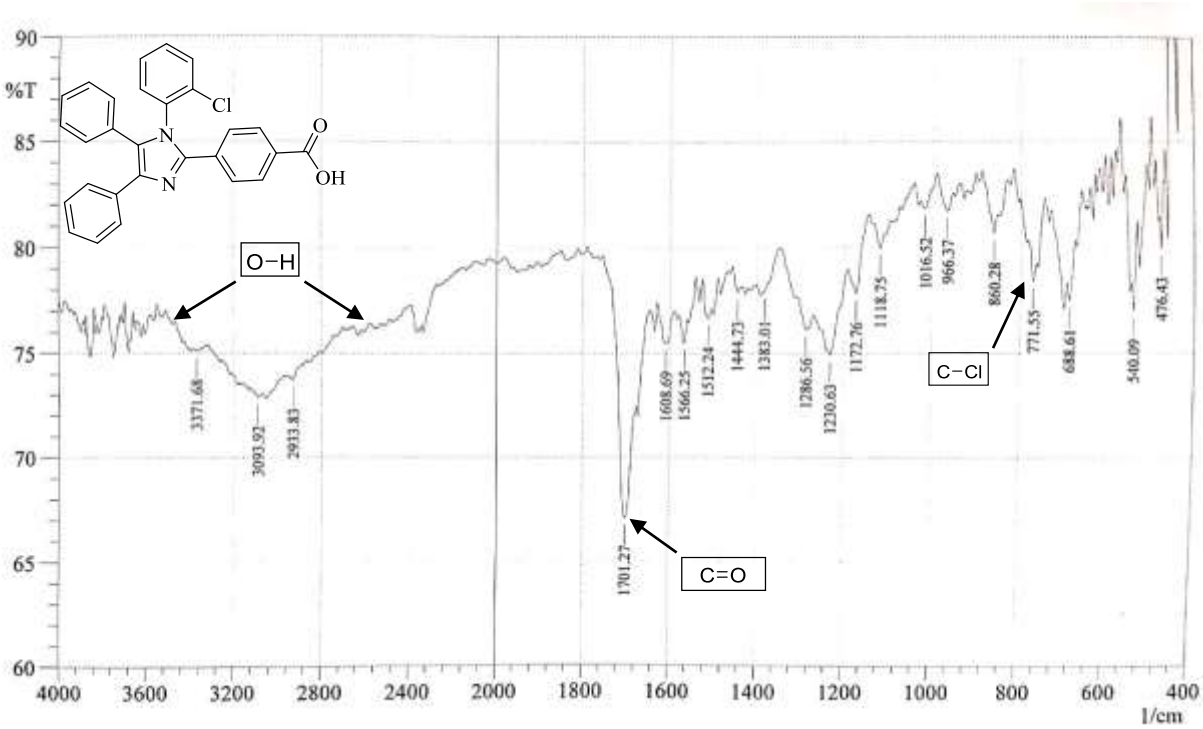

Figure 3-5: FTIR spectrum of (PP5)

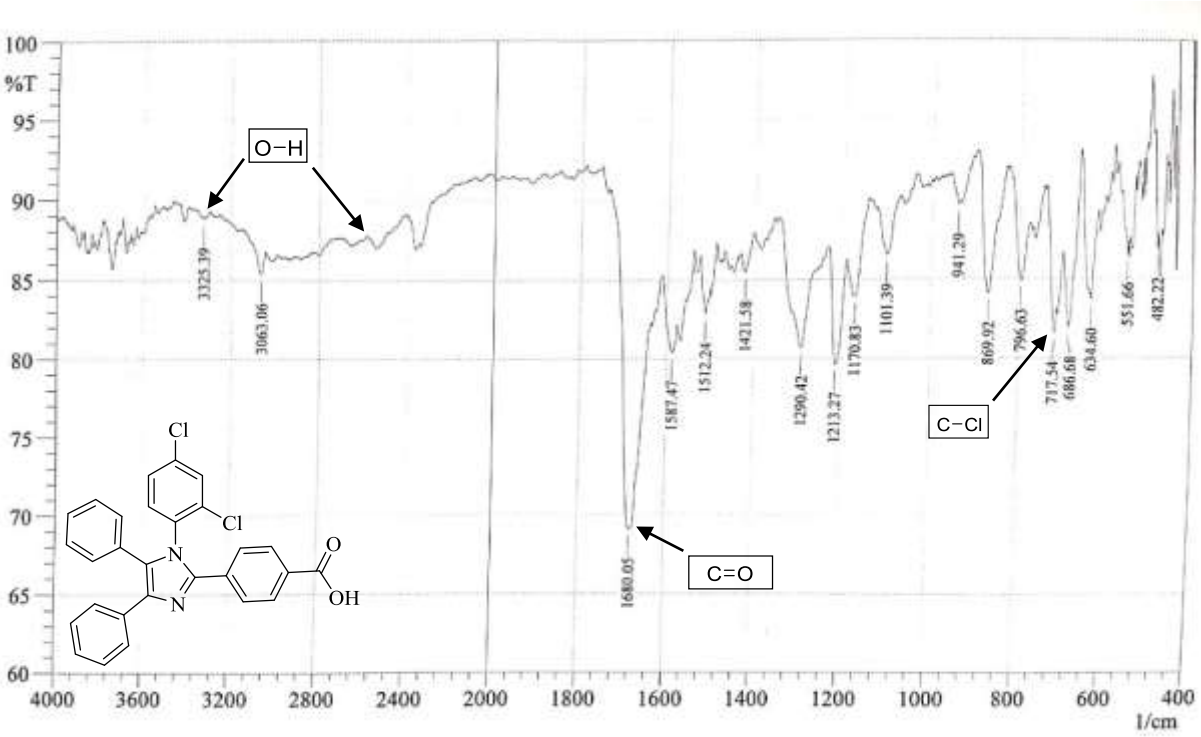

Figure 3-6: FTIR spectrum of (PP6)

^{1}HNMR was also utilized to analyze the structure of the dyes (PP1, PP2, PP3, PP4, PP5 and PP6).The ^{1}HNMR spectrum of PP1 exhibited a singlet signal at 10.1 ppm (Fig. 3-7) assigned to one proton in N-H of imidazole ring while in the other dyes this signal was disappeared due to presence a substituent group on N-H of imidazole ring, so there is no proton on N of imidazole. All the dyes showed a singlet signal at 12.96 - 13.25 ppm (Fig. 3-7 to 3-12) corresponding to proton in carboxylic group except PP3 showed a singlet signal at 10.10 ppm . The PP3 (Fig. 3-9) showed triplet signal at 0.55 ppm of protons (2× -CH_3), quartet at 2.10 ppm of protons (2× -C$\underline{H}_2$-) and triplet at 2.24 ppm of protons (2× -C$\underline{H}_2$-) in aliphatic amine was substituted on imidazole ring. Moreover, the mass spectra of compounds showed molecular ion peaks M+ and M+H at m/z corresponding to their respective calculated molecular masses as shown in (Table 3-1) with some physical properties of the dyes was synthesized.

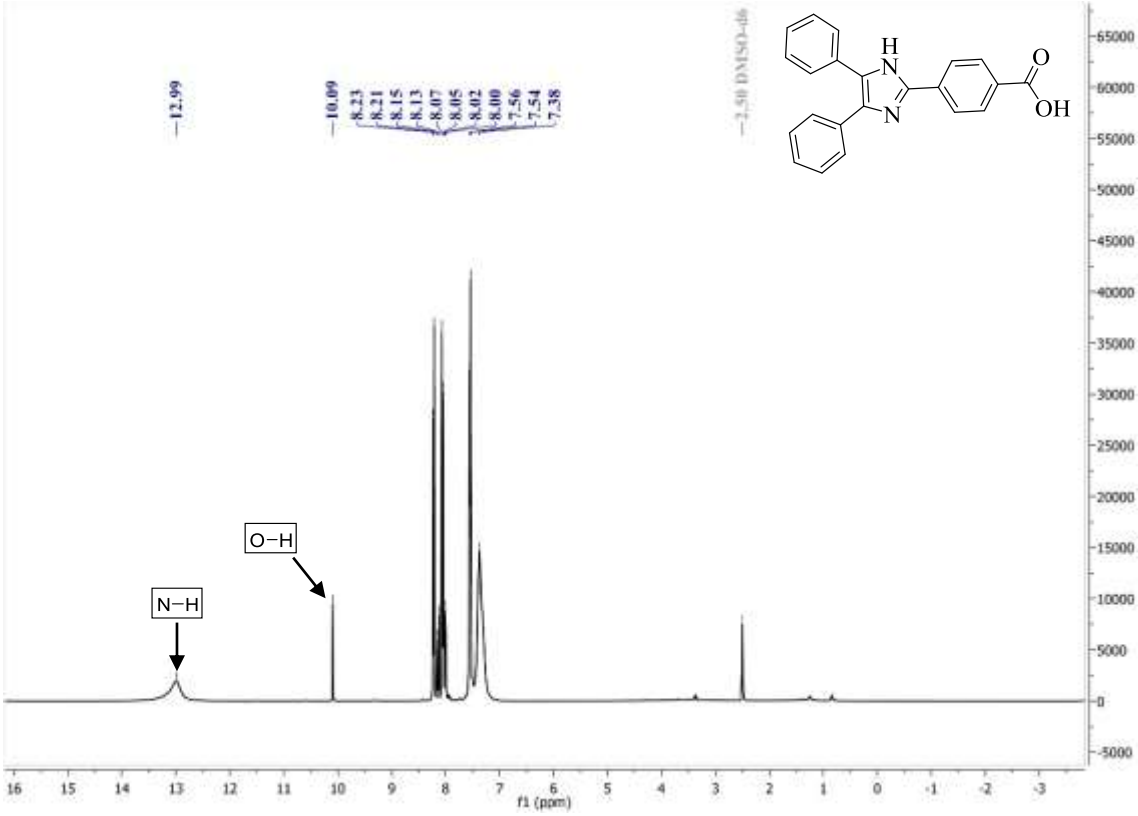

Figure 3-7:^{1}HNMR spectrum of (PP1)

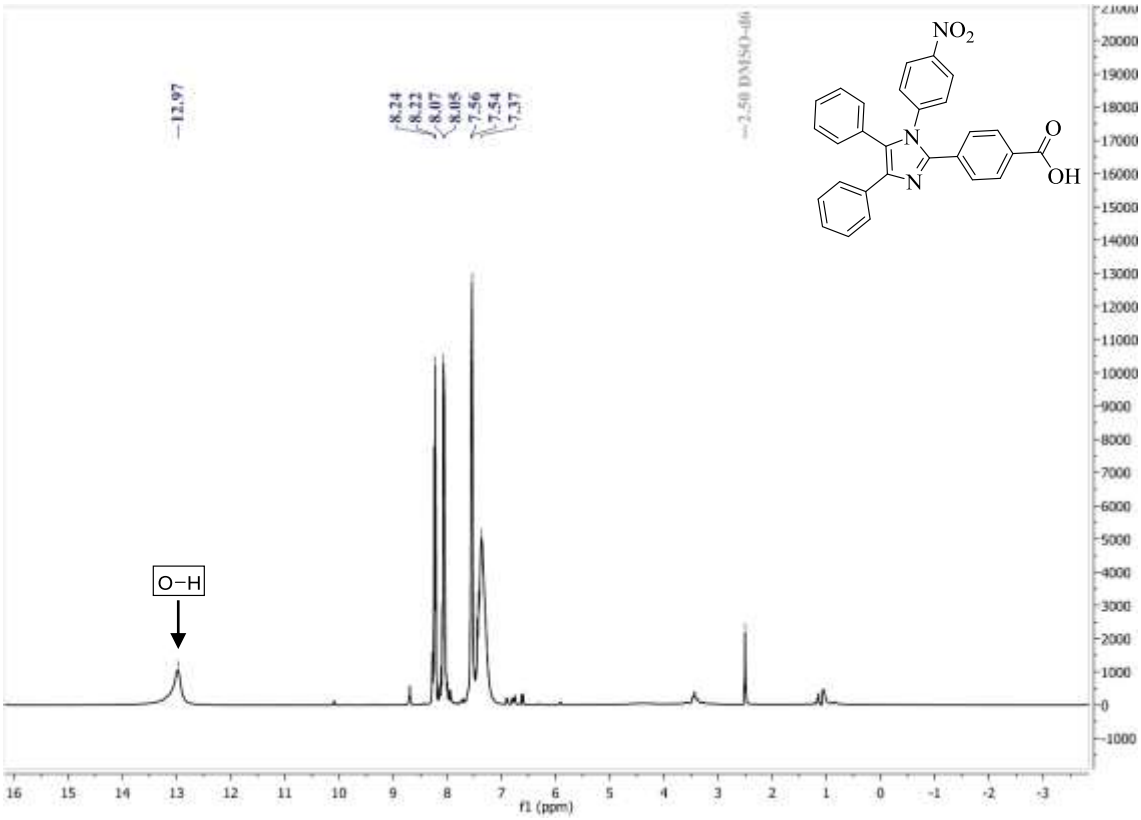

Figure 3-8:^{1}HNMR spectrum of (PP2)

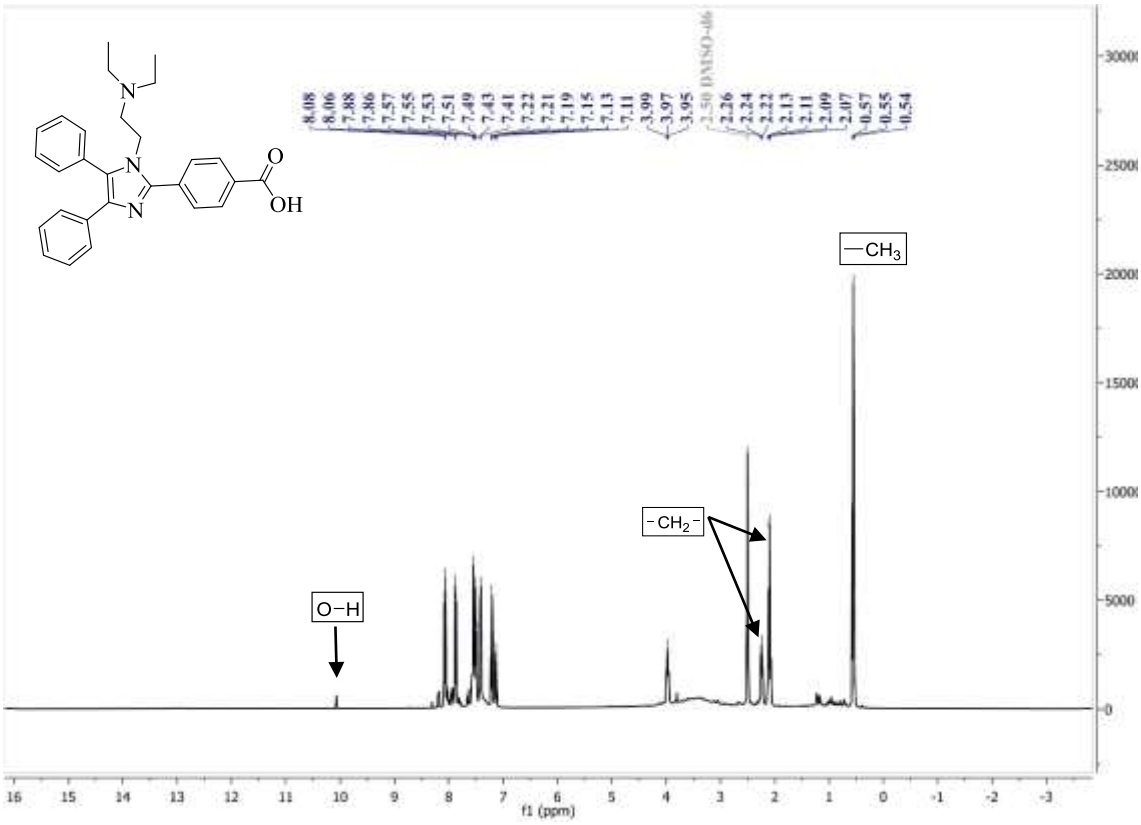

Figure 3-9:^{1}HNMR spectrum of (PP3)

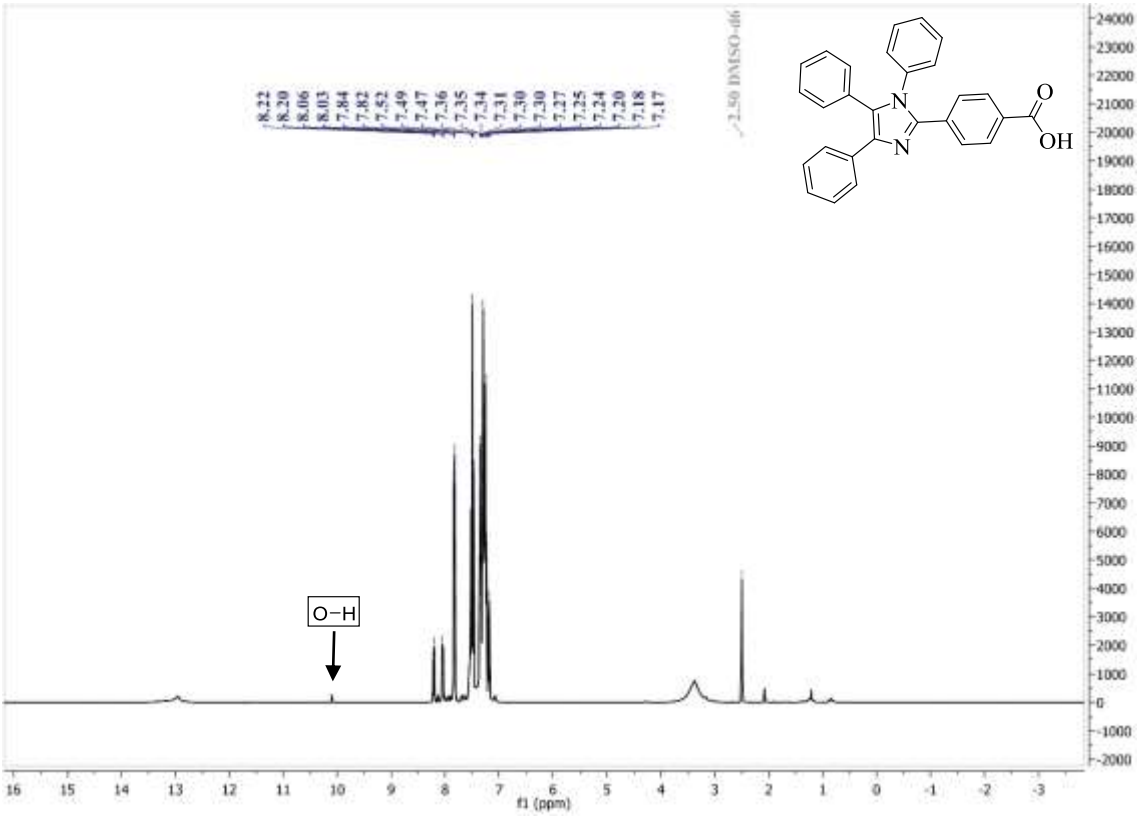

Figure 3-10:^{1}HNMR spectrum of (PP4)

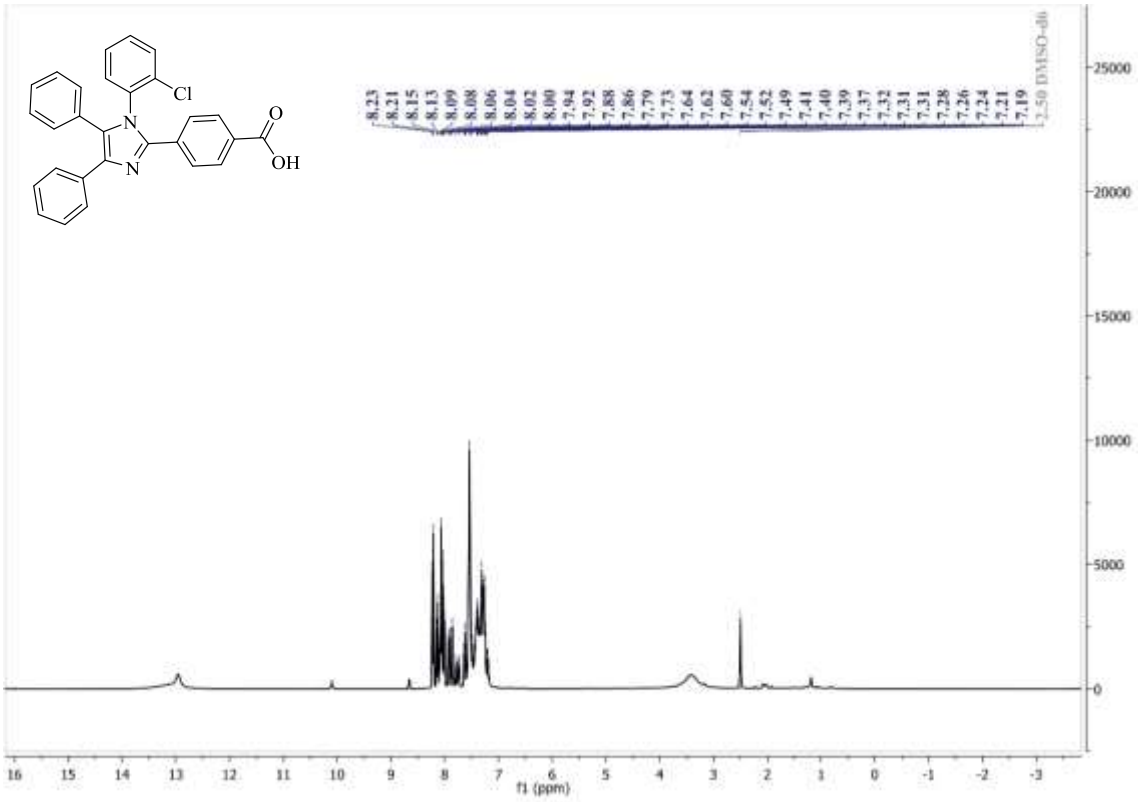

Figure 3-11:^{1}HNMR spectrum of (PP5)

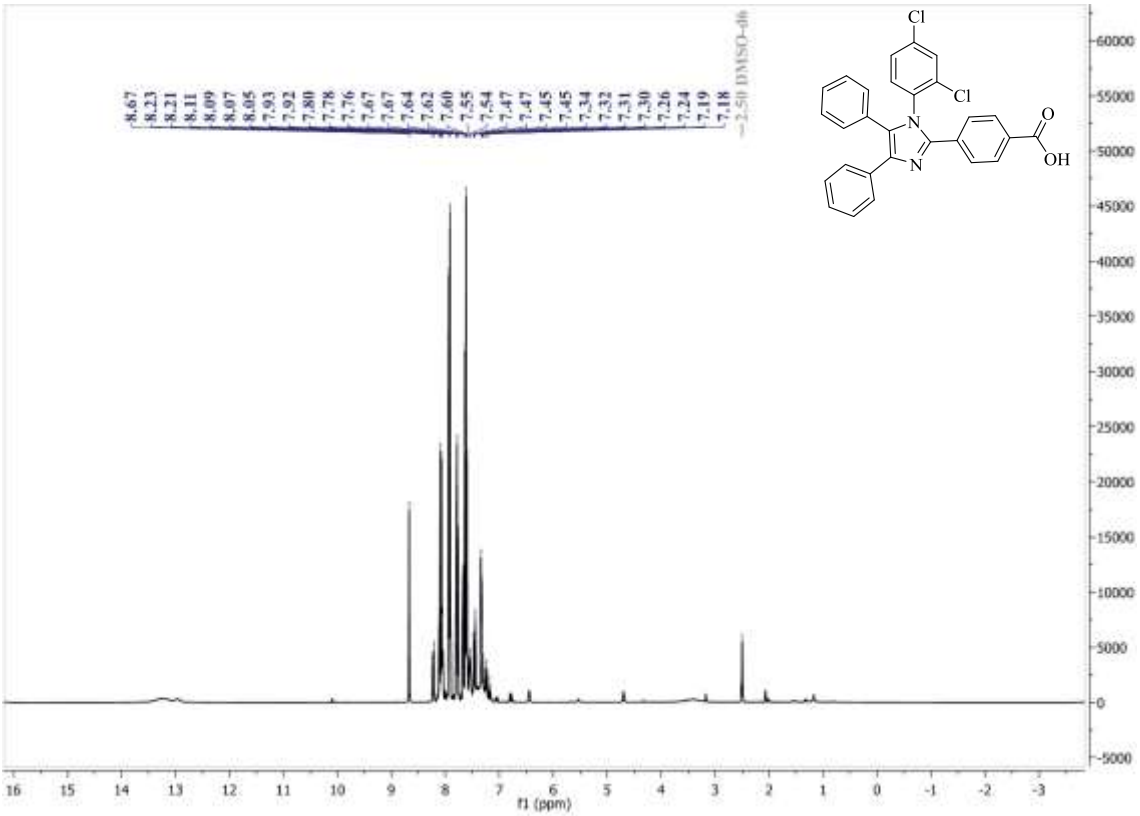

Figure 3-12:^{1}HNMR spectrum of (PP6)

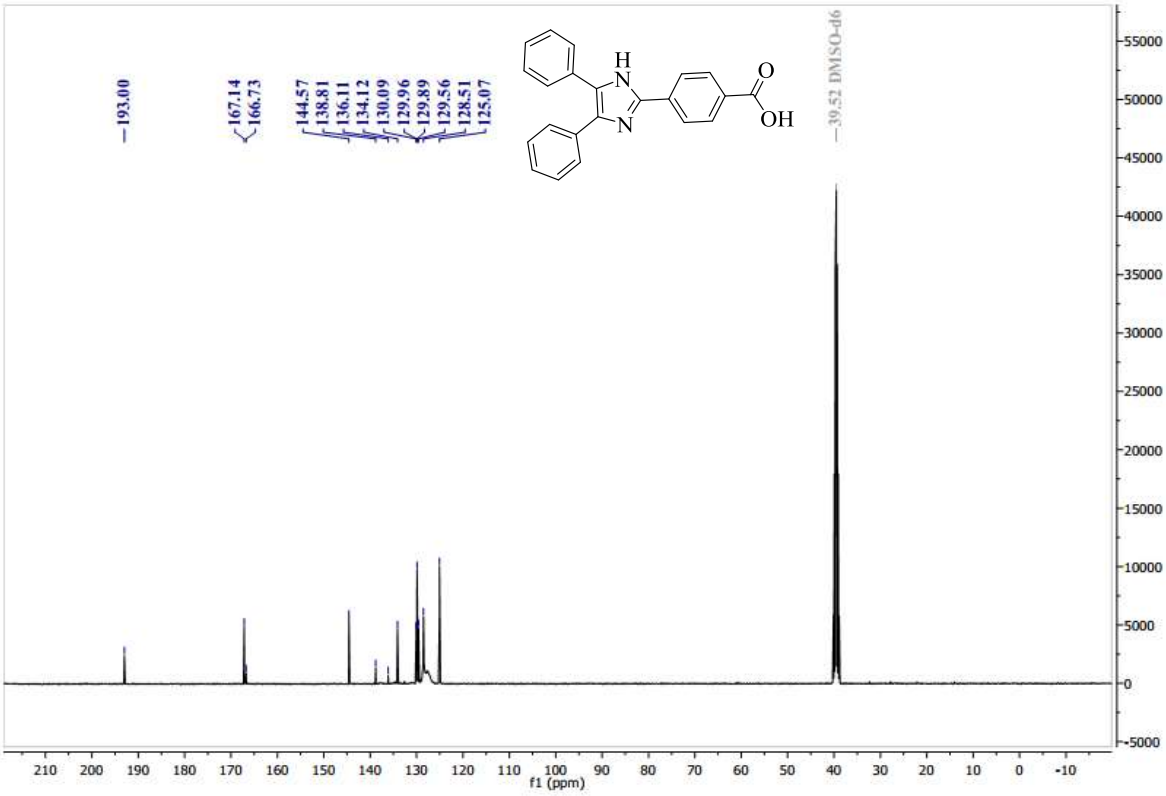

Figure 3-13: ^{13}C NMR spectrum of (PP1)

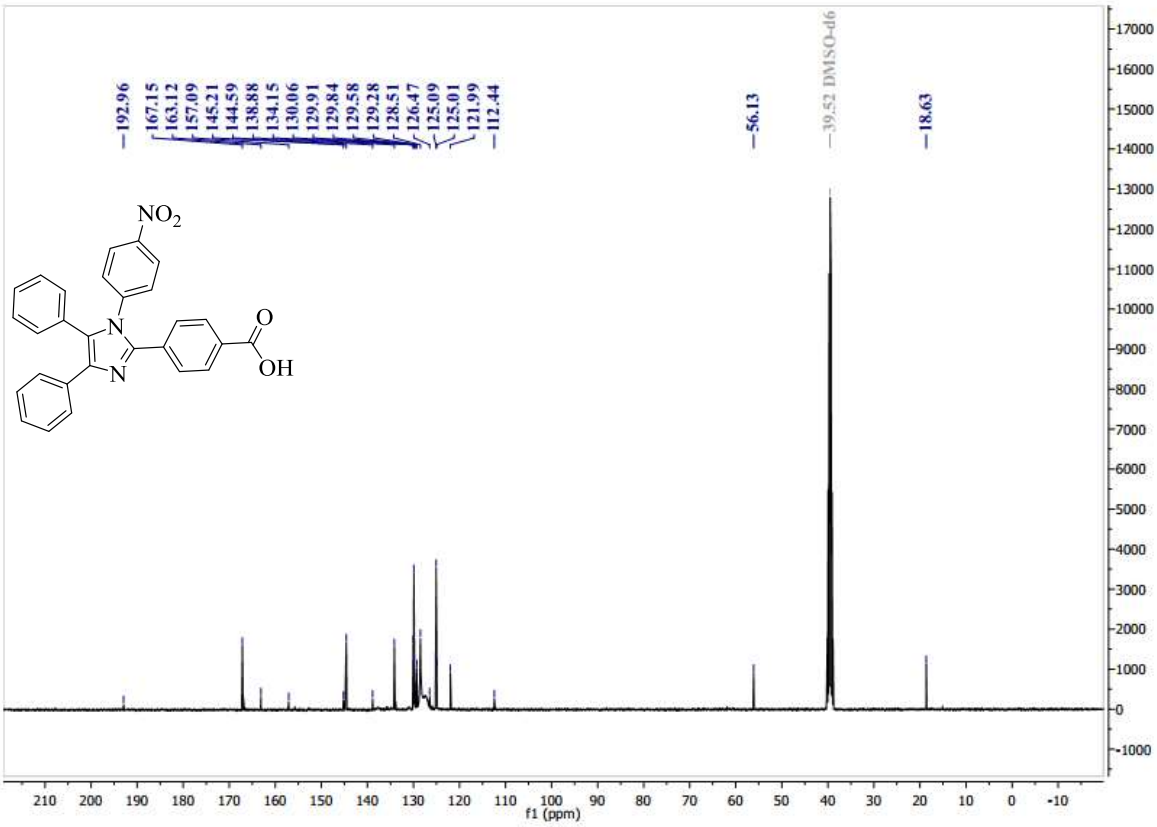

Figure 3-14: ^{13}C NMR spectrum of (PP2)

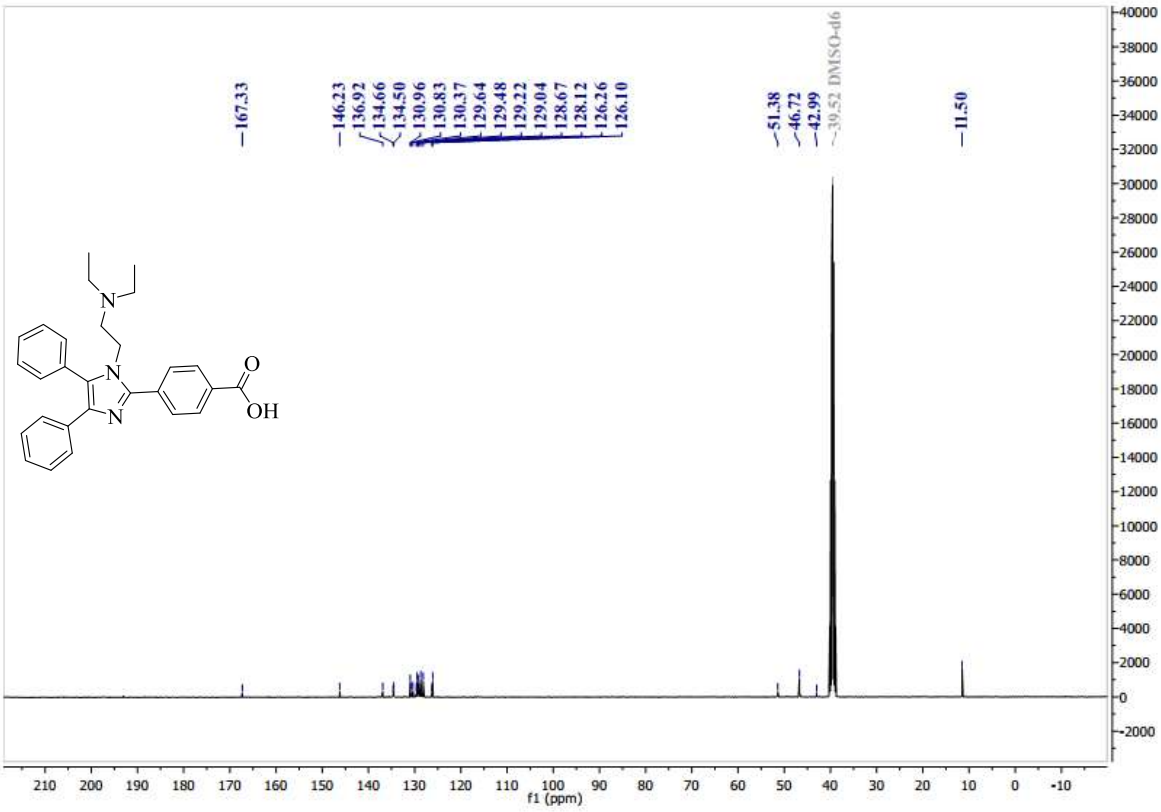

Figure 3-15: ^{13}C NMR spectrum of (PP3)

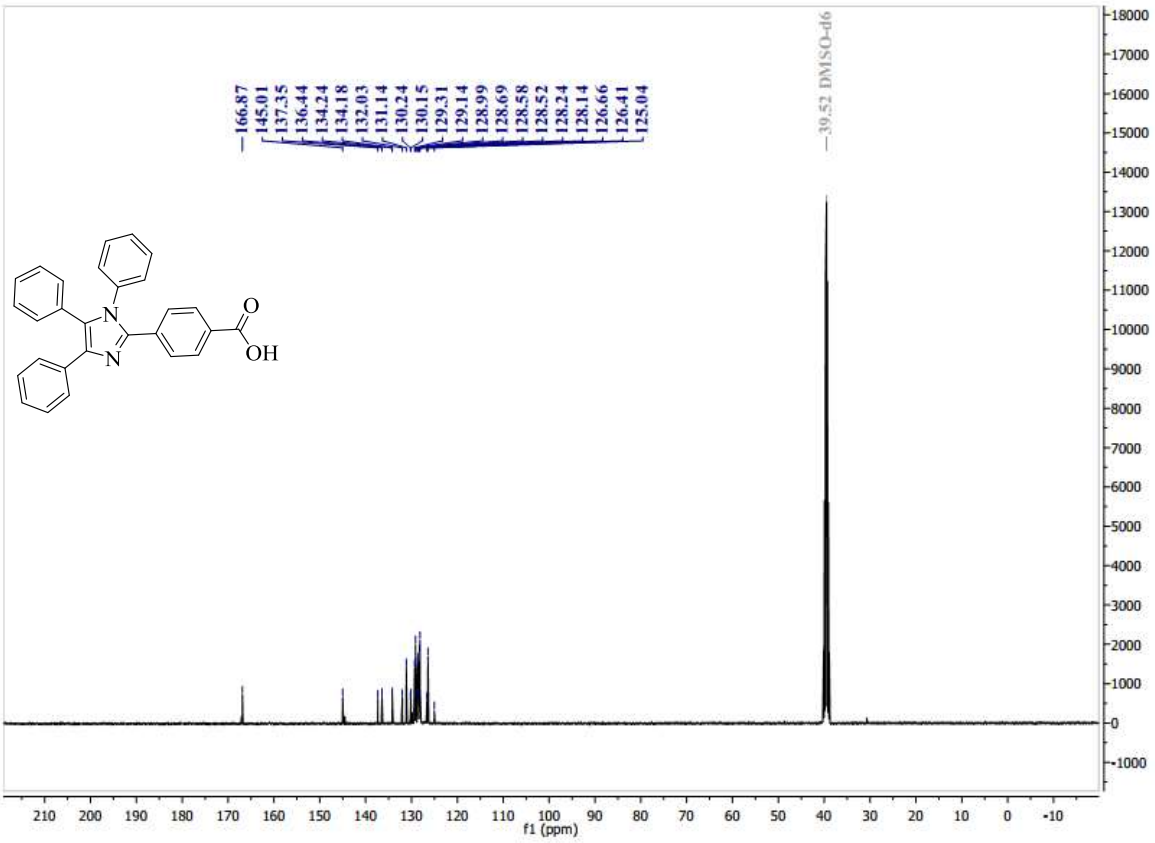

Figure 3-16: ^{13}C NMR spectrum of (PP4)

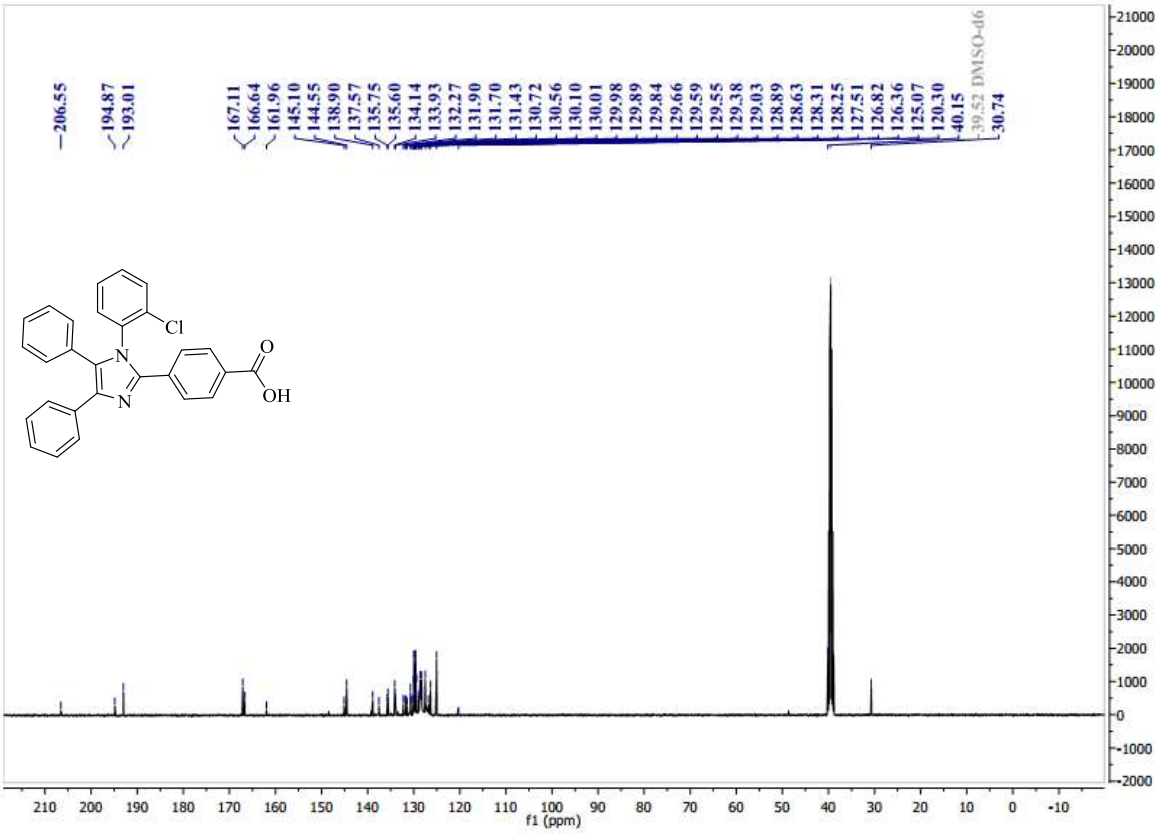

Figure 3-17: ^{13}C NMR spectrum of (PP5)

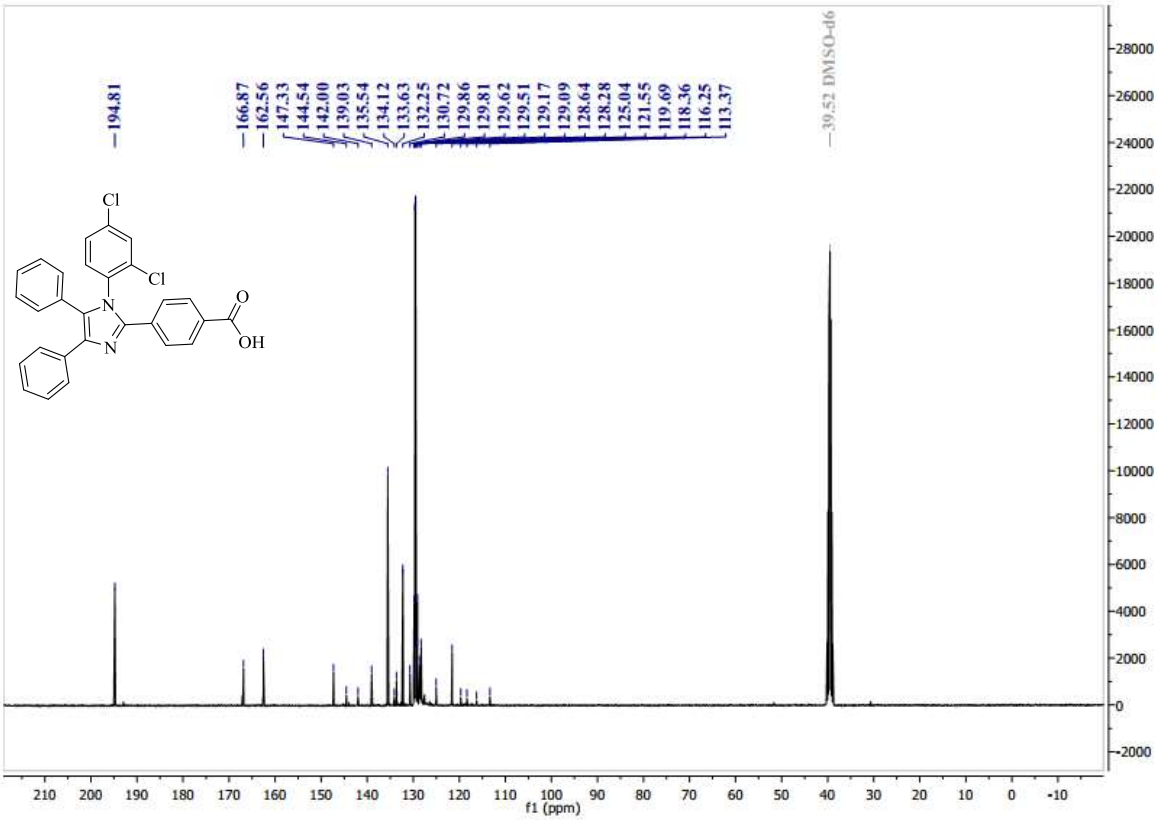

Figure 3-18: ^{13}C NMR spectrum of (PP6)

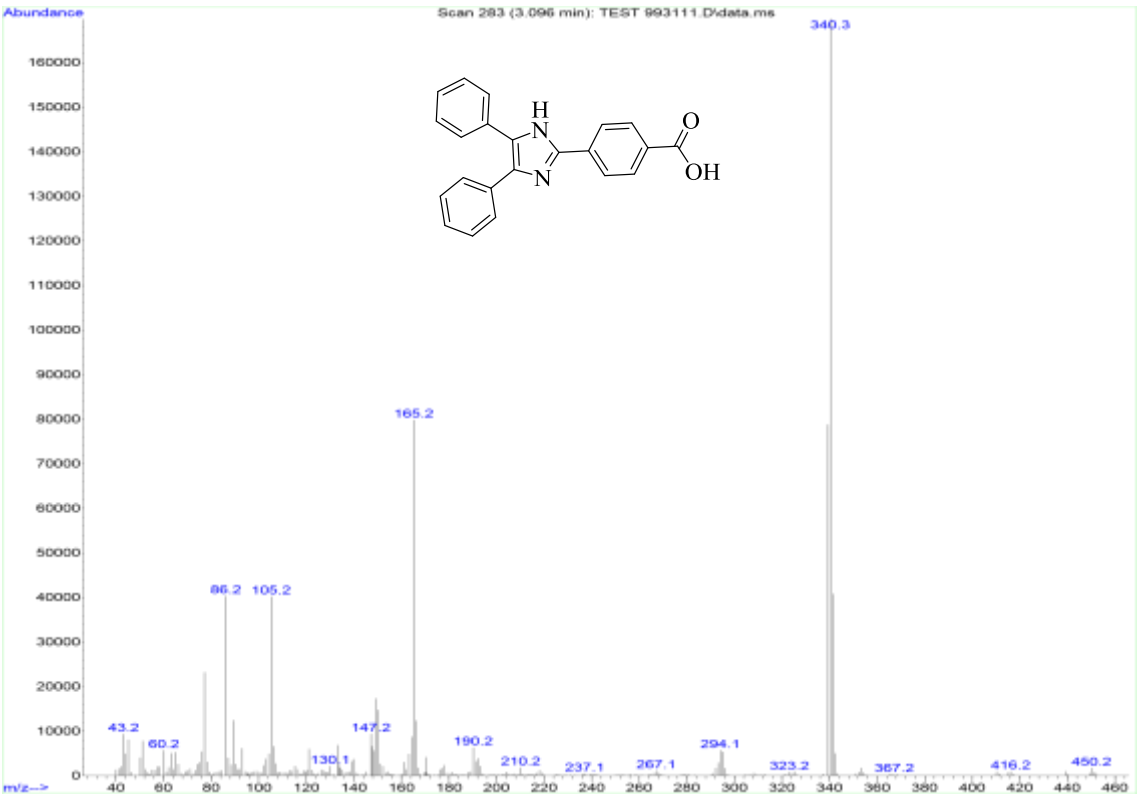

Figure 3-19: Mass spectrum of (PP1)

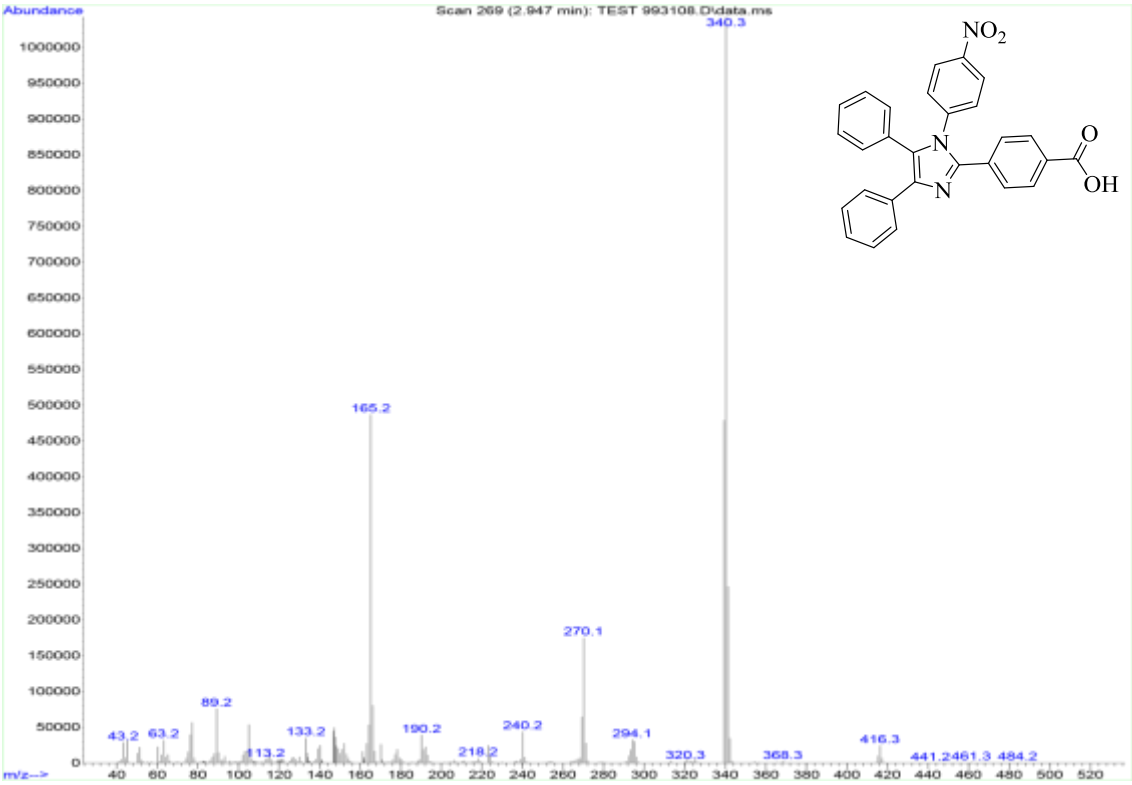

Figure 3-20: Mass spectrum of (PP2)

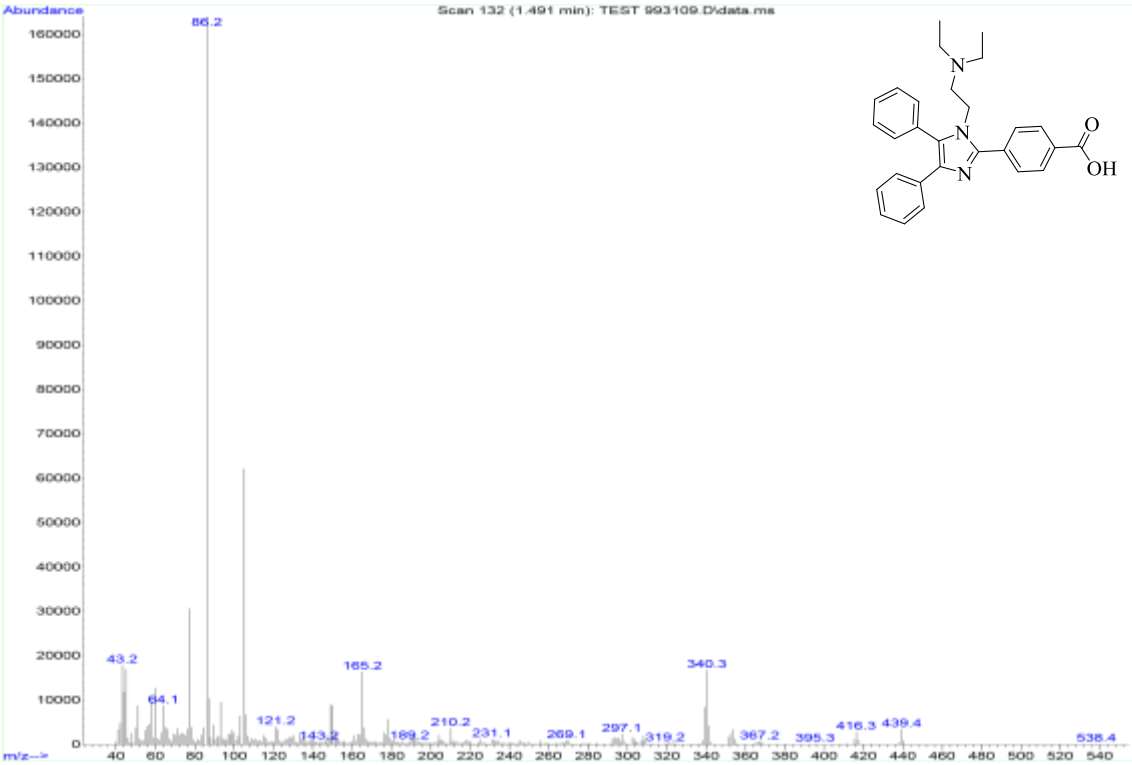

Figure 3-21: Mass spectrum of (PP3)

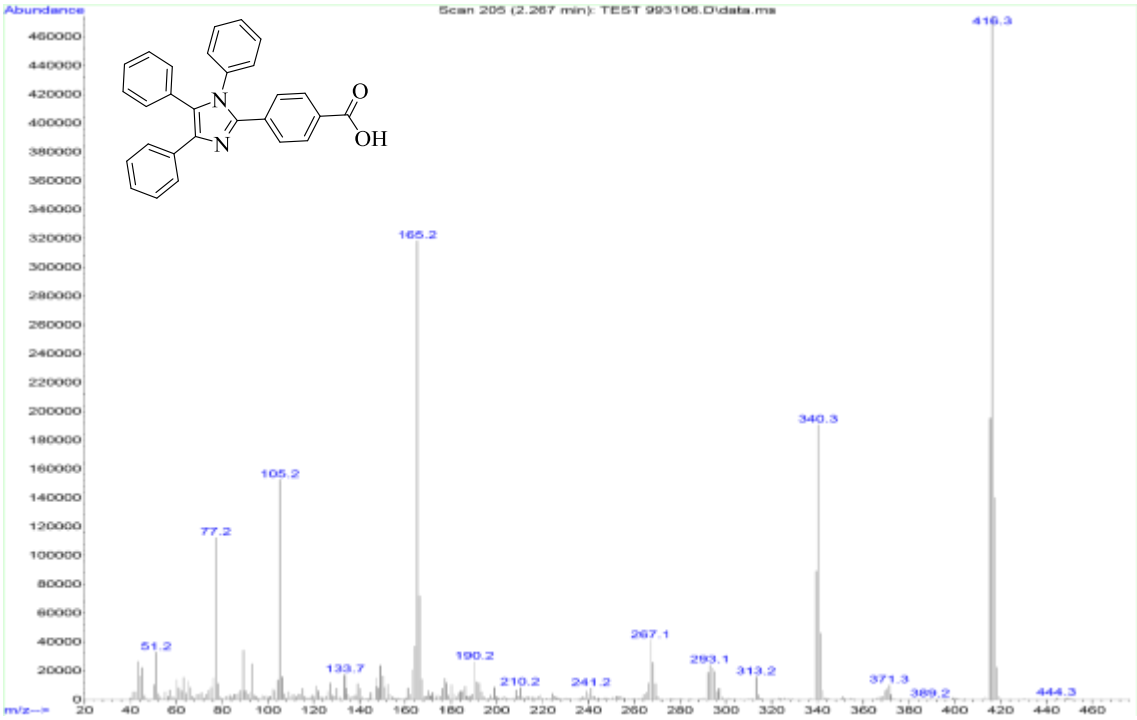

Figure 3-22: Mass spectrum of (PP4)

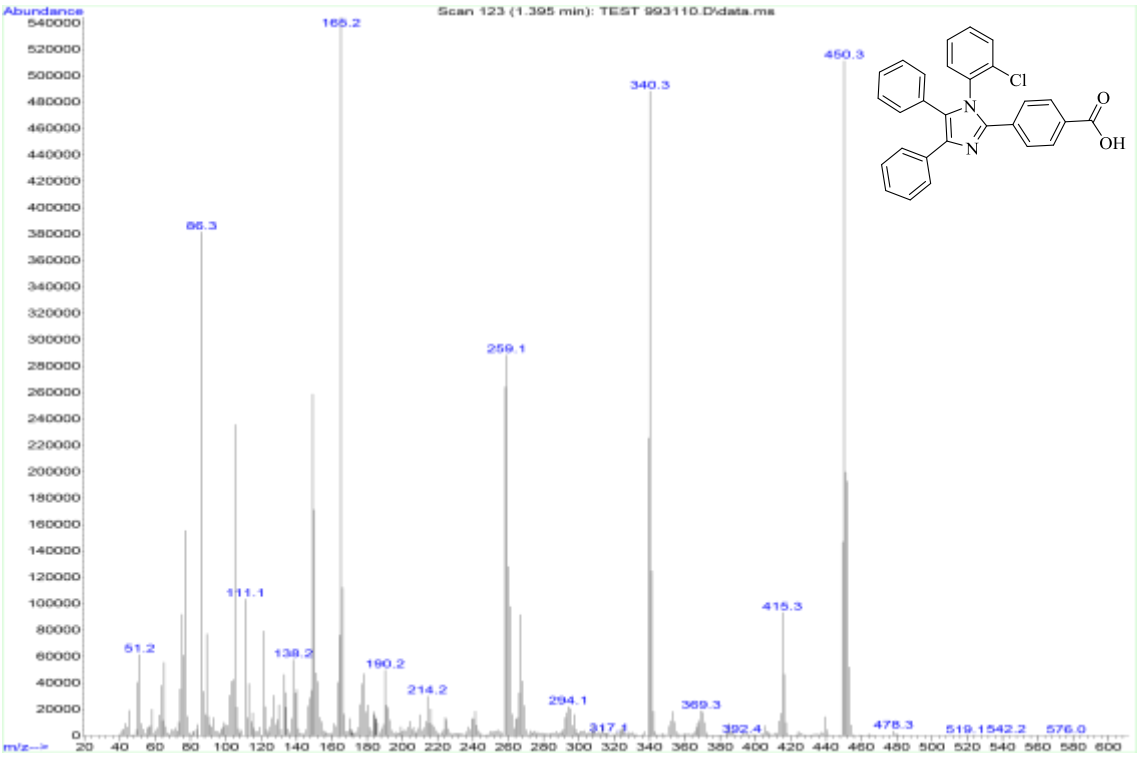

Figure 3-23: Mass spectrum of (PP5)

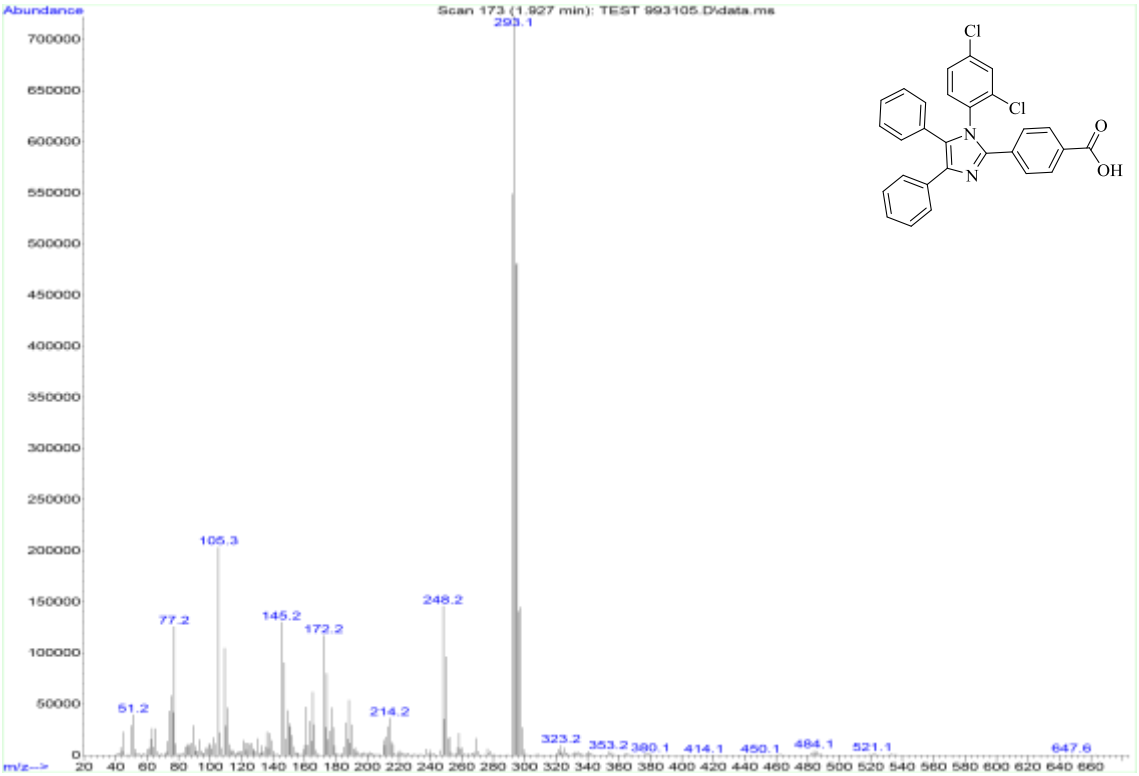

Figure 3-24: Mass spectrum of (PP6)

Table (3-1): Some of physical properties of the synthesized dyes and mass data

Dyes	Structure	Name	Molecular formula	M. Wt. (g/mol)	m.p. (°C)	Yield (%)	Mass Data (m/z) [M+]
PP1	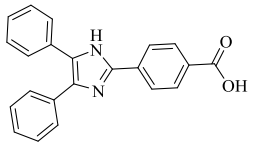	4-(4,5-diphenyl-1H-imidazol-2-yl)benzoic acid	$C_{22}H_{16}N_2O_2$	340.12	264-266	76	340.3 Figure (3-19)
PP2	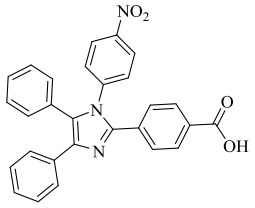	4-(1-(4-nitrophenyl)-4,5-diphenyl-1H-imidazol-2-yl)benzoic acid	$C_{28}H_{19}N_3O_4$	461.13	269	70	461.3 Figure (3-20)
PP3	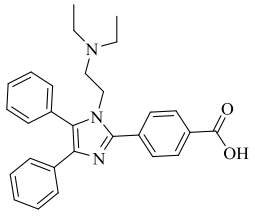	4-(1-(2-(diethylamino) ethyl)-4,5-diphenyl-1H-imidazol-2-yl)benzoic acid	$C_{28}H_{29}N_3O_2$	439.22	216-217	68	439.4 Figure (3-21)
PP4	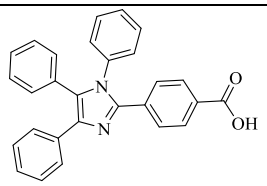	4-(1,4,5-triphenyl-1H-imidazol-2-yl)benzoic acid	$C_{28}H_{20}N_2O_2$	416.15	250-252	71.5	416.3 Figure (3-22)
PP5	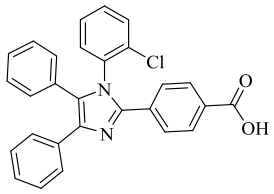	4-(1-(2-chlorophenyl)-4,5-diphenyl-1H-imidazol-2-yl)benzoic acid	$C_{28}H_{19}ClN_2O_2$	450.11	220-222	77	450.3 Figure (3-23)
PP6	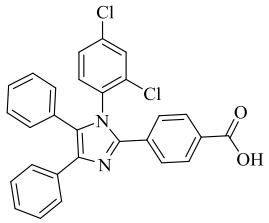	4-(1-(2,4-dichlorophenyl) -4,5-diphenyl-1H-imidazol-2-yl)benzoic acid	$C_{28}H_{18}Cl_2N_2O_2$	484.07	234-235	73	484.1 Figure (3-24)

3.3 Optical Properties

The UV–visible absorption spectra of the dyes PP1, PP2, PP3, PP4, PP5, and PP6 appeared between 329 and 335 nm (Fig.3-25) in EtOH as the solvent. These bands are a result of the donor segment's confined (high energy) aromatic π-π* transition and intramolecular charge transfer (ICT) electronic transitions [73-75]. These absorption bands are a result of the imidazole moiety being introduced into the phenyl core. The charge transfer is thought to originate from the donor 4,5-diphenyl-1*H*-imidazole to the acceptor benzoic acid [76-78]. Notably, the dye PP2 has a significantly higher molar extinction coefficient (17200 M^{-1} cm^{-1}) and a stronger absorption band than other dyes, indicating that it is an excellent light harvester. This result could be attributed to the imidazole and nitrobenzene donating and accepting groups respectively, and (table 3-2) is shown the optical properties and simulation energy for all synthesized dyes. The optical energy gap (E_g, opt) was essentially calculated using the Einstein-Plank equation (equation 1) [79,80], and PP2 had the smallest optical energy gap (2.96 eV) if compared to other dyes, indicating that it has a better electron transition from HOMO to LUMO than other dyes.

$$Eg\ opt = \frac{1240}{\lambda onset} \quad \text{.....(1)}$$

Where λ_{onset} is the onset of absorption spectra on the low energy side.
1240 = hc where h = 4.136 x 10^{-15} eV·s is the Planck's constant and c = 3 x 10^{17} nm·s^{-1} is the speed of light.

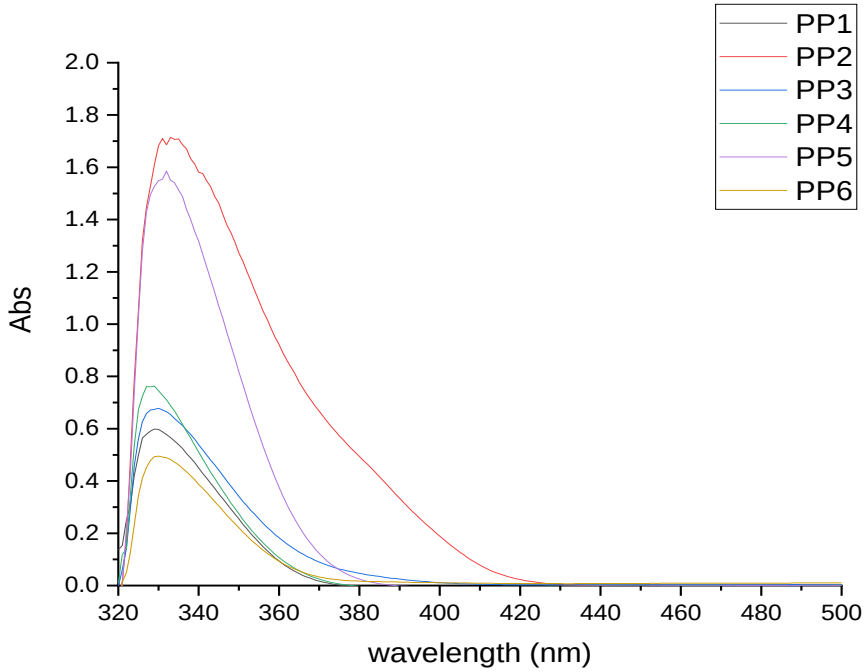

Figure 3-25: The absorption spectra of PP1, PP2, PP3,PP4, PP5 and PP6 dyes (EtOH 1×10^{-4} M)

Table 3-2: The optical properties and simulation energy for all synthesized dyes.

Dye	λ_{max}/nm	ε/M^{-1} cm^{-1}[a]	$E_{g,opt}$/eV	HOMO/eV[b]	LUMO/eV[b]	E_g/eV[b]
PP1	329	6000	3.35	-5.77	-2.53	3.24
PP2	333	17200	2.96	-6.05	-3.46	2.58
PP3	330	6400	3.18	-5.72	-2.43	3.29
PP4	329	7900	3.36	-5.74	-2.48	3.26
PP5	332	16000	3.32	-5.78	-2.01	3.77
PP6	330	5000	3.31	-5.90	-2.12	3.78

[a] Extinction coefficient (given from $A=\varepsilon cl$)

[b] Values obtained by computational study (DFT calculation)

3.4 Computational Studies

For optimization geometry and frequency calculations, all dyes are calculated in vacuum using the 6-311G* basis set. In all computational calculations, there are no created imaginary frequencies which were indicating that the optimized structures are energy minima. The electron distributions of the highest occupied molecular orbital (HOMO) and the lowest unoccupied molecular orbital (LUMO) in the molecule are displayed to illustrate the electron localization between donor and acceptor portions. As illustrated in (Fig. 3-26), the HOMOs in all dyes are predominantly located in the auxiliary donor area (phenyl-imidazole unit), whereas the LUMOs are located in the nitrobenzene for PP2 and the acceptor area (benzoic acid) for PP1, PP3, PP4, PP5, and PP6 dyes, which may result in the highest electron injection efficiency between the TiO_2 surface and the dye [81-84].

The computed HOMO (E_{HOMO}), LUMO (E_{LUMO}), and E_g energies for each of the six dyes are given in (Table 3-2). The energy level diagrams of all six dyes, as well as the conduction band (CB) energy level of TiO_2, and the redox potential energy of the I_3^-/I^- redox electrolyte (4.8 eV), are shown in (Fig. 3-27). All six dyes have LUMOs with energies greater than the TiO_2 CB (4.0 eV), resulting in effective electron injection from the dye's LUMO into the TiO_2 CB. Similarly, the energy of all five dyes' HOMOs is lower than the energy level of the I_3^-/I^- redox electrolyte [85].

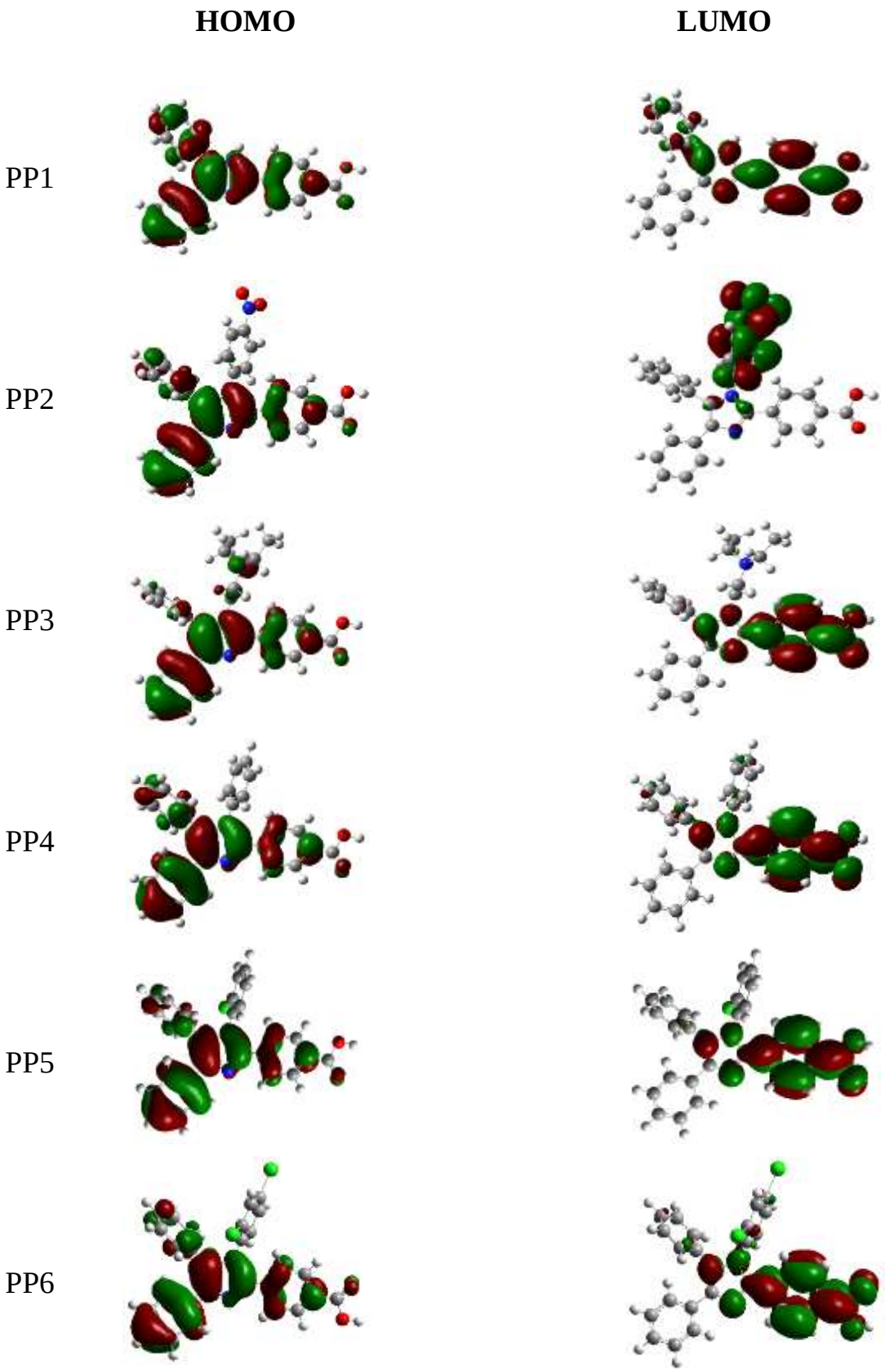

Figure 3-26: HOMOs and LUMOs for all dyes, predicted by DFT calculation.

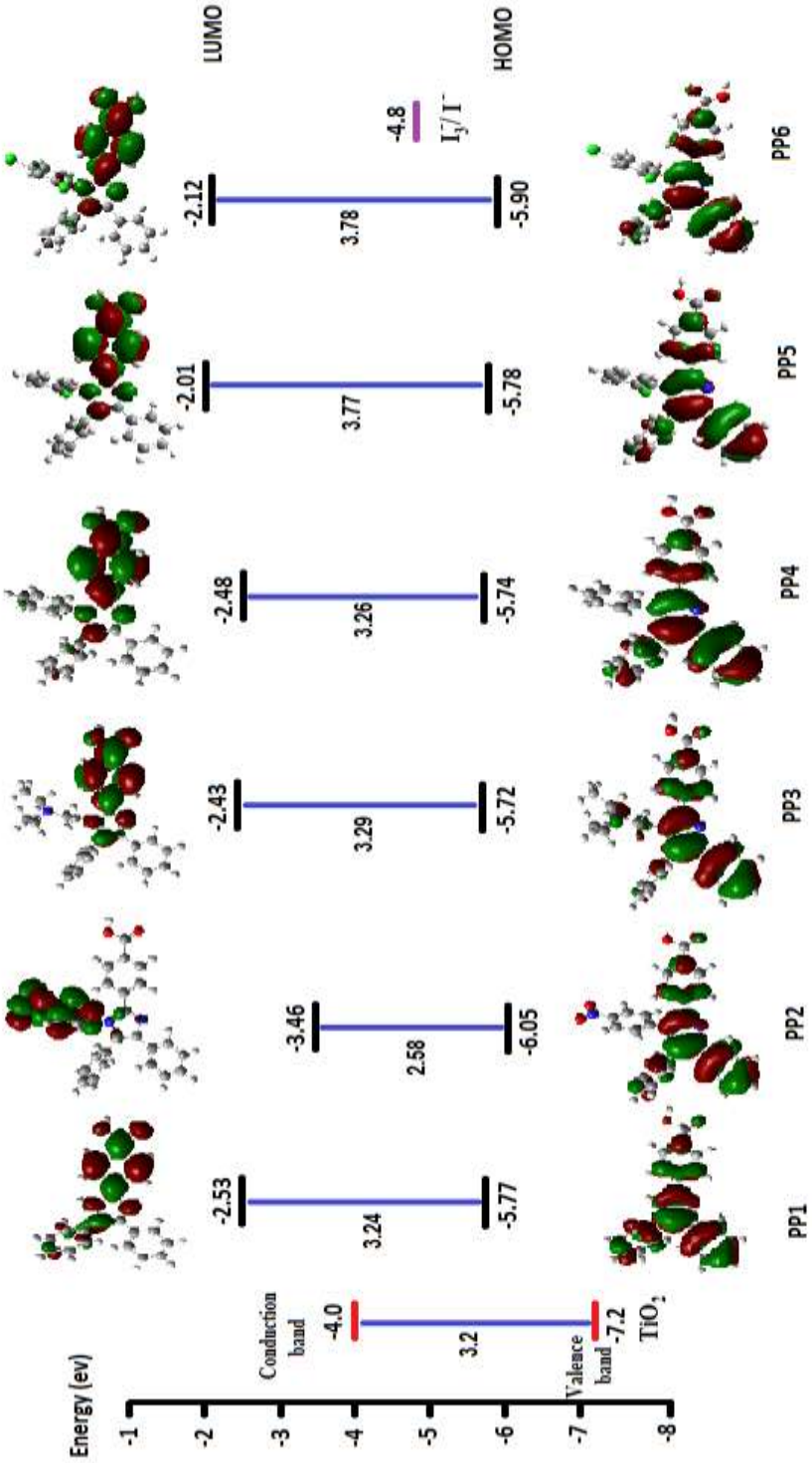

Figure 3-27: The energy level diagram of six dyes with CB of TiO_2 and redox potential energy of I_3^-/I^-

3.5 DSSCs test

The open-circuit voltage (V_{oc}) and short circuit current (J_{sc}) were calculated from the *J-V* curve. The fill factor (FF) and efficiency of the solar cells were determined using the following equations[86-88]:

$$FF = \frac{Jmax\ Vmax}{Jsc\ Voc} \ldots\ldots\ldots\ldots (2)$$

$$\eta = \frac{Jsc\ Voc\ FF}{Io} \ldots\ldots\ldots\ldots (3)$$

Where J_{max} is the maximum power point current, V_{max} is the maximum power point voltage of the solar cell, and I_o is the total incident irradiance.

The J-V curves for all dyes are depicted in (Fig. 3-28), as are the results for J_{SC}, V_{oc}, FF, and PCE (Table 3-3). In comparison to other dyes, PP3 dye had the highest PCE, which might be related to its solubility due to its alkyl chain bonding with the N of the imidazole ring, which prevents the dye from aggregating on the surface of TiO_2. While PP2 had the lowest PCE, this could be owing to the electron distribution of LUMO being concentrated on nitrobenzene rather than benzoic acid, which prevents an electron from the dye from being injected into the TiO_2. When compared to PP1, PP3, PP4, PP5, and PP6 compounds, the PP2 dye displayed the lowest PCE and J_{sc} values, which might be attributable to the dye's short electron lifetime and separation of the LUMO from the acceptor group.

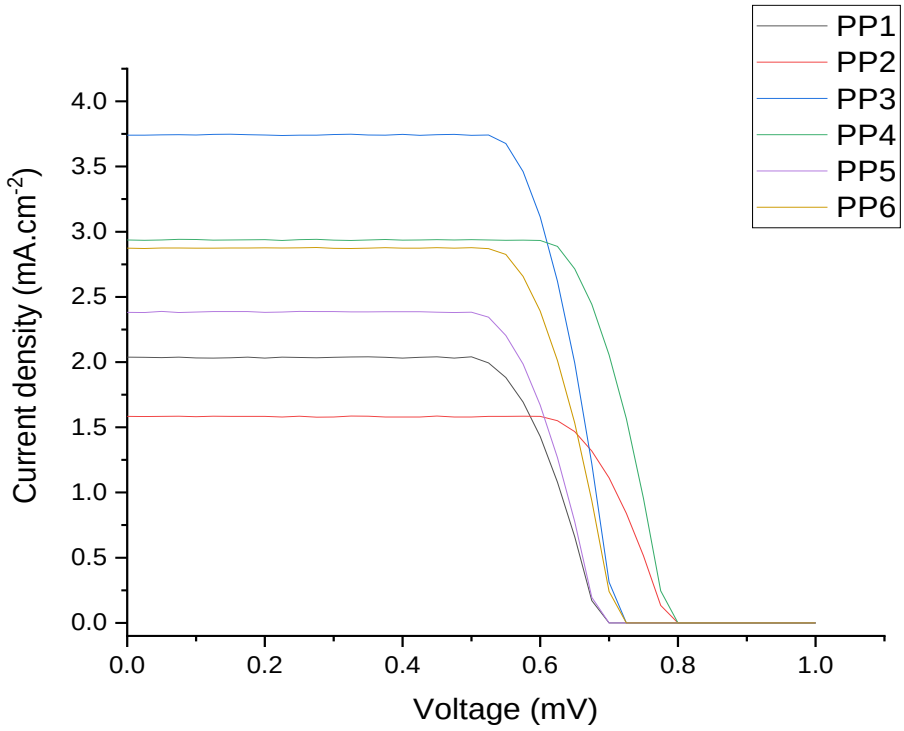

Figure 3-28: *J-V* curve of DSSCs sensitized by PP1, PP2, PP3, PP4, PP5 and PP6

Table 3-3: Photovoltaic parameters for all dyes under standard condition.

Dye	*Jsc* (mA.cm^{-2})	*Voc* (mV)	*FF* (%)	PCE (%)
PP1	2.03	0.700	73.6	1.05
PP2	1.59	0.800	61.6	0.960
PP3	3.75	0.730	73.9	2.01
PP4	2.91	0.790	76.7	1.78
PP5	2.39	0.690	73.7	1.46
PP6	2.39	0.690	73.3	1.55

3.6 Conclusion

1) A series of six organic dyes based on an imidazole ring was designed and synthesized as a donor, π-bridge, and acceptor groups to apply in DSSCs.
2) Investigate the efficiency of the solar cells by using different types of substitutions group on imidazole ring and these groups have enhanced the solubility by minimizing the aggregation of the dye.
3) PP2 has the smallest optical energy gap (2.96 eV) when compared to other dyes, higher molar extinction coefficient (17200 M^{-1} cm^{-1}) and a stronger absorption band than other dyes
4) The PP2 dye has the lowest energy gap (2.55 eV) and lowest PCE value 0.96% (J_{sc} = 1.59 mA cm^{-2}, V_{oc} = 0.080 mV, FF = 61.6%), and that could be attributed to the electron distribution on LUMO which is delocalized on the nitrobenzene instead of benzoic acid part and that is effective to the efficient of the electron injection from the dye to the surface of TiO_2.
5) The PP3 has the best efficiency of 2.01% (J_{sc} = 3.75 mA cm^{-2}, V_{oc} = 0.73 mV, FF = 73.9%) and that could be attributed to the excellent solubility of the dye and good electron distribution of HOMO and LUMO.

3.7 Future Works

1) Synthesis new imidazole derivatives dyes with new substituents groups as a donor and accepter.
2) Supporting the experimental part with a theoretical study to know the appropriate dyes for application in dye-sensitized solar cells.

References

[1] R. A. Stockman, "Heterocyclic chemistry," *Annu. Rep. Prog. Chem*. vol. 103, pp. 107-124, 2007.

[2] T. Eicher and S. Hauptmann, " The Chemistry of Heterocycles", 2nd Ed., 2003.

[3] H. S. Jabbar, A. K. Al-Edan, A. A. H. Kadhum, W. N. Roslam, and M. Sobri, "Synthesis and characterization of imidazole derivatives and catalysis using chemical pharmaceutical compounds," *J. Adv. Res. Dyn. Control Syst.*, vol. 11, pp. 1928–1939, 2019.

[4] A. Bhatnagar, P. K. Sharma, and N. Kumar, "A review on 'imidazoles': Their chemistry and pharmacological potentials," *Int. J. PharmTech Res.*, vol. 3, no. 1, pp. 268–282, 2011.

[5] J. Sivanadanam, I. S. Aidhen, and K. Ramanujam, "New cyclic and acyclic imidazole-based sensitizers for achieving highly efficient photoanodes for dye-sensitized solar cells by a potential-assisted method," *New J. Chem.*, vol. 44, pp. 10207–10219, 2020.

[6] S. M. J. Nabavi, H. Alinezhad, B. Hosseinzadeh, R. Ghahary, and M. Tajbakhsh, "Design, Synthesis and Application of Imidazole-Based Organic Dyes in Dye Sensitized Solar Cells," *J. Electron. Mater.*, vol. 49, pp. 3735–3750, 2020.

[7] D. Panday, D. S. Gupta, D. B. Yogi, J. Singh, and R. Kaur, "a Review Article on Synthesis of Imidazole," *World J. Pharm. Res.*, vol. 9, pp. 253–273, 2020.

[8] M. Waheed, N. Ahmed, M. A Alsharif, M. I. Alahmdi, and S. Mukhtar, "An Efficient Synthesis of 2,4,5-Trisubstituted and 1,2,4,5-Tetrasubstituted Imidazoles Using Dihydroquinolines as Novel Organocatalyst," *ChemistrySelect*, vol. 2, pp. 7946–7950, 2017.

[9] R. Bansal, P. K. Soni, and A. K. Halve, "Green Synthesis of 1,2,4,5-Tetrasubstituted and 2,4,5-Trisubstituted Imidazole Derivatives Involving One-pot Multicomponent Reaction," *J. Heterocycl. Chem.*,

vol. 55, pp. 1308–1312, 2018.

[10] S. Walki, L.Naik, H. M. Savanur, K. C. Yogananda, S. Naik, M. K. Ravindra, G. H. Malimath and K. M. iMahadevan, “Design of new imidazole-derivative dye having donor-π-acceptor moieties for highly efficient organic-dye-sensitized solar cells,” *Optik.*, vol. 208, pp. 164074–164104, 2020.

[11] K. M. Manikandan, A. Yelilarasi, S. S. Saravanakumar, P. Senthamaraikannan, A. Khan, and A. M. Asiri, “Effect of imidazole based polymer blend electrolytes for dye-sensitized solar cells in energy harvesting window glass applications,” *Chinese J. Chem. Eng.*, vol. 27, pp. 2807–2814, 2019.

[12] M. Mao, X. L. Zhang, and G. H. Wu, “Novel imidazole substituted bodipy-based organic sensitizers in dye-sensitized solar cells,” *Int. J. Photoenergy*, vol. 2018, pp. 1–9, 2018.

[13] S. Ashraf, J. Akhtar, H. M. Siddiqi, and A. El-Shafei, “Thiocyanate-free ruthenium(II) sensitizers with a bi-imidazole ligand in dye-sensitized solar cells (DSSCs),” *New J. Chem.*, vol. 41, pp. 6272–6277, 2017.

[14] M. Velusamy, Y. C. Hsu, J. T. Lin, C. W. Chang, and C. P. Hsu, “1-alkyl-1H-imidazole-based dipolar organic compounds for dye-sensitized solar cells,” *Chem. - An Asian J.*, vol. 5, pp. 87–96, 2010.

[15] B. Xu, Y. Li, P. Song, F. Ma, and M. Sun, “Photoactive layer based on T-shaped benzimidazole dyes used for solar cell: From photoelectric properties to molecular design,” *Sci. Rep.*, vol. 7, pp. 1–17, 2017.

[16] M. S. Tsai, Y. C. Hsu, J. T. Lin, H. C. Chen, and C. P. Hsu, “Organic dyes containing 1H-phenanthro[9,10-d]imidazole conjugation for solar cells,” *J. Phys. Chem. C*, vol. 111, pp. 18785–18793, 2007.

[17] X. Chen, C. Jia, Z. Wan, and X. Yao, “Organic dyes with imidazole derivatives as auxiliary donors for dye-sensitized solar cells:

Experimental and theoretical investigation," *Dye. Pigment.*, vol. 104, pp. 48–56, 2014.

[18] Y. S. Yen, J. S. Ni, T. Y. Lin, W. I. Hung, J. T. Lin, and M. C. P. Yeh, "Imidazole-Based Sensitizers Containing Double Anchors for Dye-Sensitized Solar Cells," *European J. Org. Chem.*, vol. 2015, pp. 7367–7377, 2015.

[19] Y. M. Ren and C. Cai, "Highly efficient , one-pot , solvent-free synthesis of highly substituted imidazoles using molecular iodine as catalyst", *Adv. Mater. Res.*, vol. 398, pp. 1871–1874, 2012.

[20] K. S. Ahmad, S. N. Naqvi, and S. B. Jaffri, "Systematic review elucidating the generations and classifications of solar cells contributing towards environmental sustainability integration," *Rev. Inorg. Chem.*, vol. 41, pp. 21–39, 2021.

[21] M. Tao, Terawatt solar photovoltaics: Roadblocks and opportunities, 2014.

[22] J. Jean, P. R. Brown, R. L. Jaffe, T. Buonassisi, and V. Bulović, "Pathways for solar photovoltaics," *Energy Environ. Sci.*, vol. 8, pp. 1200–1219, 2015.

[23] J. M. Gordon, T. Fasquelle, E. Nadal, and A. Vossier, "Providing large-scale electricity demand with photovoltaics and molten-salt storage," *Renew. Sustain. Energy Rev.*, vol. 135, pp. 110261-110267, 2021.

[24] Z. I. Alferov, V. M. Andreev, and V. D. Rumyantsev, "Solar photovoltaics: Trends and prospects," *Semiconductors*, vol. 38, pp. 899–908, 2004.

[25] O. Shevaleevskiy, "The future of solar photovoltaics: A new challenge for chemical physics," *Pure Appl. Chem.*, vol. 80, pp. 2079–2089, 2008.

[26] S. William, "Electrons and holes in semiconductors, with applications to transistor electronics," D. Van nortrand vompany, inc, 1950.

[27] G. L. Pearson, “Conversion of Solar to Electrical Energy,” *Am. J. Phys.*, vol. 25, pp. 591–598, 1957.

[28] N. A. S. Symposium and P. Rappaport, “developed, yielding,” *PNAS*, vol. 47, pp. 6–9, 1961.

[29] D. Kishore Kumar, J. Kríz̆, N. Bennett , B. Chen, H. Upadhayaya , K. R. Reddy, “Functionalized metal oxide nanoparticles for efficient dye-sensitized solar cells (DSSCs): A review,” *Mater. Sci. Energy Tech.* vol. 3, pp. 472–481, 2020.

[30] M. Alipour, H. Salim, R. A. Stewart, and O. Sahin, “Residential solar photovoltaic adoption behaviour: End-to-end review of theories, methods and approaches,” *Renew. Energy*, vol. 170, pp. 471–486, 2021.

[31] A. Mohammad Bagher, “Types of Solar Cells and Application,” *Am. J. Opt. Photonics*, vol. 3, pp. 94–113, 2015.

[32] S. Sharma, K. K. Jain, and A. Sharma, “Solar Cells: In Research and Applications-A Review,” *Mater. Sci. Appl.*, vol. 06, pp. 1145–1155, 2015.

[33] B. Srinivas, S. Balaji, M. Nagendra Babu, and Y. S. Reddy, “Review on present and advance materials for solar cells,” *Int. J. Eng. Res.*, vol. 3, pp. 178–182, 2015.

[34] A. Le Donne, A. Scaccabarozzi, S. Tombolato, S. Binetti, M. Acciarri, and A. Abbotto, “Solar Photovoltaics: A Review,” *Rev. Adv. Sci. Eng.*, vol. 2, pp. 170–178, 2013.

[35] P. R. Mohanta1, J. Patel, J. Bhuva, “A Review on Solar Photovoltaics and Roof Top Application of It,” *Int. J. Adv. Res. Eng. Sci. Tech.*, vol. 2, pp. 1–4, 2015.

[36] M. N. Mustafa and Y. Sulaiman, “Review on the effect of compact layers and light scattering layers on the enhancement of dye-sensitized solar cells,” *Sol. Energy*, vol. 215, pp. 26–43, 2021.

[37] J. Gonga, K. Sumathy, Q. Qiao, "Review on dye-sensitized solar cells (DSSCs): Advanced techniques and research trends," Renew. Sustain. *Energy Rev.*, vol. 68, pp. 234–246, 2017.

[38] N. Tomar, A. Agrawal, V. S. Dhaka, and P. K. Surolia, "Ruthenium complexes based dye sensitized solar cells: Fundamentals and research trends," *Sol. Energy*, vol. 207, pp. 59–76, 2020.

[39] A. M. Ammar, H. S. H. Mohamed, M. M. K. Yousef, G. M. Abdel-Hafez, A. S. Hassanien, and A. S. G. Khalil, "Dye-Sensitized Solar Cells (DSSCs) based on extracted natural dyes," *J. Nanomater.*, vol. 2019, pp. 1–10, 2019.

[40] A. Omar, M. S. Ali, and N. Abd Rahim, "Electron transport properties analysis of titanium dioxide dye-sensitized solar cells (TiO2-DSSCs) based natural dyes using electrochemical impedance spectroscopy concept: A review," *Sol. Energy*, vol. 207, pp. 1088–1121, 2020.

[41] R. Alfanaar, P. E. Elim, Y. Yuniati, H. S. Kusuma, and M. Mahfud, " Synthesis of TiO 2 /ZnO-Anthocyanin Hybrid Material for Dye Sensitized Solar Cell (DSSC) ," *IOP Conf. Ser. Mater. Sci. Eng.*, vol. 1053, pp. 012088-012100, 2021.

[42] J. Zhang, J. Zhang, H. B. Li, J. Z. Zhang, Y. Wu, Y. Geng, Q. Fu and Z. M. Su, "A promising anchor group for efficient organic dye sensitized solar cells with iodine-free redox shuttles: A theoretical evaluation," *J. Mater. Chem.* A, vol. 1, pp. 14000–14007, 2013.

[43] N. K. Moluguri, C. R. Murthy, and V. Harshavardhan, "Solar Energy System and Design - Review," Mater. Today Proc., vol. 3, pp. 3637–3645, 2016.

[44] M. S. M. Yahya , A. Bouziani , C. Ocak , Z. Sefero˘glu, "Organic/metal-organic photosensitizers for dye-sensitized solar cells (DSSC): Recent developments, new trends, and future perceptions," *Dye. Pigment.*, vol. 192, pp. 1–38, 2021.

[45] S. Bera, D. Sengupta, S. Roy, and K. Mukherjee, "Research into dye-sensitized solar cells: A review highlighting progress in India," *JPhys Energy*, vol. 3, pp. 1–30, 2021.

[46] M. R. Nalzala Thomas, V. J. Kanniyambatti Lourdusamy, A. A. Dhandayuthapani, and V. Jayakumar, "Non-metallic organic dyes as photosensitizers for dye-sensitized solar cells: a review," *Environ. Sci. Pollut. Res.*, vol. 28, pp. 28911–28925, 2021.

[47] S. Shalini, R. Balasundaraprabhu, T. S. Kumar, N. Prabavathy, S. Senthilarasu, and S. Prasanna, "Status and outlook of sensitizers/dyes used in dye sensitized solar cells (DSSC): a review," *Int. J. energy Res.*, vol. 40, pp. 1303–1320, 2016.

[48] L. A. Kosyachenko, Solar Cells: Dye-Sensitized Devices. BoD–Books on Demand, 2011.

[49] A. Carella, F. Borbone, and R. Centore, "Research progress on photosensitizers for DSSC," *Front. Chem.*, vol. 6, pp. 1–24, 2018.

[50] A. Hagfeldt, G. Boschloo, L. Sun, L. Kloo, and H. Pettersson, "Dye-Sensitized Solar Cells," *Chem. Rev.*, vol. 110, pp. 6595–6663, 2010.

[51] Y. Ooyama and Y. Harima, "Photophysical and electrochemical properties, and molecular structures of organic dyes for dye-sensitized solar cells," *ChemPhysChem*, vol. 13, pp. 4032–4080, 2012.

[52] M. M. Al Mogren, N. M. Ahmed, and A. A. Hasanein, "Molecular modeling and photovoltaic applications of porphyrin-based dyes: A review," *J. Saudi Chem. Soc.*, vol. 24, pp. 303–320, 2020.

[53] P. Semalti and S. N. Sharma, "Dye Sensitized Solar Cells (DSSCs) Electrolytes and Natural Photo-Sensitizers: A Review," *J. Nanosci. Nanotechnol.*, vol. 20, pp. 3647–3658, 2019.

[54] J. V. S. Krishna, M. Mrinalini, S. Prasanthkumar, and L. Giribabu, "Recent advances on porphyrin dyes for dye-sensitized solar cells,"

Dye-Sensitized Sol. Cells, pp. 231–284, 2019.

[55] D. Devadiga, M. Selvakumar, P. Shetty, and M. S. Santosh, "Dye-Sensitized Solar Cell for Indoor Applications: A Mini-Review," *J. Electron. Mater.*, vol. 50, pp. 3187–3206, 2021.

[56] J. Gong, J. Liang, and K. Sumathy, "Review on dye-sensitized solar cells (DSSCs): Fundamental concepts and novel materials," *Renew. Sustain. Energy Rev.*, vol. 16, pp. 5848–5860, 2012.

[57] L. Zhang and J. M. Cole, "Anchoring Groups for Dye-Sensitized Solar Cells," *Appl. Mater. Interfaces*, vol. 7, pp. 3427–3455, 2015.

[58] V. Pramananda, T. A. Hadyan Fityay, and E. Misran, "Anthocyanin as natural dye in DSSC fabrication: A review," *IOP Conf. Ser. Mater. Sci. Eng.*, vol. 1122, pp. 012104–012111, 2021.

[59] A. A. F. Husain, W. Z. W. Hasan, S. Shafie, M. N. Hamidon, and S. S. Pandey, "A review of transparent solar photovoltaic technologies," *Renew. Sustain. Energy Rev.*, vol. 94, pp. 779–791, 2018.

[60] N. Ruba , P. Prakash, S. Sowmya, B. Janarthana, A. N. Prabu, J. Chandrasekaran, T. Alshahrani, H. Y. Zahran & I. S. Yahia "Recent Advancement in Photo-Anode, Dye and Counter Cathode in Dye-Sensitized Solar Cell: A Review," *J. Inorg. Organomet. Polym. Mater.*, vol. 31, pp. 1894–1901, 2021.

[61] N. T. R. N. Kumara, A. Lim, C. M. Lim, M. I. Petra, and P. Ekanayake, "Recent progress and utilization of natural pigments in dye sensitized solar cells: A review," *Renew. Sustain. Energy Rev.*, vol. 78, pp. 301–317, 2017.

[62] P. Mahadevi and S. Sumathi, "Mini review on the performance of Schiff base and their metal complexes as photosensitizers in dye-sensitized solar cells," *Synth. Commun.*, vol. 50, pp. 2237–2249, 2020.

[63] F. Schoden, M. Dotter, D. Knefelkamp, T. Blachowicz, and E. Schwenzfeier-Hellkamp, "Review of State of the Art Recycling

Methods in the Context of Dye Sensitized Solar Cells," *Energies*, vol. 14, pp. 3741–3753, 2021.

[64] O. Adedokun, K. Titilope, and A. O. Awodugba, "Review on Natural Dye-Sensitized Solar Cells (DSSCs)" , *Int. J. Eng. Technol. IJET*, vol. 2, pp. 1–34, 2016.

[65] M. Kidwai, P. Mothsra, V. Bansal, R. K. Somvanshi, A. S. Ethayathulla, S. Dey, T. P. Singh, "One-pot synthesis of highly substituted imidazoles using molecular iodine: A versatile catalyst," *J. Mol. Catal. A Chem.*, vol. 265, pp. 177–182, 2007.

[66] Y. M. Ren and C. Cai, "A solvent-free synthesis of 1,2,4,5-tetrasubstituted imidazoles using molecular iodine as catalyst," *J. Chem. Res.*, vol. 34, pp. 133–134, 2010.

[67] S. M. Abdalhadi, A. Y. Al-Baitai, and H. A. Al-Zubaidi, "Synthesis and characterization of 2,3-diaminomaleonitrile derivatives by one-pot schiff base reaction and their application in dye synthesized solar cells," *Indones. J. Chem.*, vol. 21, pp. 443–451, 2021.

[68] N. Chander and V. K. Komarala, "Fabrication and characterization of dye sensitized solar cells: A photographic guide," *Indian J. Pure Appl. Phys.*, vol. 55, pp. 737–744, 2017.

[69] Abdalhadi, S.M., Synthesis and study of new organic and organometallic compounds with photovoltaic applications, 2017, University of Glasgow.

[70] T. T. Nguyen, N. P. Thi Le, T. T. Nguyen, and P. H. Tran, "An efficient multicomponent synthesis of 2,4,5-trisubstituted and 1,2,4,5-tetrasubstituted imidazoles catalyzed by a magnetic nanoparticle supported Lewis acidic deep eutectic solvent," *RSC Adv.*, vol. 9, pp. 38148–38153, 2019.

[71] M. Alikarami and M. Amozad, "One-pot synthesis of 2,4,5-trisubstituted imidazole derivatives catalyzed by BTPPC under

solvent-free conditions," *Bull. Chem. Soc. Ethiop.*, vol. 31, pp. 177–184, 2017.

[72] A. Parveen, M. R. S. Ahmed, K. A. Shaikh, S. P. Deshmukh, and R. P. Pawar, "Efficient synthesis of 2,4,5-triaryl substituted imidazoles under solvent free conditions at room temperature," *Arkivoc*, vol. 2007, pp. 12–18, 2007.

[73] Q. Cui, Q. Yang, W. Wang, J. Yao, Z. Liu, X. Zuo, K. Zhu, G. Li and S. Jin, "Controllable synthesize core-shelled Zn0.76Co0.24S nanospheres as the counter-electrode in dye-sensitized solar cells and its enhanced electrocatalytic performance," *J. Mater. Sci. Mater. Electron.*, vol. 31, pp. 1797–1807, 2020.

[74] S. Sambathkumar S. Priyadharshini, M. Fleisch, D.W. Bahnemann, G. Gnana Kumar, S. Senthilarasu and R. Renganathan, "Design and synthesis of imidazole-triphenylamine based organic materials for dye sensitized solar cells," *Mater. Lett.*, vol. 242, pp. 28–31, 2019.

[75] S. Kula, P. Krawczyk, M. Filapek, and A. M. Maroń, "Influence of N-donor substituents on physicochemical properties of phenanthro[9,10-d]imidazole derivatives," *J. Lumin.*, vol. 233, pp. 1–11, 2021.

[76] S. Kula, P. Ledwon, A. M. Maro´n, M. Siwy, J. Grzelak, M. Szalkowski, S. Ma´ckowski, and E. S. Balcerzak, "Synthesis, photophysical properties and electroluminescence characterization of 1-phenyl-1H-phenanthro[9,10-d]imidazole derivatives with N-donor substituents," *Dye. Pigment.*, vol. 192, pp. 1–9, 2021.

[77] S.Sambathkumar, S.Priyadharshini, M.Fleisch, D. W .Bahnemann, G. G. Kumar, S. Senthilarasu and R. Renganathan, "Design and synthesis of imidazole-triphenylamine based organic materials for dye sensitized solar cells," *Mater. Lett.*, vol. 242, pp. 28–31, 2019.

[78] D. Karthik, V. Kumar, K. R. Justin Thomas, C. T. Li, and K. C. Ho, "Synthesis and characterization of thieno[3,4-d]imidazole-based

organic sensitizers for photoelectrochemical cells," *Dye. Pigment.*, vol. 129, pp. 60–70, 2016.

[79] A. R. Zolghadr, O. Estakhr, M. Heydari Dokoohaki, and H. Salari, "Comparison between Bi2WO6and TiO2Photoanodes in Dye-Sensitized Solar Cells: Experimental and Computational Studies," *Ind. Eng. Chem. Res.*, vol. 60, pp. 12292–12306, 2021.

[80] M. Cariello, "Synthesis of novel organic semiconductors for optoelectronic devices," pp. 1-254, 2016.

[81] C. A. Huerta Aguilar, T. Pandiyan, J. A. Arenas-Alatorre, and N. Singh, "Oxidation of phenols by TiO2Fe3O4M (M = Ag or Au) hybrid composites under visible light," *Sep. Purif. Tech.*, vol. 149, pp. 265–278, 2015.

[82] J. S. Al-otaibi, A. H. Almuqrin, Y. S. Mary, and R. Thomas, "Modeling the conformational preference , spectroscopic properties , UV light harvesting ef fi ciency , biological receptor inhibitory ability and other physico-chemical properties of fi ve imidazole derivatives using quantum mechanical and molecular mecha," *J. Mol. Liq.*, vol. 310, pp. 112871–112875, 2020.

[83] K. Galappaththi, P. Ekanayake, and M. I. Petra, "A rational design of high efficient and low-cost dye sensitizer with exceptional absorptions: Computational study of cyanidin based organic sensitizer," *Sol. Energy*, vol. 161, pp. 83–89, 2018.

[84] Y. S. Priya, K. R. Raob, P. V. Chalapathic, A. V. Katta, E. Srikanthd, Y. S. Marye and R. Thomas, "Intricate spectroscopic profiling, light harvesting studies and other quantum mechanical properties of 3-phenyl-5-isooxazolone using experimental and computational strategies," *J. Mol. Struct.*, vol. 1203, pp. 127461–127510, 2020.

[85] S. Mandal, S. Rao, and K. Ramanujam, "Understanding the photo-electrochemistry of metal-free di and tri substituted thiophene-based

organic dyes in dye-sensitized solar cells using DFT/TD-DFT studies," *Ionics (Kiel).*, vol. 23, pp. 3545–3554, 2017.

[86] S. Umale, V. Sudhakar, S. M. Sontakke, K. Krishnamoorthy, and A. B. Pandit, "Improved efficiency of DSSC using combustion synthesized TiO2," *Mater. Res. Bull.*, vol. 109, pp. 222–226, 2019.

[87] M. R. S. A. Janjua, M. U. Khan, M. Khalid, N. Ullah, R. Kalgaonkar, K. Alnoaimi, N. Baqader and S. Jamil "Theoretical and Conceptual Framework to Design Efficient Dye-Sensitized Solar Cells (DSSCs): Molecular Engineering by DFT Method," *J. Clust. Sci.*, vol. 32, pp. 243–253, 2021.

[88] N. Kutlu, "Investigation of electrical values of low-efficiency dye-sensitized solar cells (DSSCs)," *Energy*, vol. 199, p. 117222, 2020.

الخلاصة

في هذا العمل، تم تحضير ست صبغات عضوية خالية من المعادن كنظام مانح- جسر - مستقبل في تفاعل تكثيف أحادي الوعاء واستخدمت كمحسس في الخلايا الشمسية المتحسسة للصبغة (**DSSCs**). الأصباغ التي تم تسجيلها هي من مشتقات الإيميدازول وهي من نوعين. النوع الأول عبارة عن مشتقات إيميدازول ثلاثية التعويض في المواقع 2,4,5 (المخطط الأول) والنوع الثاني من الأصباغ هو مشتقات إيميدازول رباعية التعويض في المواقع 1,2,4,5 (المخطط الثاني).

النوع الأول هو PP1 والنوع الثاني يمثل خمسة أنواع مختلفة من الاستبدال (نيتروبنزينPP2، *N,N*- ثنائي اثيل بروبان-1-امين PP3، فنيل PP4، كلوروبنزين PP5 وثنائي كلورو بنزين PP6) في موضع- NH على حلقة إيميدازول للتحقق من تأثير هذه المجاميع في كفاءة **DSSCs**. تم اختيار وحدتي البنزين والإيميدازول كمجموعات مانحة، لخاصية التبرع بالإلكترون ولتجنب تراكم الصبغة على سطح TiO_2. في الأساس، تم استخدام وحدات إيميدازول 2,4,5- trisubstituted لدراسة المقارنة لأداء المحسّسات في الأجهزة النهائية. تم اختيار حلقة البنزين كجسر وتم اختيار حامض الكربوكسيل كمجموعة مستقبلة ومرتبطة على سطح TiO_2. شُخصت هذه الأصباغ بـتقنية الـ FTIR، ^{1}H -NMR، ^{13}C–NMR و Mass spectra ومدعومة بالحسابات النظرية. أظهرت الصبغة PP3 مع استبدال سلسلة الألكيل أعلى كفاءة تحويل للطاقة (PCE) بنسبة 2.01%(J_{sc} = 3.75 مللي أمبير سم $^{-2}$، V_{oc} = 0.73 مللي فولت، FF = 73.9٪) بينما أظهرت صبغة PP2 باستبدال النيتروبنزين أقلها فجوة الطاقة (2.55 eV) وأدنى PCE 0.96٪ (J_{sc} = 1.59 مللي أمبير سم $^{-2}$، V_{oc} = 0.080 مللي فولت، FF = 61.6٪).

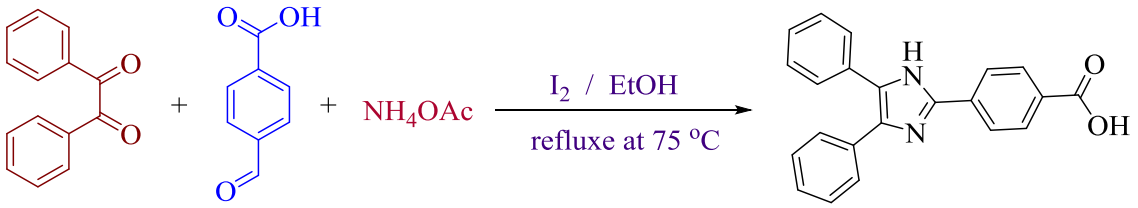

PP1

المخطط الأول: تحضير مشتقات الايميدازول ثلاثية التعويض في المواقع 2,4,5

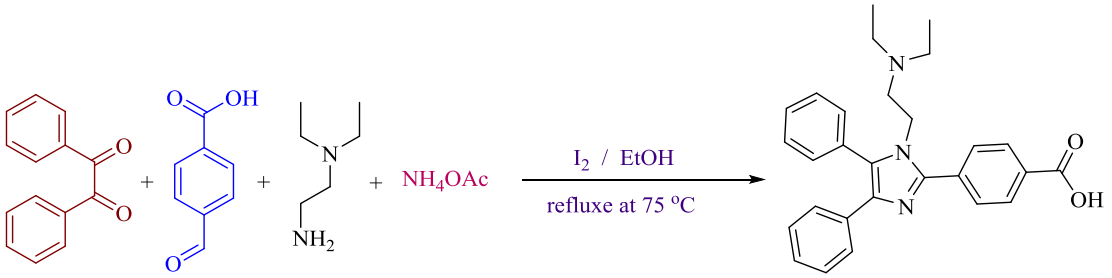

PP3

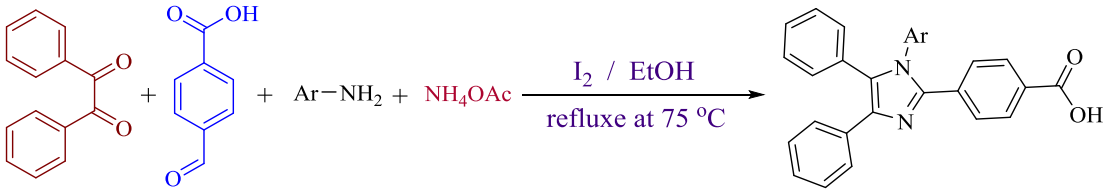

PP2, PP4, PP5 and PP6

Where Ar = 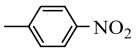

(PP2),  **(PP4),** 

(PP5), 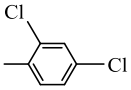

(PP6)

المخطط الثاني: تحضير مشتقات الايميدازول رباعية التعويض في المواقع 1,2,4,5

جامعة كربلاء

كلية العلوم

قسم الكيمياء

تحضير ودراسة نظرية لمشتقات صبغات الايميدازول الجديدة وتطبيقها في الخلايا الشمسية المحفزة بالصبغة

رسالة مقدمة الى
مجلس كلية العلوم – جامعة كربلاء
كجزء من متطلبات نيل درجة الماجستير
علوم في الكيمياء

تقدم بها

سيف الدين فاهم عبد الحسين

اشراف

أ. د. هيثم دلول حنون

أ.م. د. سيف الدين موفق عبد الهادي

2022م

1443هـ